International Scientific-Technical and Production Journal

The Paton WELDING JOURNAL

February 2003 # 2

English translation of the monthly «Avtomaticheskaya Svarka» (Automatic Welding) journal published in Russian since 1948

Founders: *The E.O. Paton Electric Welding Institute of the NAS of Ukraine*
International Association «Welding»

Publisher: *International Association «Welding»*

Address:

E.O. Paton Electric Welding Institute,
International Association «Welding»,
11, Bozhenko str., 03680, Kyiv, Ukraine
Tel.: (38044) 227 67 57
Fax: (38044) 268 04 86
E-mail: journal@paton.kiev.ua
http://www.nas.gov.ua/pwj

State Registration Certificate
KV 4790 of 09.01.2001

Subscriptions:

$460, 12 issues per year,
postage and packaging included.
Back issues available.

CONTENTS

MATHEMATICAL MODELLING OF PROCESSES OF INTERACTION OF METAL WITH GASES IN ARC WELDING

I.K. POKHODNYA
The E.O. Paton Electric Welding Institute, NASU, Kyiv, Ukraine

Results of thermodynamic investigations of interaction of molten metal with a gas, containing hydrogen, oxygen and compounds of fluorine, and also with a slag phase are given. Taking into account the non-stationary conditions and variable rate of crystallization the laws of redistribution of hydrogen in a crystallizing weld pool are established. The formulated mathematical models are based on a differential equation of mass transfer, in particular, the Fick's equation with boundary conditions of Stefan type on the moving phase interface. Kinetics of hydrogen redistribution near the fusion line, and also in molten metal at a cellular crystallization was studied. The process of growth of a gas bubble in weld pool is described.

Key words: *arc welding, absorption of gases, hydrogen, crystallization, weld pool, porosity*

The arc welding is the high-temperature metallurgical process. At all its stages the metal and slag interaction with hydrogen, nitrogen and oxygen is occurred. Specialists of the E.O. Paton Electric Welding Institute pay a great attention to the study of these processes whose results of investigation are described in works [1–14].

High temperatures and rate of reactions, existing in arc welding, small volumes and large specific surfaces of reacting phases, and also non-equilibrium conditions of different stages of the process complicate significantly the conductance of experiments. Methods of physical and mathematical modelling give an opportunity to obtain the additional information using advanced computer engineering.

The present article describes the results of works, obtained mainly at the E.O. Paton Electric Welding Institute, on physical and mathematical modelling of behaviour of gases in arc welding of steels.

Metal evaporation and absorption of gases. Calculation of hydrogen solubility in a molten iron depending on the temperature was made by I.I. Frumin [4], and the experimental investigations were performed by V.I. Lakomsky [5]. The results obtained showed that the maximum hydrogen solubility in iron is observed at 2700 K temperature and decreased to zero at the metal boiling temperature.

As is followed from the results of investigations [1], the heat content of electrode metal drops depends on current and its polarity (Figure 1). In many cases the temperature of drops exceeds the temperature of a maximum solubility of gases in iron. Therefore, the difference in temperature of drops in the 200–300 K range in case of a consumable electrode welding at current of straight and reverse polarity can influence greatly on the absorption of gases.

Figure 2 presents the experimental data (circles) about the nitrogen content in drops of the Cr–Ni electrode metal in welding at current of straight polarity in Ar + 10 % N_2 [1]. O.M. Portnov made calculation of nitrogen absorption by electrode metal drops and its results are shown in Figure 2 by a solid line. As is seen from the Figure the satisfactory coincidence of calculated and experimental data is observed.

Thermodynamical evaluation of metal interaction with a slag and gas. The thermodynamic approaches were used for analysis of the process of bind-

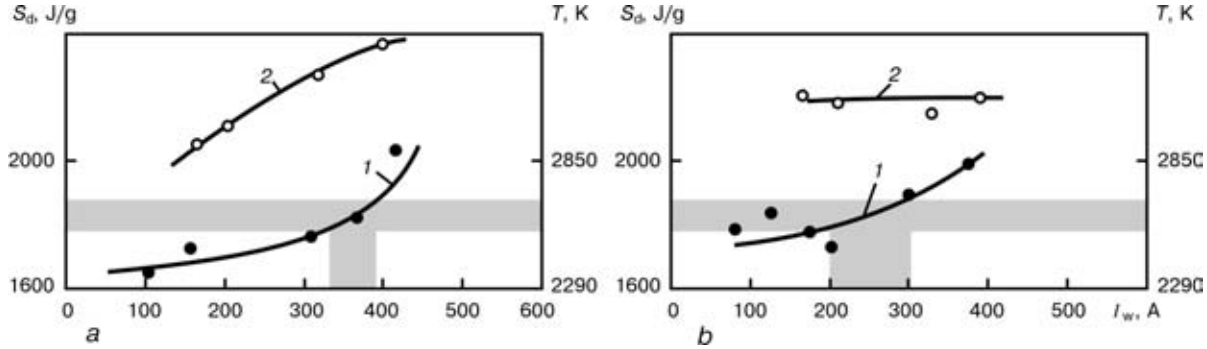

Figure 1. Effect of welding current I_w and its polarity on heat content of drops S_d of electrode metal in welding low-carbon steel using 2 mm diameter wire Sv-08A in mixture of inert gases He + N_2 (*a*) and Ar + N_2 (*b*): *1*, *2* — current of straight and reverse polarity, respectively (regions of temperatures of maximum solubility of nitrogen and current at which these temperatures are reached are hatched)

ing hydrogen, located in the gas phase in the form of water vapours, into hydrogen fluoride, insoluble in a molten iron, at temperature 2000–2500 K and pressure $1 \cdot 10^5$ Pa [6]. Calculations were made as regards to welding with a flux-cored wire in CO_2. The initial conditions were characterized by the formation of phases of the following compositions: gas — carbon monoxide with a small amount of water vapours, metal — iron, and slag — CaF_2 and SiO_2, Al_2O_3, TiO_2 and CaO in different proportions. To create the oxidizing atmosphere some amount of FeO was introduced into the calculated composition of the slag melt.

Different slag systems were analyzed: SiO_2–CaO–CaF_2, TiO_2–CaO–CaF_2, Al_2O_3–CaO–CaF_2. In addition, the process of hydrogen binding was investigated at different temperatures and content of water vapours in a gas phase, as well as at additional adding of SiF_4 and oxygen into this phase.

Figure 3, *a* shows the dependence of a mass share of hydrogen in a molten metal on the initial content of CaF_2 in the slag system TiO_2–CaO–CaF_2, obtained by a calculated method. At the absence of CaO the region, where the mass share of CaF_2 is 60–75%, is considered optimum. With increase in the mass share of CaO in the slag the region of optimum composition is shifted to the side of decrease in CaF_2 content. However, in this case a high content of hydrogen in metal corresponds to the above-mentioned zone. Similar data were obtained also for the system Al_2O_3–CaO–CaF_2 (Figure 3, *b*). In system SiO_2–CaO–CaF_2 (Figure 3, *c*) the mass share of CaO does not influence the hydrogen content in the molten metal, which is decreased with the increase in the mass share of CaF_2 in the slag.

With increase in oxidizing potential of the gas phase due to adding of a molecular oxygen the hydrogen content in metal is decreased negligibly. With SiF_4 adding to the gas phase the mass share of hydrogen in the molten metal is greatly decreased due to developing of the reaction of hydrogen interaction with free atoms of fluorine forming in dissociation of SiF_4 (Figure 4). This method of decrease in hydrogen content in the molten metal is more effective as compared with adding of a large mass share of SiO_2 and CaF_2 into slag composition with allowance for exchange reaction proceeding

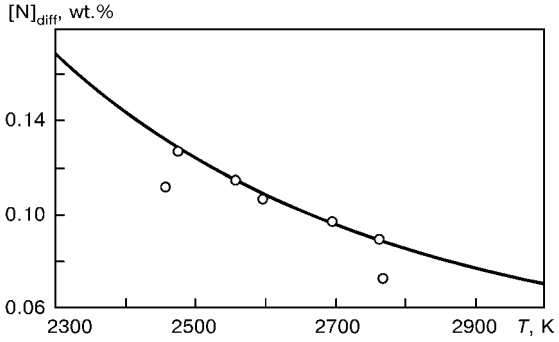

Figure 2. Effect of drops temperature T on nitrogen absorption with electrode metal drops in welding at straight polarity current in Ar + 10 % N_2 mixture

$$2CaF_2 + SiO_2 \rightarrow 2CaO + SiF_4. \quad (1)$$

To investigate the kinetics of development of thermochemical reactions in solid and liquid substances with a gas phase participation, a dynamic thermogravimetry is used at which the mass of sample and rate of its change in the controllable atmosphere depending on temperature and time is continuously recorded. Using the data obtained it is possible to study the kinetics of the processes of evolution of gases at the high rate of heating which is typical of the arc welding. For this purpose, a method of calculation is used, based on determination of energy of activation of reaction of a thermal decomposition and other kinetic parameters from the data of series of thermogravimetric analyses at different rates of heating [13, 14].

Results of the thermogravimetric analysis of mixture CaF_2 + SiO_2, and also powders Na_2SiF_6 and $BaSiF_6$ are given in Figure 5. A noticeable interaction of CaF_2 and SiO_2 is started at temperatures above 700 °C, and dissociation of Na_2SiF_6 and $BaSiF_6$ occurs, respectively, at 500–700 and 300–400 °C. However, in case of hexafluorosilicates the process of thermal decomposition has a comparatively high energy of activation (≈ 280–320 kJ/mol), while the energy of activation of the reaction of formation of silicon

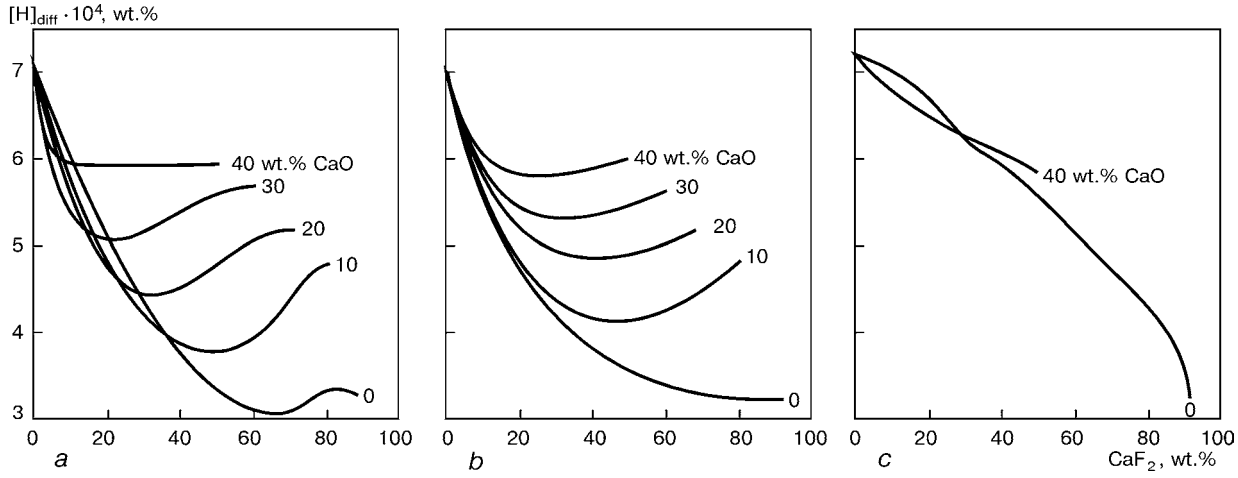

Figure 3. Change in hydrogen content in molten metal depending on mass share of CaF_2 in different slag systems: *a* — TiO_2–CaO–CaF_2; *b* — Al_2O_3–CaO–CaF_2; *c* — SiO_2–CaO–CaF_2

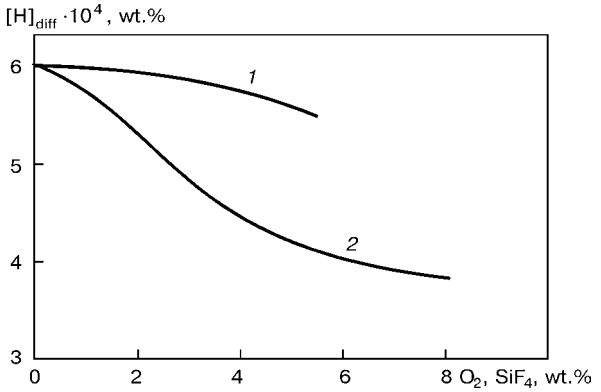

Figure 4. Effect of mass share of oxygen and SiF_4 in gas phase on hydrogen content in a molten metal (slag — 45 % SiO_2, 45 % CaF_2 and 10 % FeO, calculated data): *1* — O_2; *2* — SiF_4

tetrafluoride is characterized by lower values (about 150 kJ/mol) as a result of exchange reaction of fluorite with silica, that leads to the dependence of temperature interval of intensive gas evolution on the heating rate.

The calculation results are confirmed experimentally in investigation of concentration of diffusive hydrogen in weld metal made by flux-cored wires with different fluorides in the core metal (Figure 6) [7].

Calculations of a partial pressure P_{SiF_4} at 4 and 11 % mass share of SiO_2 in electrode coating, and also experimental data on diffusive hydrogen concentration in weld metal are given in Figure 7. The Figure shows a noticeable reduction in concentration of the diffusive hydrogen with increase in a mass share of SiO_2 and CaF_2 in the coating [8].

Evaluation of hydrogen behaviour in arc discharge. The physical bases for construction of a calculated model were conceptions about the presence of a local thermodynamic equilibrium in the arc column. The arc column is characterized by a convex shape of a radial distribution of temperature. Here, the effect of near-electrode zones was not taken into account. The physical model, taken in calculations, and its mathematical description are given in [9].

Hydrogen and oxygen in the arc are dissociated completely at temperature 4000 K, fluorine — even at temperature 1600 K, as it has a low energy of dissociation (1.38 eV). In a larger part of the arc

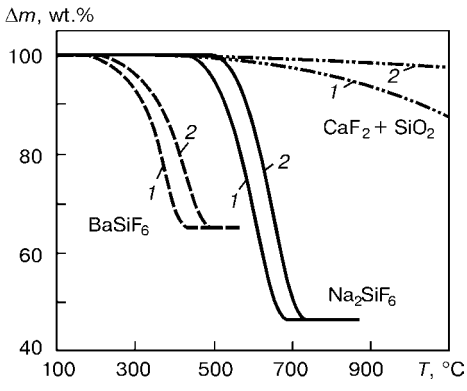

Figure 5. Results of thermogravimetric analysis of dissociation of fluorides and silicon fluorides at heating rate of 10 (*1*) and 20 (*2*) °C/min (Δm — change in sample mass)

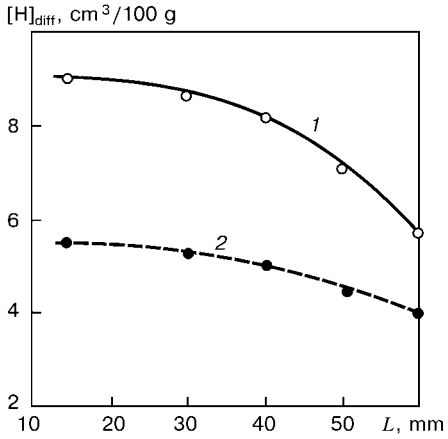

Figure 6. Change in concentration of diffusion hydrogen in weld metal made by flux-cored wires with different fluorides in core metal [7]: *1* — $CaF_2 + SiO_2$; *2* — Na_2SiF_6 (L — length of wire stickout)

column section HF and OH are also dissociated completely (Figure 8, *a*).

The improvement of efficiency of arc protection with decrease in temperature is shown in Figure 8, *b*. 1 % HF and 1 % OH were introduced additionally into the arc (partial pressure $P_{HF} = P_{OH} = 1000$ Pa). It is seen from comparison of distribution of HF and OH particles in such arc (Figure 8, *b*) that in case of reduction in arc temperature the effectiveness of hydrogen binding into HF and OH is increased. The width of zone, where dissociation is occurred, is 1.5 times larger for HF than for OH. The comparison of curves in Figure 8 showed that at equal partial pressure HF and OH have the same degree of dissociation at temperatures, differed approximately by 1000 K.

The effective hydrogen binding by these compounds can be provided only at low temperatures which exist at the periphery of the arc column and beyond it, where the temperature for HF does not exceed 3000, and 2500 K for OH.

Hydrogen in weld pool. Distribution of hydrogen in the process of weld pool crystallization will be

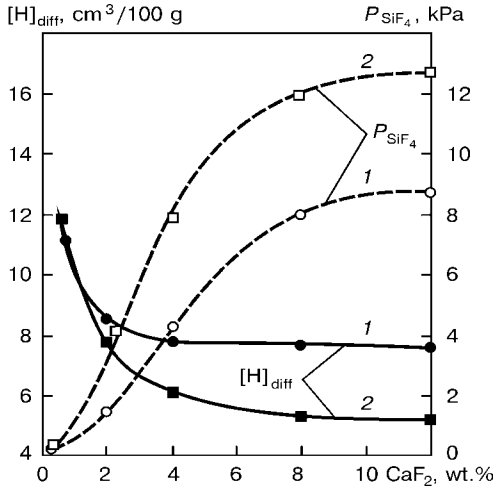

Figure 7. Effect of CaF_2 and SiO_2 in the coating on calculated values of partial pressure of silicon tetrafluoride P_{SiF_4} in arc atmosphere and experimental values of hydrogen concentration in deposited metal [8]: *1* — 4 wt.% SiO_2; *2* — 11 wt.% SiO_2

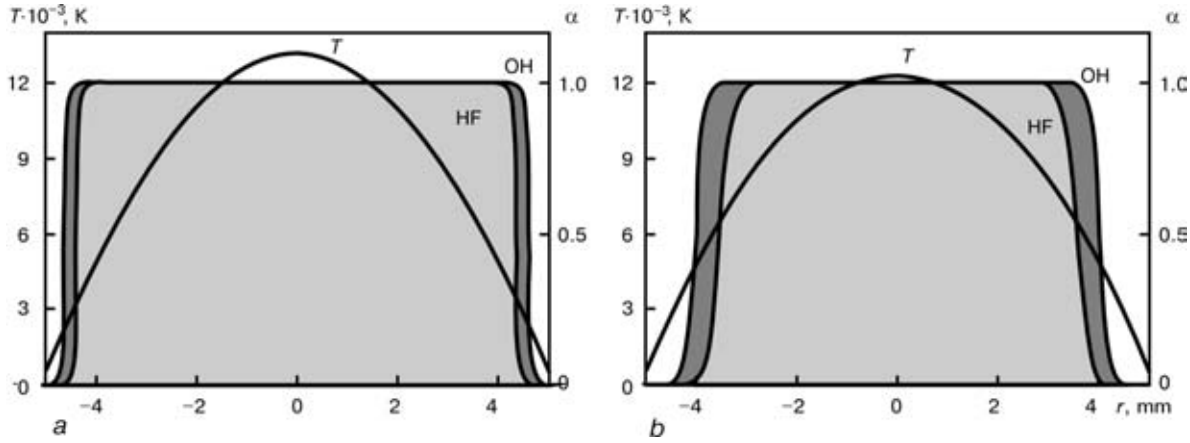

Figure 8. Dependence of degree of dissociation of particles HF and OH, α, on radius of arc column, r, at increased (*a*) and lower (*b*) temperature in the column axis zone

considered for the case of plane and cellular fronts of crystallization.

Hydrogen distribution at a plane front of crystallization. Gas transfer is realized by diffusion; the coefficient of diffusion depends on temperature and rate of crystallization. Analytical solution of the problem is given in [10]. Figure 9 shows a typical pattern of hydrogen distribution at intermittent crystallization of the weld pool in case of welding of low-carbon steel. In calculations the following values of parameters are taken: $D_S = 1 \cdot 10^{-4}$ cm^2/s; $D_L = 1 \cdot 10^{-3}$ cm^2/s; $k = 0.53$; $v_{\text{cryst}} = 0.2$ cm/s; $t_{st} = 0.2$ s; $C_L(0) = 5$ cm^3/100 g; $C_S(0) = 0$; $t_d(i) = 0.05 + di$ (here D_S and D_L are the coefficients of hydrogen diffusion in solid and liquid phase, respectively; k is the coefficient of hydrogen distribution; v_{cryst} is the rate of crystallization; t_d, t_{st} is the time of process of crystallization and its interruption; $C_L(0)$ and $C_S(0)$ is the initial hydrogen concentration in liquid and solid phase, respectively; $i = 0, 1, 2, \ldots, n$ is the number of a crystallization layer, counted from the fusion line).

Analysis of calculated data showed that at an intermittent crystallization in the liquid phase the formation of a diffusion boundary layer, enriched with hydrogen, is observed in the form of a concentration packing which is tended to a quasi-stationary condition at v_{cryst} = const. During interruption between the periods of growth of crystals the decay of the concentration packing is occurred under the action of the following factors: diffusion in liquid phase, which reduces the hydrogen concentration directly near the front of crystallization and enriches the molten metal layer at some distance from the front of crystallization; decrease in hydrogen concentration in liquid phase at the interface proceeding proportionally to the decrease in hydrogen content in solid phase.

With interruption of the crystallization process the flow of diffusive hydrogen is directed from the solid phase to liquid phase. In the liquid phase, enriched with hydrogen, the conditions for formation of gas bubbles are created at its initial concentration 10–12 cm^3/100 g. The total gas distribution in weld metal caused by a lamellar crystallization is characterized by two peculiar features: existence of enriched hydrogen layer, locating in the solidified metal in the place of liquid phase enriched during interruption of liquid phase, and the presence of a hydrogen-depleted region at the boundary of the crystallization layer from the solid metal side.

In weld metal cooling this non-homogeneity is decreased due to hydrogen diffusion. The hydrogen distribution between the weld pool and solidified metal depends on the rate of crystallization. As the calculations showed the 10 times decrease in a preset value of the coefficient of hydrogen diffusion in solid phase, the same as the change in duration of crystallization pauses in the solid phase growth, has no great influence on the hydrogen distribution nature.

Hydrogen distribution at a cellular front of crystallization. The change in geometric structure of the crystallization front causes a radically new distribution of hydrogen, dissolved in weld pool. Figure 10 shows the field of hydrogen concentrations in a growing cell and intercrystalline liquid. During calculations the following values of parameters were taken: $D_S = 1 \cdot 10^{-3}$ cm^2/s; $D_L = 1.6 \cdot 10^{-3}$ cm^2/s; $v_{\text{cryst}} = 0.4$ cm/s; cell size $l = 25$ μm; rate of cooling $v_{\text{cool}} = 50$ °C/s; 0.2 % mass share of carbon.

Analysis of calculated data showed the following:

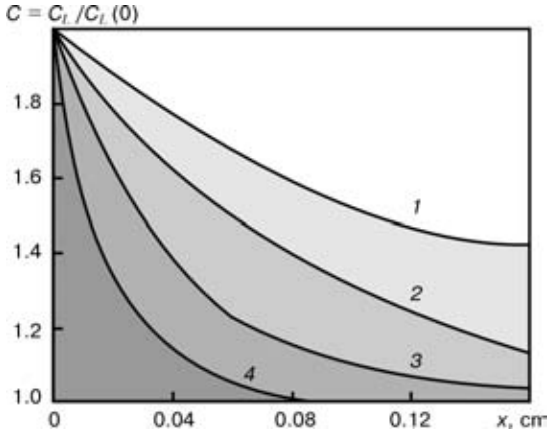

Figure 9. Distribution of hydrogen concentration C in molten metal during moving the plane front of crystallization at $v_{\text{cryst}} = 0.01$ (*1*), 0.02 (*2*), 0.04 (*3*) and 0.08 (*4*) cm/s (x — coordinate counted from the crystallization front)

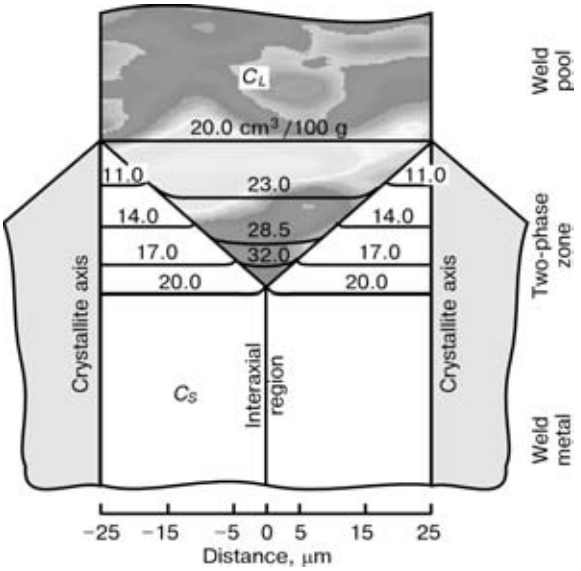

Figure 10. Field of hydrogen concentration in solid C_S and liquid C_L phase at a cellular front of crystallization

• enrichment of metal with dissolved hydrogen is mainly localized in an intercrystalline liquid; average gas concentration is observed in a weld pool liquid phase;

• due to high diffusion mobility of hydrogen in solid phase the non-homogeneity of hydrogen distribution in section of a completely solidified cell is negligible.

Growth of a gas bubble. Factor, limiting the bubble growth from the initially-formed nuclei is the process of transportation of a gas dissolved in a liquid metal to the gas–liquid interface. The transfer of the dissolved gas to metal is realized by two methods: diffusion and convection. Calculations were based on the conceptions about the presence of a boundary layer of molten metal near the crystallization front, which was not participating in a convective stirring of the main mass of the weld pool metal, and also on the assumptions that the formed bubble nucleus is growing in this layer during some period of time. It was assumed that the nucleus and dissolved bubble have a spherical shape. It was assumed in the initial calculations that the contact surface area of the bubble growing at the front of crystallization with a solid phase is much smaller than that with a liquid phase. In addition, it was allowed that the non-homogeneity of diffusion oversaturation ahead of the crystallization

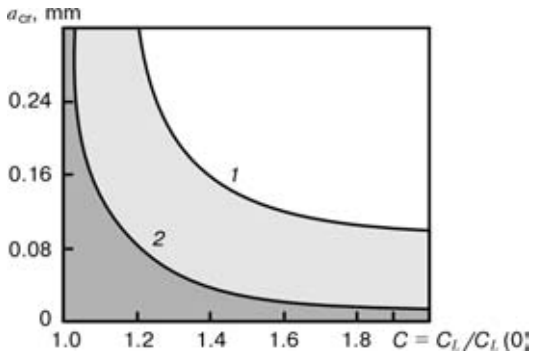

Figure 11. Dependence of critical radius a_{cr} of bubble on relative concentration C of nitrogen (*1*) and hydrogen (*2*) in melt

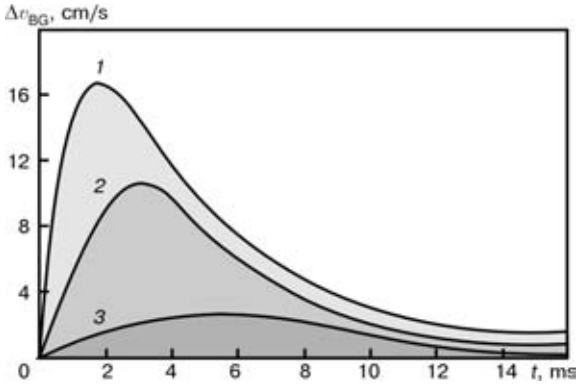

Figure 12. Change in rate of bubble growth Δv_{BG} of hydrogen at the moment of time t: *1* — $C_L(0) = 42$ cm³/100 g, $\sigma = 1 \cdot 10^{-4}$ J/cm²; *2* — $C_L(0) = 42$ cm³/100 g, $\sigma = 1.8 \cdot 10^{-4}$ J/cm²; *3* — $C_L(0) = 35$ cm³/100 g, $\sigma = 1.15 \cdot 10^{-4}$ J/cm²

front is small. Dendritic-cellular nature of crystallization corresponds mostly to these conditions.

Physical model and procedure of its numerical realization in computer are described in [10]. Dependence of bubble critical radius on relative gas concentration in melt is presented in Figure 11. As the calculations showed, the gas diffusion into bubble results in formation of a layer, depleted with gas, moving together with the bubble, in a molten metal. The rate of bubble growth depends on the gas concentration in weld pool ahead of the crystallization front. Maximum rate is observed at the initial stage of the bubble growth (Figure 12).

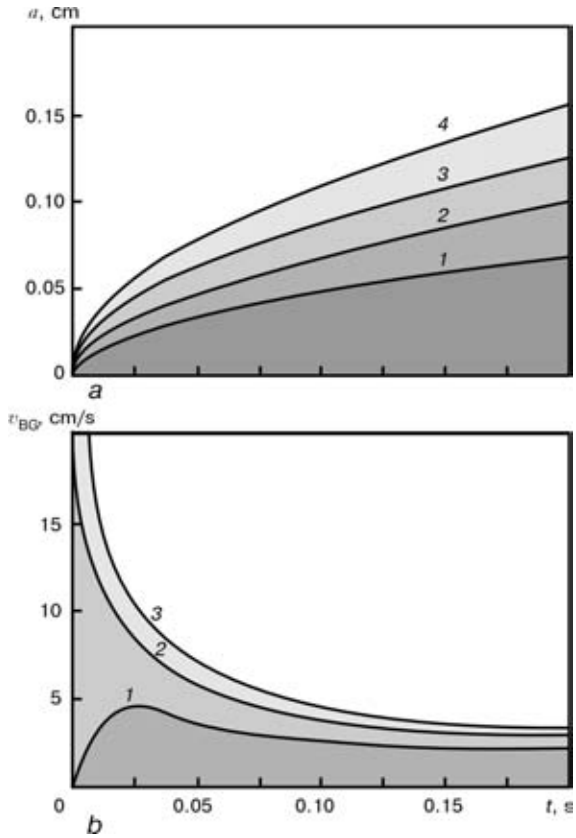

Figure 13. Kinetics of growth of a gas bubble (*a*) and rate of its growth (*b*) depending on ratio β of area of bubble contact with melt to a total surface of bubble: *1* — β = 1; *2* — 0.9; *3* — 0.8; *4* — 0.7 (*a* — radius of gas bubble)

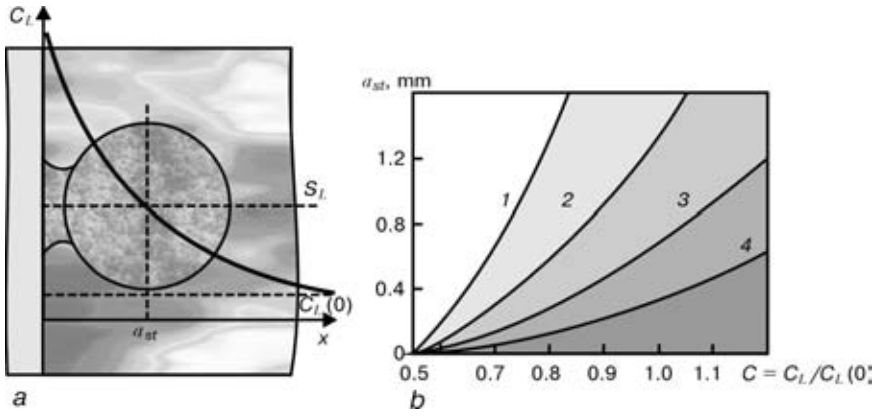

Figure 14. Scheme of determination of a stopping radius of bubble a_{st} (*a*) and dependence of its values at which its growth is interrupted on hydrogen concentration C and rate of crystallization (*b*): *1* — v_{cryst} = 0.01; *2* — 0.02; *3* — 0.04; *4* — 0.08 cm/s

The bubble growth rate depends also on the surface tension at the metal–gas interface. With increase in the surface tension the maximum values of growth rate are decreased and shifted to the side of large periods of time. After reaching the maximum growth rate its instantaneous reduction to values comparable with the rate of weld pool crystallization are observed. The effect of surface tension at such rate is negligible.

It was assumed in construction of the above-described model of a gas bubble growth that the area of surface contact of the growing bubble with a solid phase is negligible. At the same time, it is initiated really at the front of crystallization. Consequently, it can be expected that the level of hydrogen diffusion into the gas bubble from the solid phase will be high.

L.A. Taraborkin suggested to make allowance for the above-mentioned effect as follows. Law of mass conservation is described in the form of a boundary condition at the bubble surface

$$\frac{dM(t)}{dt} = [P_S\beta(t) + P_L(1 - \beta(t))]\sigma(t), \qquad (2)$$

where M is the mass of hydrogen in a bubble; P_S, P_L are the flows of diffused gas from solid and liquid phases, respectively; $\beta(t)$ is the fraction of area of the bubble surface at the moment of time t; $\sigma(t)$ is the area of bubble surface at the moment of time t.

The gas flow from the solid phase is determined by the solution of a non-linear problem of diffusion with a boundary condition, here the reaction of hydrogen solvation at the rate proportional to the square of concentration of gas atoms in the external layer is taken into account:

$$P_S = KC^2_{S_{surf}}(t), \qquad (3)$$

where K is the coefficient of proportionality (constant of solvation reaction rate); $C^2_{S_{surf}}$ is the surface concentration of gas atoms at the bubble boundary. It was taken into account in the last condition that the chemical potential of gas in bubbles is much higher than in solid metal, so the diffusion flow from the gas phase to the solid phase (to metal) can be considered negligible.

Results of calculation experiments (Figure 13) illustrate the kinetics of growth and rate of growth of the gas bubble (hydrogen bubble) in the solidifying melt with allowance for the hydrogen diffusion from the solid phase.

Formation of pores in weld. Results of numerical experiments on redistribution of gases in weld pool

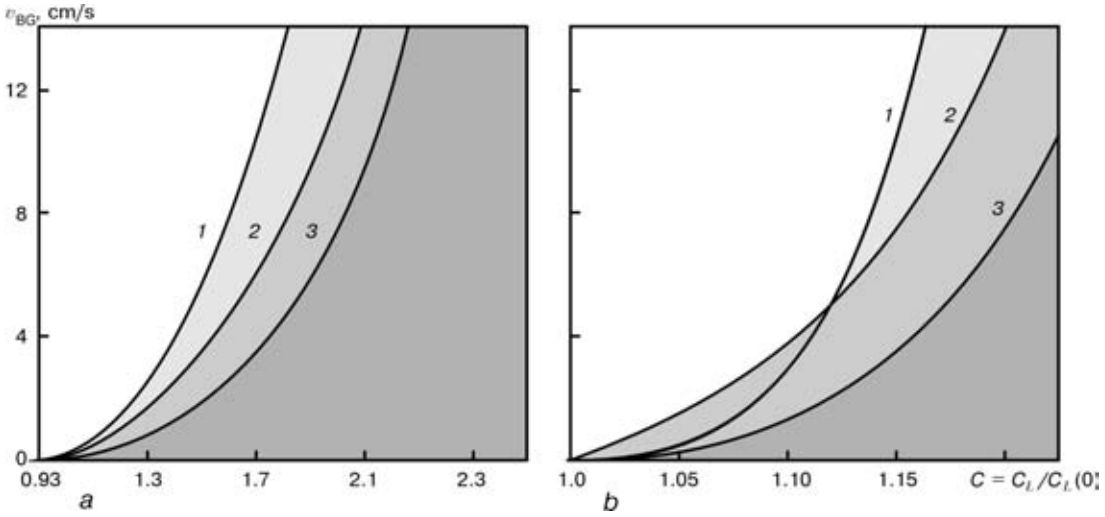

Figure 15. Dependence of rate of hydrogen $2a$ diameter bubble growth v_{BG} on hydrogen concentration C in molten metal: *a* — 1.3 < C < 2.5 — high oversaturations; *b* — 1.00 < C < 1.25 — small oversaturations; *1* — $2a$ = 0.5; *2* — 1.0; *3* — 2.0 mm

Table 1. Change of relative degree of oversaturation of intercrystalline liquid C', critical radius of gas bubble a_{cr} and transverse sizes of liquid phase ξ in length of a two-phase zone

Distance from axes of first order, mm	$C' = C_L/S_L$	a_{cr}, *mm*	ξ
0.8	1.156	0.104	0.014
0.9	1.225	0.068	0.009
1.1	1.300	0.050	0.008
1.4	1.375	0.038	0.005
1.7	1.450	0.032	0.004

crystallization and growth of gas bubbles were used to analyze the causes of formation of pores in welds [10].

Two cases were considered.

1. Concentration of dissolved gas is within the interval of its solubility in solid S_S and liquid S_L metal:

$$S_S < C_L(0) \le S_L. \quad (4)$$

2. Concentration of dissolved gas exceeds the limit of its solubility in molten metal at the same conditions:

$$C_L(0) > S_L. \quad (5)$$

Case 1. At a plane front of crystallization the distribution of dissolved gas ahead of the front is described by the formula

$$C_L(x) = C_L(0)\left(1 + \frac{1-k}{k}\exp\left(-\frac{v_{cryst}x}{D_L}\right)\right), \quad (6)$$

where $C_L = C_L(x)$ is the current gas concentration in weld pool; k is the coefficient of hydrogen distribution equal to ratio S_S/S_L.

In accordance with the formula (6) the gas concentration is changed from $C_L(0)/k$ (maximum directly at the crystallization front) to $C_L(0)$ (at some distance from it). In the region of a concentration packing which is adjacent to the phase interface the concentration of the dissolved gas ecxeeds its equilibrium solubility S_L in molten metal, i.e.

$$S_S < C_L < C_L(0)/k. \quad (7)$$

The molten metal in the second region is depleted as regards to S_L. In the oversaturated region the formation of gas bubbles and their growth are possible (Figure 14, *a*). The latter can occur also in case when the part of its surface covers the depleted region. The bubble growth is interrupted if the area of its surface, which covers the depleted region, becomes larger than the area of the bubble surface in an enriched layer.

Assuming $x = a_{st}$, $C_L(x) = S_L$ in equation (6) it is possible to determine a radius of bubble a_{st}, at which its growth is interrupted. Figure 14, *b* gives the results of calculation a_{st} depending on the hydrogen concentration and rate of crystallization.

At the moment of bubble growth interruption the front of crystallization «by passes» the bubble and as if fixes it in the solidified metal. Results of calculation showed that the increase in crystallization rate leads to the decrease in thickness of the diffusion boundary layer. In addition, the bubble radius should be reduced to the value of the smallest critical radius of the nucleus. In this case the formed bubble nucleus is dissolved.

Thus, with increase in welding speed the probability of pore formation in the weld pool near the fusion line is decreased, if the concentration of the dissolved gas in the weld pool $C_L(0)$ is in the range of $S_S < C_L(0) \le S_L$.

If the rate of crystallization and bubble growth have close values, then the pores of an elongated shape are formed. The gas enter into these pores can occur not only from the side of the molten metal, but also from the side of the solidified metal, because with the decrease in temperature an oversaturated solution of gas is formed in the solid metal and, in accordance with laws of thermodynamics, the conditions for gas transfer from the solution to the pores are created.

In transition of the crystallization front from plane to cellular-dendritic, the structure of the diffusion boundary layer is changed. At temperature above the liquidus temperature the oversaturation of the molten metal with hydrogen is not occurred.

At hydrogen concentration $C_L(0)$ in the weld pool in the range of $S_S < C_L(0) \le S_L$ the gas bubble nucleation ahead of the crystallization front (more exactly, ahead of growing cells) is improbable. At cellular and dendritic front of crystallization the origin of gas bubble nuclei capable to the further growth is possible only in oversaturated volumes of the intercrystalline liquid.

Calculations proved that at cooling rates typical of arc welding, the critical radius of the nuclei bubble radius is occurred to be larger than the transverse sizes of the liquid phase (Table 1). Therefore, the growth of gas bubbles in intercrystalline volumes of

Table 2. Content of gases in metal in welding with different types of flux-cored wires and presence of pores in weld

Type of wire core	*Welding speed, m/h*	*Concentration of* $[H]_{diff}$, $cm^3/100\ g$	*Mass share of gases in metal, %*		*Presence of pores*
			N	*O*	
Carbonate-fluorite	16	13.0	0.038	0.054	Yes
	30	14.1	0.032	0.027	No
Rutile-organic	12	26.8	0.021	0.080	Same
	30	27.1	0.022	0.090	Yes

liquid is impossible, and all the gas from the weld pool is transferred into the solidified metal with the formation of the oversaturated solid solution. The calculation experiment gives an opportunity to understand the physical nature of the process of weld metal oversaturation with hydrogen which was observed earlier in experiments [11].

Case 2. Concentration of the dissolved gas exceeds the limit of its solubility in the molten metal — $C_L(0) > S_L$. The rate of growth of gas bubbles near the fusion line at the plane front of crystallization is much higher than the rate of the crystallization. This is contributed by the higher degree of oversaturation of molten metal ahead of crystallization front as compared with the rest volume of molten metal. For example, for bubbles, growing directly at the fusion line the relative degree of hydrogen oversaturation at the crystallization front is 2.2 cm/s, while the rate of the bubble growth exceeds 12 cm/s (Figure 15, *a*).

In this case the nucleation and growth of gas bubbles in the weld pool volume is also possible.

At small gas oversaturation in the weld pool the conditions for formation of pores at cellular and dendritic nature of crystallization may occur. This is possible in case if the rate of crystallization is higher than that of growth of the gas bubbles (Figure 15, *b*). With increase in welding speed the probability of pores formation in weld axis is increased. And vice versa, the increase in oversaturation degree leads to the acceleration of growth of bubbles, i.e. promotes the decrease in probability of porosity formation.

Conceptions about mechanism of pore formation, formulated on the basis of the physical model and calculation experiments, were tested experimentally in welding with two types of self-shielding flux-cored wires. The experimental data obtained have a good correlation with calculated data (Table 2). As is seen from the Table the pore formation is determined by two factors, such as content of gases in the weld pool and rate of its crystallization.

CONCLUSIONS

1. Modelling of complex processes proceeding in welding metals should be based on fundamental knowledge in the field of thermodynamics, kinetics of metallurgical processes, metal physics, etc.

2. Modelling is rational, in particular for study of the processes, whose direct experimental investigation using the physical-chemical methods is difficult at present. However, the best results are provided by modelling in combination with experimental investigations.

3. The use of advanced computer engineering makes it possible to construct the dynamic three-dimensional models and to provide more profound knowledge with their help about the welding processes.

1. Pokhodnya, I.K. (1972) *Gases in welds*. Moscow: Mashinostroenie.
2. Pokhodnya, I.K. (1997) Hydrogen behaviour in welded joints. In: *Proc. of Joint Seminar on Hydrogen Management in Steel Weldments*, Australia, DSTO and WTIA.
3. Makhnenko, V.I. (2000) Computer modelling of welding processes. In: *Advanced materials science: 21st century*. Ed. by I.K. Pokhodnya. Cambridge: Cambridge Int. Sci. Publ.
4. Frumin, I.I. (1961) *Automatic electric arc surfacing*. Kharkov: Metallurgizdat.
5. Lakomsky, V.I. (1962) Solubility of hydrogen in liquid iron up to boiling temperature. *Doklady AN SSSR*, **3**, 628–629.
6. Pokhodnya, I.K., Tsybulko, I.I., Orlov, L.N. (1993) Influence of flux composition on hydrogen content in CO_2 welding liquid metal. *Avtomatich. Svarka*, **11**, 3–5.
7. Pokhodnya, I.K., Paltsevich, A.P., Golovko, V.V. et al. (1998) Technology and metallurgy methods for decreasing diffusible hydrogen. *IIW Doc. II-1335–98*.
8. Gorpenyuk, V.N., Taraborkin, L.A., Makarenko, V.D. et al. (1983) Estimation of thermodynamic probability of formation of titanium and silicon tetrafluorides in basic electrode slags. In: *Proc. of All-Union Conf. on Welding Consumables*, Cherepovets, Oct. 10–11, 1983. Kyiv: PWI.
9. Pokhodnya, I.K., Shvachko, V.I., Utkin, S.V. (1998) Calculated estimation of hydrogen behaviour in arc charge. *Avtomatich. Svarka*, **9**, 4–11.
10. Pokhodnya, I.K., Demchenko, V.F., Demchenko, L.I. (1979) *Mathematical modelling of gases behaviour in welds*. Kyiv: Naukova Dumka.
11. Pokhodnya, I.K., Paltsevich, A.P., Yavdoshchin, I.R. et al. (1975) Influence of welding condition and baking temperature of rutile electrodes on weld porosity. *Avtomatich. Svarka*, **8**, 34–38.
12. Pokhodnya, I.K., Demchenko, L.I., Paltsevich, A.P. et al. (1976) Kinetics of hydrogen diffusion redistribution between weld and base metal in arc welding. *Ibid.*, **8**, 1–5.
13. Shlepakov, V.N., Suprun, S.A., Kotelchuk, A.S. (1986) Kinetics of gassing in flux-cored wire welding. In: *Inform. Materials: CMEA. Coord. Center on Problem «Development of scient. fundamentals and new technol. processes of welding, surfacing and thermal cutting of different materials and alloys to produce the welded structures and to create the efficient welding consumables and equipment»*. Issue 1. Kyiv: Naukova Dumka.
14. Kotelchuk, A.S. (2001) Kinetics of thermal destruction of powder materials and their mixtures. In: *Arc welding. Materials on the threshold of the 21st century*. Proc. of 2nd Int. Conf. on Welding Consumables of CMEA Countries, Oryol, June 4–8, 2001.

POWER SYSTEM OF FLASH-BUTT WELDING MACHINES WITH A TRANSISTOR INVERTER

V.K. LEBEDEV and **A.A. PISMENNY**
The E.O. Paton Electric Welding Institute, NASU, Kyiv, Ukraine

The paper gives analysis and comparison of various power systems of flash-butt welding machines by their power characteristics, namely single-phase systems of industrial frequency and three-phase systems with converters of frequency and phase number (with thyristor inverters and bipolar transistors). It is shown that a system with an inverter converter, using power transistors, has an advantage over the system with a thyristor converter in terms of distribution of currents in the mains phases, as power consumer. High power factor, close weight and dimensional indices of the lower-frequency transformer to those of commercial-frequency transformer and absence of powerful rectifier diodes in the secondary circuit are indicative of the good prospects for application of the transistor inverter with the set frequency of 30 Hz.

Key words: *flash-butt welding, symmetrical power system, transistor inverter, power factor*

Advance of power converters enabled development of new types of power systems for high-capacity flash-butt welding machines. The currently used machines with the power system, consisting of a three-phase rectifier, higher-frequency inverter and transformer with a rectifier in the secondary circuit, have a low efficiency. Power losses in the valves are close to, and in some cases are higher than the power, consumed in formation of a welded joint. The only method to increase the efficiency is elimination of rectifiers in the machine secondary circuit, i.e. transition to alternating current. Such machines were produced many years ago, and they operated at a frequency of about 5 Hz. Such a low frequency was selected to decrease the machine impedance, and, hence, also its power, but in this case the transformer weight increased many times [1]. Machines with such transformers have found a limited application and are not currently used. The frequency could be increased, but in this case, the load on the mains phases becomes the more non-uniform, the closer is the converted frequency to the mains frequency. Frequency increase requires increasing the power.

Work [2] describes a new power system, close to the one, mentioned above, but differing in that a uniform loading of the phases is achieved only during three half-cycles of converted (low) frequency. The system cannot be regarded as symmetrical in the full sense of this term. The instant power does not remain constant at any moment (main feature of a symmetrical system), but the currents in the phases are equalized within a short time period, and in these terms the system is symmetrical. A system, considered in [2], is not ideal, but it is superior in many respects to those currently used.

A similar system is considered here, but it has a transistor inverter (Figure 1). Transistors of the inverter key permit switching to be performed at any moment of time. In this case switching is performed after a time, multiple of 1/3 of the mains half-cycle. Depending on the number of «sinusoid crowns», the presented system can be set to the following frequencies:

$$f = \frac{3}{0.02n}.$$

Let us consider a system with the set frequency of 30 Hz ($n = 5$). Voltage and current plots are shown in Figure 2. Let us compare the main indices of this power system to those of widely used single- and three-phase systems, fitted with a thyristor inverter [2]. Let us represent the equivalent circuit of the machine (including the transformer, secondary circuit and welding contact) as resistance r and reactance (inductance) X, connected in series. In this case

$$i = C \exp\left(-\frac{t}{\tau}\right) + \frac{U}{r},$$

where i is the current; $U = 1.35U_1$ is the active value at converter input; $\tau = X/\omega r = \text{tg}\,\varphi/\omega$ is the time constant; φ is the phase shift of current curve relative to voltage curve; t is the time; U_1 is the active value of linear voltage; $C = -2\frac{U}{r}\left(1 + \exp\left(-\frac{t_p}{\tau}\right)\right)$ is the

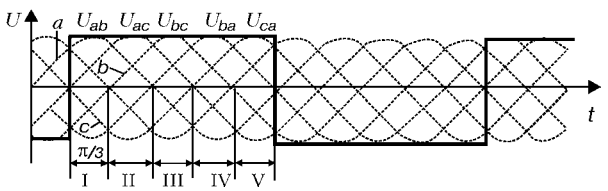

Figure 1. Power system of a flash-butt welding machine with a transistor inverter (for description of sections I–V see the text)

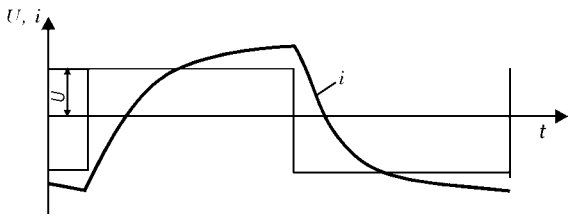

Figure 2. Graphs of voltage and current at converter output

free component of current; $\omega = 2\pi f = 314$ s^{-1} is the angular frequency; $t_p = T/2$ is half of the cycle of converted frequency.

High-capacity flash-butt welding machines for joining large-sized parts with great thicknesses have a significant inductance X, much higher than ohmic resistance r. Therefore, we will take U, X as basic values, and we will further move from absolute time to the time, calculated by the angle of mains voltage. We further assume that in the considered half-cycle of converted frequency (30 Hz) the current flows as follows (Figure 1): in phase a — sections I, II, IV and V, each of $\pi/3$ duration; in b — I, III and IV; in c — II, III and V. Let us denote the active values of currents, expressed in relative units, which are reduced to the primary circuit, as follows: welding — ie and phase — ia, ib, ic. Let us conduct integration within one half-cycle of low frequency (0–$5\pi/3$). Calculation results are presented in tabulated form and Figure 3.

As is seen from the Table, phase currents have different values, but during 1.5 cycle their value is averaged and becomes equal to

$$ij = \sqrt{[(ia^2 + ib^2 + ic^2)/3]}.$$

Figure 3 shows for comparison the same values of phase currents for one half-cycle of a low frequency, taken from [2]. As follows from the compared diagrams, the advantages of the transistor converter in terms of distribution of currents by phases are indubitable. Let us determine the power factor of a three-phase converter and compare it with the power factor of a system with single-phase power. Power factor

$$K = \frac{P}{S} = 0.955\,\frac{ie}{\text{tg}\,\varphi},\quad P = \left(\frac{U}{X}\right)^2 ie^2 r,\quad S = 3U_{\text{av}}\,\frac{U}{X}\,ij,$$

where P, S are the active and apparent power; $U_{\text{av}} = \dfrac{U}{1.73 \cdot 1.35}$.

Dependence of power factor of a converter with three-phase power on power factor of a system with single-phase power (Figure 4) confirms the advantages of a system with the inverter, compared to the simplest single-phase system at unchanged load for both the systems. A transistor inverter has a somewhat higher power factor than does the thyristor inverter. The ratio of phase current of three-phase mains, powering a transistor inverter through a rectifier, to the converted current is the same, as when a regular bridge

Relative value of welding and phase currents depending on tg φ

tg φ	*ia*	*ib*	*ic*	*ie*	*ij*
0.5	0.45	0.409	0.360	0.450	0.367
1.0	0.69	0.601	0.636	0.788	0.644
1.5	0.95	0.799	0.895	1.018	0.831
2.0	1.25	1.045	1.171	1.165	0.951

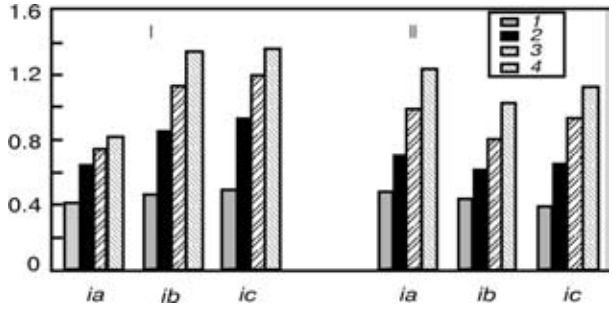

Figure 3. Comparison of phase currents of thyristor (I) and transistor (II) systems: *1* — tg φ = 0.5; *2* — 1; *3* — 1.5; *4* — 2

rectifier is used and it is equal to 0.816, irrespective of the power factor.

Frequency lowering at a specified value of welding current increases the number of flux linkages in the transformer. At the frequency of 50 Hz

$$U_{m1} \sin \omega t = \frac{d\psi_{(1)}}{dt},$$

whence

$$\psi_{(1)} = \frac{\sqrt{2}\,U_{(1)}}{\omega},$$

where U_{m1} is the amplitude value of voltage, applied to the transformer primary winding; $U_{(1)}$ is the active value of primary voltage; $\psi_{(1)}$ is the flux linkage in a commercial-frequency transformer.

In a three-phase system with an inverter

$$\psi = \int U dt = Ut + C.$$

At $t = 0$

$$\psi = Ut - \psi_{(3)} = -\psi_{(3)},$$

where $\psi_{(3)}$ is the flux linkage in the transformer, designed for 30 Hz frequency.

In a low-frequency half-cycle $T/2$

$$\psi_{(3)} = U\,\frac{T}{2} - \psi_{(3)},$$

whence

$$\psi_{(3)} = U\,\frac{T}{4} = \frac{U}{4f} = \frac{U}{120},$$

where $U = U_{(1)}\,1.35/\sqrt{2}$.

Ratio of flux linkages is

$$\frac{\psi_{(1)}}{\psi_{(3)}} = \frac{120\sqrt{2}\,U_{(1)}}{314U}.$$

From the condition of equality of welding currents we find

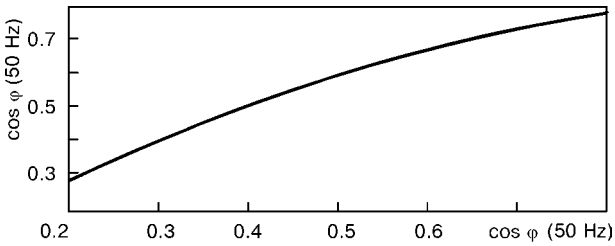

Figure 4. Dependence of power factor of a three-phase system of power conversion on the power factor of a welding circuit at commercial frequency

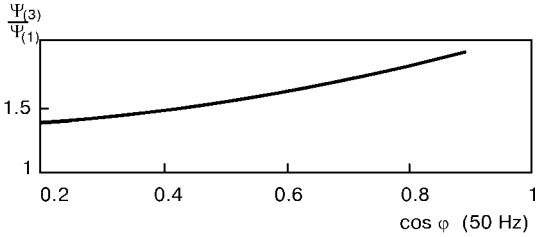

Figure 5. Dependence of the ratio of maximum number of flux linkages in a transformer at 30 Hz frequency to the maximum number of flux linkages of a transformer at 50 Hz on the power factor of welding circuit at 50 Hz frequency

$$\frac{U_{(1)}}{Z} = \frac{U}{X} ie,$$

where Z is the load circuit impedance.

Using the latter relationship, we obtain the following expression for the ratio of flux linkages:

$$\frac{\Psi_{(1)}}{\Psi_{(3)}} = 1.77 \frac{\sin \varphi}{ie}.$$

At a high power factor the flux linkage in the transformer, designed for a lower frequency, is greater than in a commercial-frequency transformer (Figure 5). At a relatively low power factor, the difference of flux linkage numbers is not so great. Therefore, dimensions of a lower-frequency transformer are close to those of a commercial-frequency transformer, if they are designed for the same welding current and are connected to a load with a relatively low power factor.

The considered transistor system has an advantage over the 30 Hz low-frequency thyristor system due to a higher quality of energy distribution between the mains phases.

The given data are indicative of the good prospects for application of a system of power conversion with a transistor inverter, set up for 30 Hz frequency, in medium and high capacity flash-butt welding machines.

1. Paton, B.E., Lebedev, V.K. (1969) *Flash-butt welding electric equipment. Elements of theory*. Moscow: Mashinostroenie.
2. Lebedev, V.K., Pismenny, A.A. (1998) Improvements to the power supply systems of flash-butt welding machines. In: *Welding and related technologies for the 21st century*. Harwood A.P.

COMPUTER SYSTEM FOR SELECTION OF WELDING CONSUMABLES FOR ARC WELDING OF STRUCTURAL STEELS

V.I. MAKHNENKO[1], **T.V. KOROLYOVA**[1] and **I.G. LAVRINETS**[2]
[1]The E.O. Paton Electric Welding Institute, NASU, Kyiv, Ukraine
[2]Research and Production Company «KORBA», Kyiv, Ukraine

Structure of the computer system developed by the authors for rational selection of consumables for electric arc welding of structural steels is described. The system is based on mathematical modelling of physical-metallurgical phenomena occurring during arc welding using data provided by manufacturers of welding consumables on chemical composition of deposited metal, welding parameters and conditions, as well as deposition efficiency.

Key words: *arc welding, welded joint, heat-affected zone, chemical composition, microstructure, mechanical properties, welding consumables, computer modelling*

Introduction. Traditionally, selection of a rational variant of consumables for arc welding of modern structural steels involves a large number of experiments to generate comparative results on certain parameters, such as conditions of formation and chemical composition of weld metal or penetration zone (PZ), microstructure of PZ and HAZ, susceptibility to hot and cold cracking, standard mechanical properties (hardness, yield stress, tensile strength, elongation or reduction in area, impact toughness) in different regions of a welded joint, as well as special functional properties (long-time strength at corresponding temperatures, corrosion resistance etc.). All this requires that corresponding tests of each of the alternative variants of welding consumables and conditions be conducted for a specific base metal. Given that welding electrodes, solid and flux-cored wires, fluxes and shielding gases for arc welding of structural steels are available in large numbers and wide ranges, the substantiated selection of a rational variant in a purely experimental way requires either large experience or numerous experiments.

Application of the system and information obtained. Computer system developed by the authors is intended primarily to reduce the number of experiments by using mathematical modelling tools and corresponding software to generate information required for a substantiated selection of welding consumables, as well as arc welding conditions and parameters. The source data used in the system include specification data provided by manufacturing companies for weld-

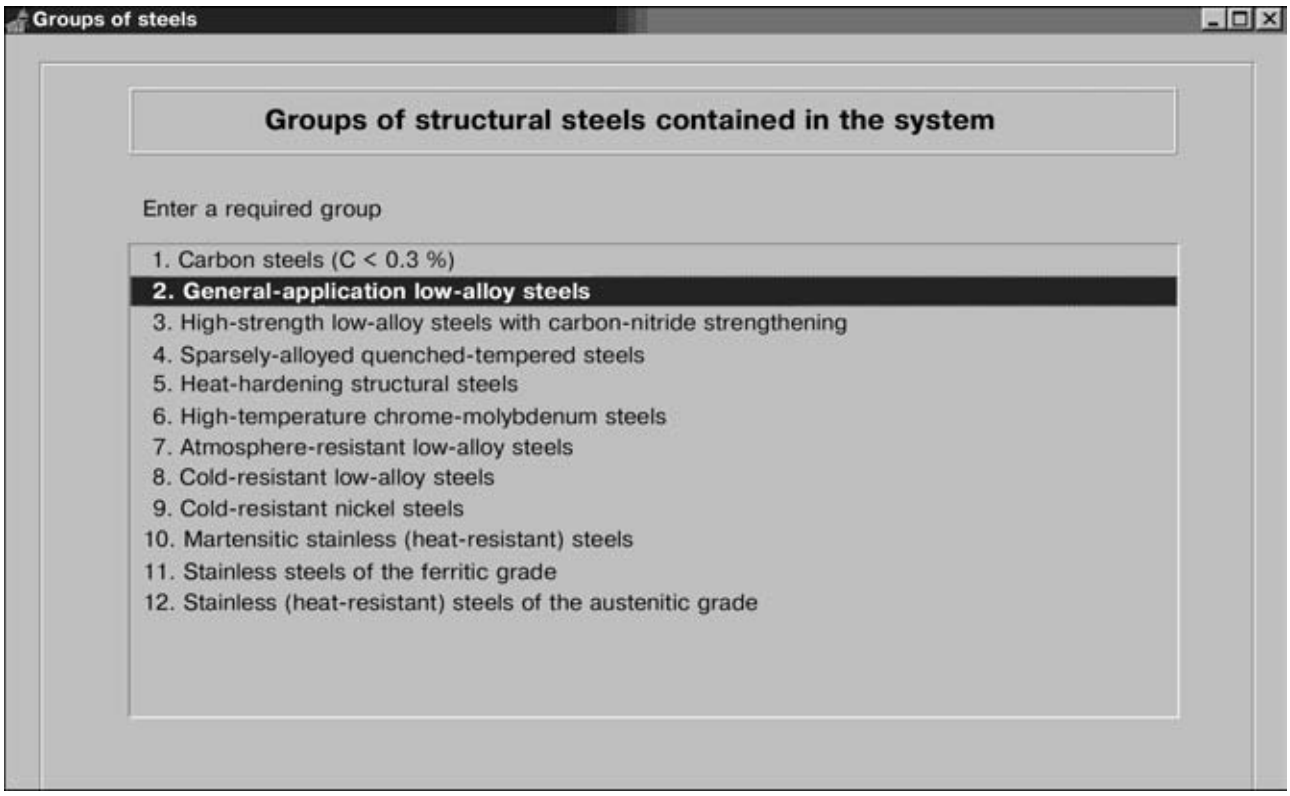

Figure 1. List of groups of structural steels offered by the system to a user

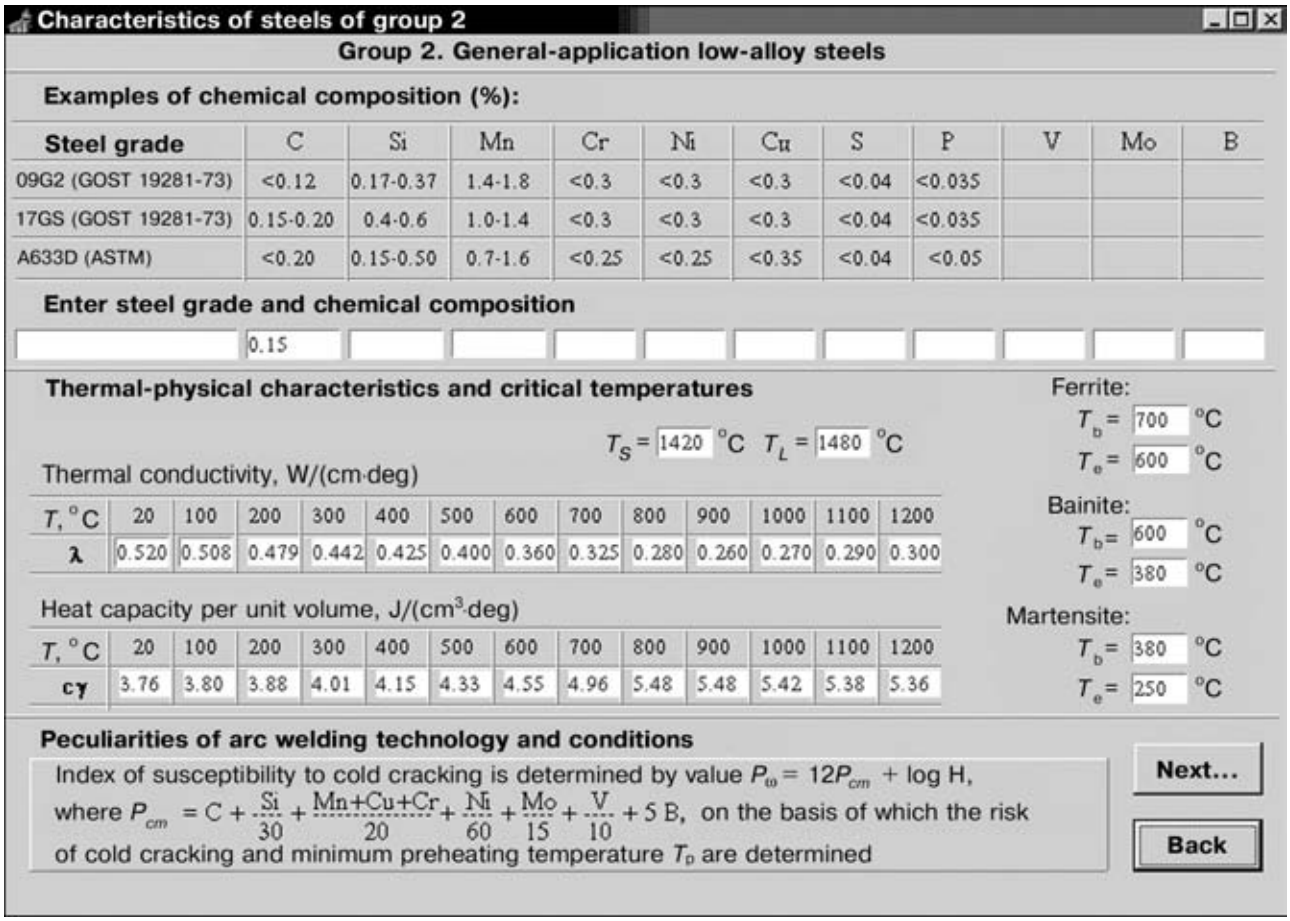

Figure 2. Example of setting of data for selection of a specific group of steels

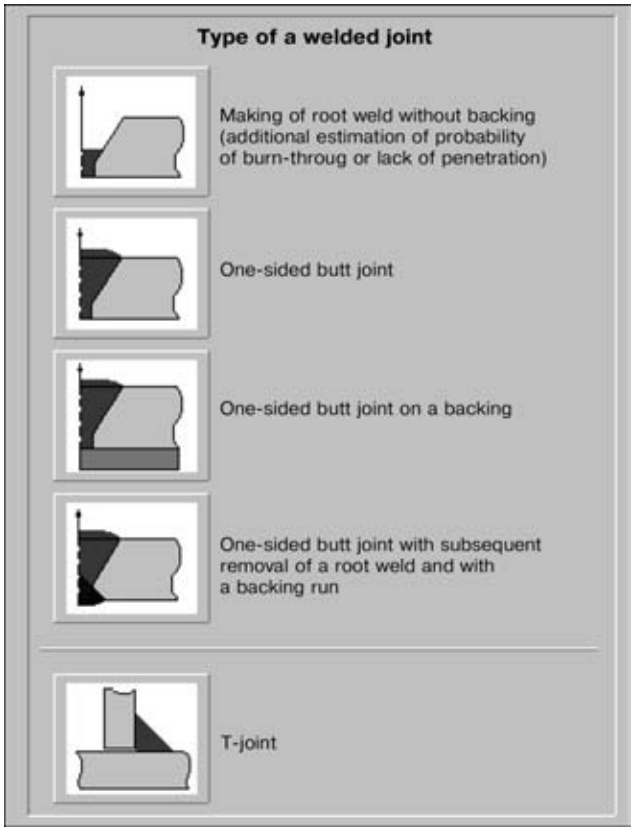

Figure 3. Types of welded joints offered to a user

ing consumables recommended for arc welding of a given type of structural steels, arc welding conditions, deposition efficiencies and chemical composition of deposited metal. These data, as well as an indication of the type of a structural steel to be welded (base metal) and its chemical composition, are entered into the system by a user. As a result, the system gives the user the following information for each alternative variant:

- size and shape of PZ for the root weld and subsequent passes (conditions of weld formation, risk of a burn-through etc.);
- chemical composition of the PZ metal;

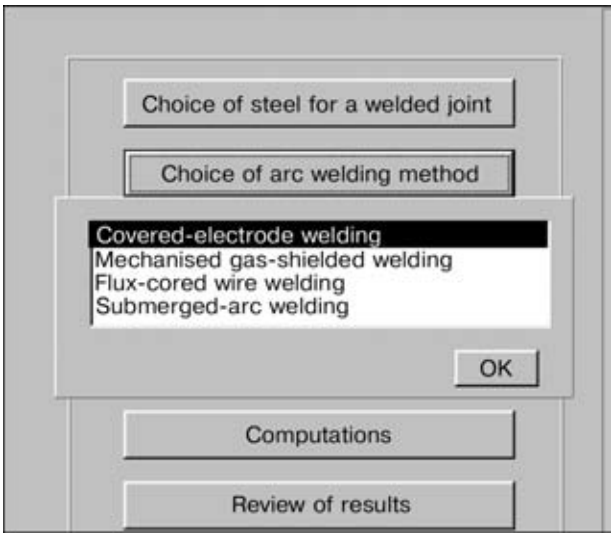

Figure 4. Arc welding methods offered to a user

- microstructural composition of the PZ and HAZ metals;
- mechanical properties (hardness, tensile strength, yield stress, elongation and reduction in area, impact toughness (KCV) at temperatures of –30 – –70 °C in PZ and HAZ);
- risk of hot and cold cracking.

Brief description of the system. Operation of the system begins from setting of the data on a base metal for the arc welding of which the consumables are selected. The system offers a user 12 groups of structural steels, and the user has to choose one of them where his base metal belongs to (Figure 1). The user, if he wants, may have a more detailed information on characteristics of steel of a specific group (Figure 2), examples of chemical composition, thermal-physical properties and peculiarities of arc welding of this steel. If the user finds the group chosen suitable, he should enter the data on chemical composition of the steel used (Figure 2).

The next step of operation of the system is associated with specifying the data on the type of a welded joint. The system offers the user several types of welded joints with butt welds and a T-joint with a fillet weld (Figure 3). The option is to use one- or multi-pass (in layers or with «stringer» welds) welding. The system automatically chooses the number of passes and arrangement of beads of the «stringer» welds. Also, it is possible to make only one root weld. For all the versions of butt joints (Figure 3) the problem of the risk of a burn-through is solved for making the root weld without backing on the basis of a balance of forces acting on the molten metal volume (surface tension, arc pressure, gravity).

The user should indicate the arc welding method (Figure 4) and choose specific variants of welding consumables by entering the corresponding data (type is shown in Figure 5) on chemical composition of just the metal being deposited, welding parameters and deposition efficiency (according to the manufacturer's specifications or on the basis of available experience).

Using the data entered, the system performs a set of operations associated with selection of the welding speed on the basis of limitations set with respect to thickness of individual layers (or cross sections of the «stringer» welds), then it computes temperature fields in a cross section of the weld for each pass starting from the root weld. The field of maximum temperatures is determined. Then, on this basis, the system estimates volumes belonging to PZ and HAZ. For this the system uses source data for the base metal with respect to melting temperatures T_{melt} and A_{c_3} (see Figure 2), as well as corresponding thermal-physical properties.

Mean chemical composition of the PZ metal is determined for each pass on the basis of knowledge of size and chemistry of regions to be melted, as well as amount and composition of a filler metal to be deposited.

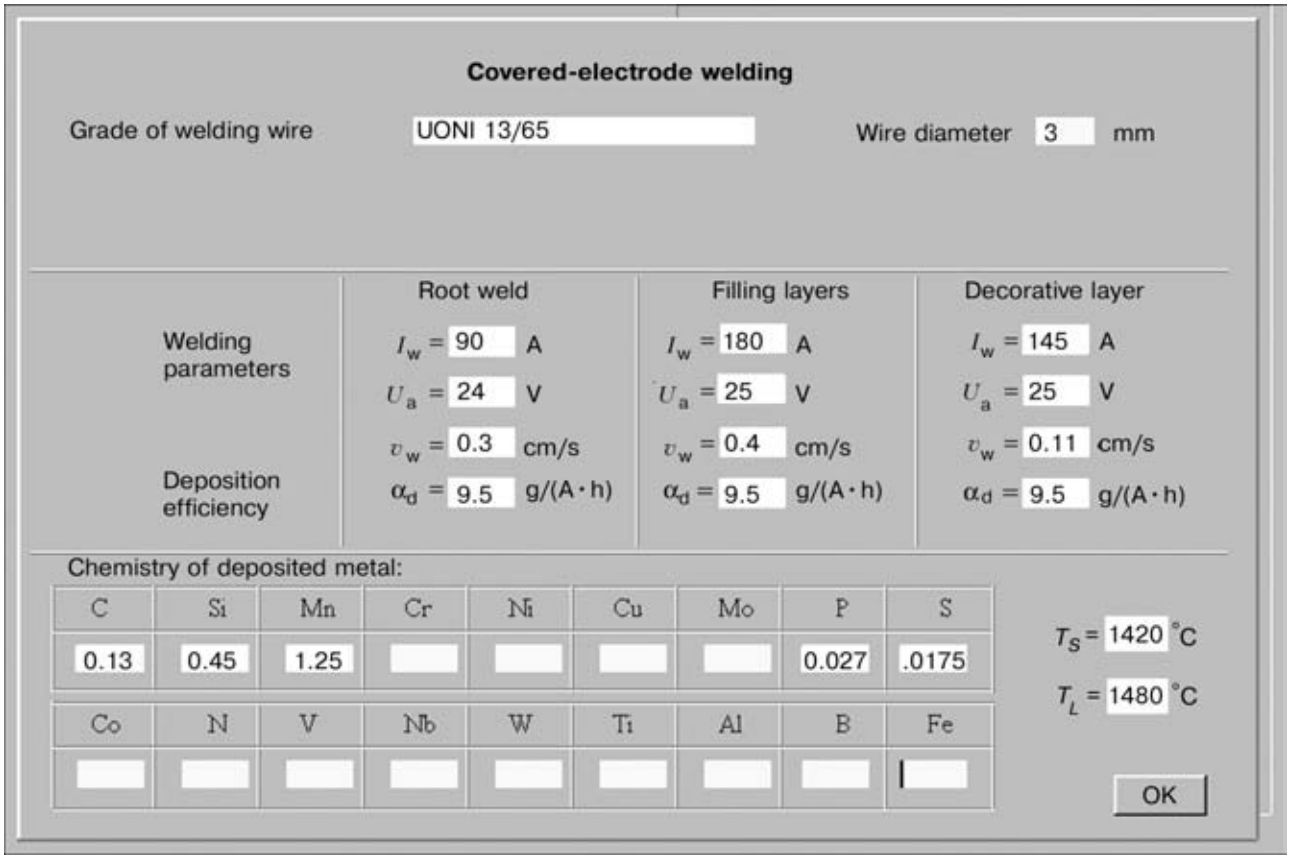

Figure 5. Example of entering data on welding conditions and chemical composition of deposited metal

Belonging of the PZ metal to a corresponding grouping of structural steels is determined from chemical composition of this zone in terms of estimation of microstructural state after cooling.

The system contains two groupings of steels (see Figure 1). The first includes structural carbon and low-alloy steels (groups 1–8), the microstructure of which is determined on the basis of the corresponding TTT diagrams. The second grouping of structural steels includes alloyed steels (groups 9–12), the microstructure of which is determined by the Schaeffler diagram (or its modifications [1]). For convenience, the system uses parametrical equations [2], allowing computation of an expected microstructure to be performed at each point of PZ and HAZ on the basis of knowledge of chemical composition and thermal cycle parameters. It is assumed that re-heating above A_{c_3} favours formation of a new microstructure on the basis of a new chemical composition and new thermal cycle parameters. Re-heating below A_{c_3} does not change microstructure, although it leads to a change in mechanical properties by the short-time tempering mechanism.

An important step of operation of the system is computation of mechanical properties at different points of PZ and HAZ. It is made on the basis of knowledge of microstructures and chemical composition. The following representation is used for all mechanical properties $X = \{HV, \sigma_t, \sigma_{0.2}, \delta_5$ and $\psi\}$:

$$X = \sum x_i V_i \quad (i = a, f, p, b, m), \qquad (1)$$

where a is austenite, f is ferrite, p is pearlite, b is bainite, m is martensite, and V_i is the mass fraction of the i-th microstructure at a given point. Regression equations are used for x_i, relating these values to chemical composition of a given group of steels [2]. For Charpy impact toughness (KCV) the averaged representation (1) does not reflect peculiarities of behaviour of a material in such tests. For these purposes the system uses regression equations which relate KCV to chemical composition, $\Delta t_{8/5}$ and test temperature T_{test}. Naturally, the regression coefficients of such a relationship may greatly depend upon the group of a structural steel.

Another important element of operation of the system is estimation of the risk of violation of integrity of the PZ or HAZ metal caused by hot or cold cracks. For high-alloy steels of the second grouping it is more realistic to account for the risk of hot cracking. Susceptibility of the PZ metal to hot cracking is estimated here with respect to Cr^{eq}/Ni^{eq}, where Cr^{eq} is the chromium equivalent and Ni^{eq} is the nickel equivalent in chemical composition of PZ [1]. Susceptibility to cold cracking and recommended preheating temperatures for steels of groups 1–4, 7 and 8 are determined by index

$$P\omega = 12P_{cm} + \log H \qquad (2)$$

and the degree of restraint of a weldment, where P_{cm} is the carbon equivalent according to [1] and H is the diffusible hydrogen content of the HAZ. For steels

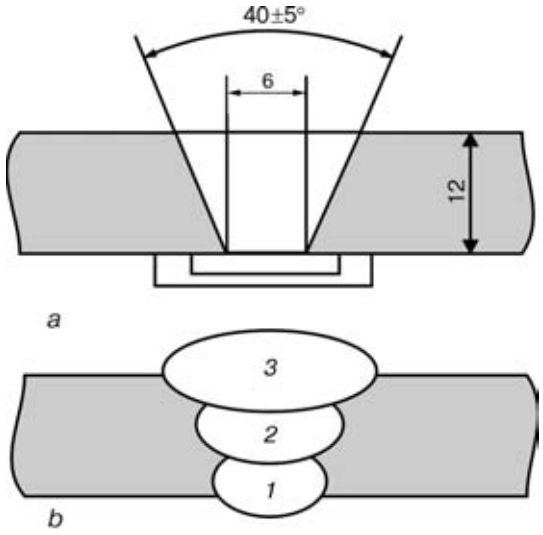

Figure 6. Schematic of groove preparation (*a*) and filling the layers (*b*)

of groups 5 and 6 the minimum preheating temperature is indicated individually.

Application examples. Consider two variants of welding of a one-sided butt joint in plates of shipbuilding steel DH32 (0.18C–1.3Mn–0.4Si–0.3Ni–0.01Al), 12 mm thick, in flat position on a ceramic backing (Figure 6, *a*); P_{cm} = 0.2633. No preheating is required at a diffusible hydrogen content of less than 3 $cm^3/100$ g in the case of a rigid restraint and 10 $cm^3/100$ g in the case of welding in a free position.

The first variant is mechanised arc CO_2 welding using the ESAB wire OK-Tubrod 15.14 with a diameter of 1.2 mm. The second variant is welding using wire JS-10 (Italy) with a diameter of 1.2 mm in a mixture of 82 % Ar + 18 % CO_2.

Specification data on recommended welding parameters and chemical composition of the deposited metal (with no participation of the base metal) are given in Table 1.

Table 2 gives results of computation of parameters of the PZ formation (heat input q_i, cross section area F, chemical composition), while Figures 7–9 (see the inset in pages 16 and 17) show the computation data on microstructures and mechanical properties of PZ and HAZ. Comparison of the computation and experimental results is given in Table 3.

The authors had at their disposal the experimental data on hardness HV and fracture toughness KCV_{-20} of the PZ and HAZ metal obtained from using a standard welding procedure for samples of the given steel under conditions given in Table 1.

Table 3 shows a good agreement between the computation and experimental data on hardness and impact toughness for the weld metal, i.e. PZ. For the HAZ metal about 1 mm wide, the experimental data on KCV are rather sensitive to the notch position. With a precisely conducted experiment, they are usually lower than for PZ. The computation data in Table 3 do not contradict this statement.

The following conclusions can be made from comparing the computation results for the two variants. Variant No.1 makes it possible to produce the PZ metal with a lower carbon content and, accordingly, with a lower P_{cm} = 0.132–0.162 (for variant No.2 in PZ P_{cm} = 0.201–0.212, which is still lower than in

Table 1. Source data for two variants of welding of a joint shown in Figure 6, *b*

Variant No.	*Wire grade and chemistry of deposited metal*	*Welding parameters*											
		1st pass			*2nd pass*			*3rd pass*			*4th pass*		
		I_w, A	U_a, V	v_w, cm/s	I_w, A	U_a, V	v_w, cm/s	I_w, A	U_a, V	v_w, cm/s	I_w, A	U_a, V	v_w, cm/s
1	OK-Tubrod 15.14 0.05C–0.5Si–1.3Mn	170	21	0.25	205	24.5	0.20	205	24.5	0.32	–	–	–
2	JS-10 0.09C–0.5Si–1.5Mn	160	21	0.30	220	25.0	0.25	220	25.0	0.25	255	31	0.42

Note. Deposition efficiency α_d = 16 g/(A·h).

Table 2. Results of computation of parameters of PZ formation for variants No.1 and No.2 from Table 1

Variant No.	*Pass No.*	q_i, J/cm	F, mm	*Chemical composition, %*
1	1	9996	60	0.08C–1.3Mn–0.477Si–0.068Ni–0.003Al; P_{cm} = 0.162
	2	17787	80	0.059C–1.3Mn–0.493Si–0.021Ni–0.002Al; P_{cm} = 0.140
	3	10865	64	0.05C–1.3Mn–0.50Si–0.0Ni–0.001Al; P_{cm} = 0.132
	4	–	–	–
2	1	7910	47	0.013C–1.448Mn–0.77Si–0.077Ni–0.003Al; P_{cm} = 0.220
	2	15400	75	0.111C–1.453Mn–0.784Si–0.07Ni–0.002Al; P_{cm} = 0.200
	3	15400	79	0.113C–1.45Mn–0.77Si–0.076Ni–0.003Al; P_{cm} = 0.212
	4	13247	59	0.102C–1.52Mn–0.87Si–0.03Ni–0.001Al; P_{cm} = 0.207

the base metal), this leading to a lower content of quenching microstructures in PZ (for variant No.1 in Figure 7, *a–c,* microstructure in PZ is as follows: V_b = 0.40–0.65, V_m < 0.12, and balance is ferritic-pearlitic mixture; for variant No.2 (Figure 7, *d–f*) V_b = 0.40–0.45 and V_m < 0.25). A higher bainite content leads to higher strength properties. Yield stress $\sigma_{0.2}$ and tensile strength σ_t for variant No.1 (Figure 8, *c, b*) are almost equal in PZ: $\sigma_{0.2}$ = 380–440 MPa and σ_t = 540–720 MPa, while for variant No.2 (Figure 8, *g, f*) $\sigma_{0.2}$ = 420–500 MPa and σ_t = = 620–720 MPa.

Accordingly, variant No.1 has higher ductile properties in PZ: elongation δ = 18–26 % and reduction in area ψ = 44–52 % (Figure 8, *a, d*). For variant No.2 these characteristics in PZ are as follows: δ = = 16–22 % and ψ = 40–46 % (Figure 8, *e, h*). In the variants under consideration, impact toughness KCV_{-20} in PZ (Figure 9, *b, e*) is higher for variant No.1 (see Table 3).

Therefore, the use of the computation system provided in a sufficiently demonstrative information, on the basis of which it is possible to give a substantiated preference to variant No.1 in terms of ductility and impact toughness requirements, and to variant No.2 in terms of the $\sigma_{0.2}$ and σ_t values.

Table 3. Results of comparison of computation and experimental data

Value, zone of a joint	*Variant No.1*	*Variant No.2*
HV, PZ	200–220 / 170–200	195–208 / 180–220
HV, HAZ	198–230 / 200–240	196–220 / 220–240
KCV_{-20}, MJ/m^2, PZ	1.2–2.3 / 1.5–2.6	1.4–2.9 / 1.2–2.0
KCV_{-20}, MJ/m^2, HAZ	– / 1.2–1.5	– / 1.0–1.4

Note. Experimental data are given in the numerator and computation data are given in the denominator.

It follows from the above-said and the given computation data that the substantiated selection of welding consumables for arc welding of specific structural steels can be done using the offered computer system, leaving generation of data for a final decision to an experiment.

1. (1998) *Welding Handbook*. Vol. 4. Materials and applications. Part 2. 8th ed. AWS.
2. Kasatkin, O.G. (1990) *Mathematical modelling of «composition–properties» dependence of welded joints and making of design-experimental system for optimisation of main technological factors of low-alloy structural steel welding*. Syn. of Thesis for Dr. of Sci. Degree (Eng.). Kyiv.

STRUCTURAL TRANSFORMATIONS AND WELDABILITY OF HARDENING HIGH-STRENGTH STEEL 20KhN4FA

V.Yu. SKULSKY, A.K. TSARYUK, V.G. VASILIEV and **G.N. STRIZHIUS**
The E.O. Paton Electric Welding Institute, NASU, Kyiv, Ukraine

Transformation of austenite in steel 20KhN4FA (GOST 4543–71) under continuous cooling conditions has been studied. Hardening of steel to form fully martensitic structure takes place at cooling rates of more than 20 °C/s, while partially bainitic decomposition occurs at lower cooling rates. Preheating to a temperature of 250–300 °C leads to a dramatic increase in cold crack resistance, which seems to be associated with sufficient conditions ensured for the γ-bainite transformation to take place. The latter is accompanied by partial self-tempering and increase in ductility of the HAZ metal of a welded joint. Issues related to selection of the preheating temperature are also considered.

Key words: *arc welding, hardening steels, structural transformations, cold cracks, implant method, preheating*

20KhN4FA steel is used to manufacture critical items, operating under the conditions of higher loading, in particular at high (300–400 °C) temperatures [1, 2]. Alloying system and content of alloying elements influence the susceptibility of steel to formation of non-equilibrium strengthening (hardening) structures at cooling from the temperatures of austenite region, which allows achieving high indices of physico-mechanical properties at appropriate heat treatment modes. After hardening and low-temperature tempering the steel yield point may be up to 1200 MPa.

According to [1], 20KhN4FA steel is currently applied only as finished rolled, forged or machined products, and not as welded structures. Nonetheless, in individual cases, questions are sometimes raised about the possibility of using this steel, for instance, for sealing joints expanded by hot rolling in casing parts, operating at high pressures. However, data on weldability of this steel is practically absent in literature.

In welding of high-strength hardening steels the main problem is cold cracking. Cold cracks initiate and propagate in the sections of overheating of the HAZ metal, having the structure of coarse-needled martensite, formed during austenite transformation.

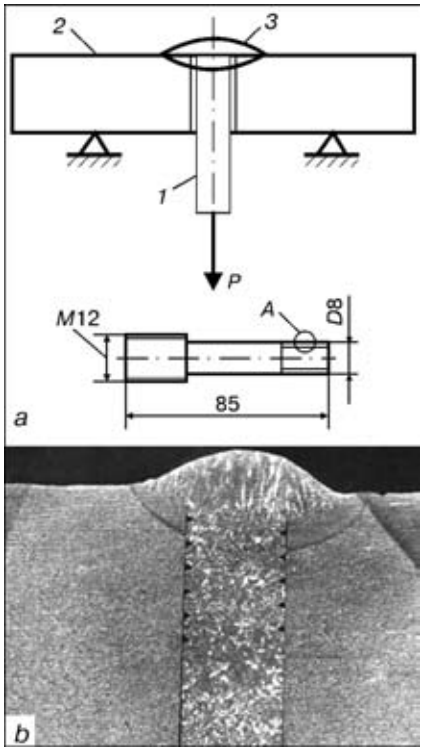

Figure 1. Schematic of testing by the implant method and appearance of the sample (*a*) and macrosection of the joint (*b*): *1* — sample; *2* — plate; *3* — weld (*P* — load)

It is believed, that welded joints of steel with more than 0.15 wt.% C and more than 3 wt.% of alloying elements are prone to initiation of this kind of defects to varying degrees [3].

Influence of steel composition on cold cracking susceptibility is usually assessed, using the calculation criterion — carbon equivalent C^{eq}. Various expressions are applied for its determination, in particular those, allowing for the dimensional factor (see for instance [3–5], etc.). Carbon equivalent was calculated, using the dependence, proposed by International Institute of Welding (IIW) [3]:

$$C^{eq} = C + \frac{Mn}{6} + \frac{Cr + Mo + V}{5} + \frac{Ni + Cu}{15} \quad (wt.\%). \quad (1)$$

For 20KhN4FA steel it is equal to 0.64–0.89 with the following content of alloying and impurity elements in it (to GOST 4543–71), wt.%: 0.17–0.24 C; 0.25–0.55 Mn; 0.17–0.37 Si; 0.7–1.1 Cr; 3.75–4.15 Ni; 0.10–0.18 V; ≤ 0.025 P; ≤ 0.025 S; ≤ 0.3 Cu. According to [3], steel with C^{eq} value higher than 0.42–0.45, should be classified in the group of difficult-to-weld materials, prone to formation of cold cracks.

It is known, that one of the main techniques, improving the crack resistance of hardening steel welded joints, is preheating and concurrent heating, which allows influencing the factors, promoting initiation of cold cracks, namely structural changes (which predetermine the proneness to brittle fracture), content of diffusible hydrogen and level of time and residual stresses. In this case, the data on kinetics of austenite transformation and features of phase formation under the conditions of different cooling rates allow selecting the thermal mode in welding.

The purpose of this study was determination of optimal preheating temperature in welding 20KhN4FA steel, providing welded joint resistance to cold cracks.

Commercial-grade steel 20KhN4FA in the form of a hot-formed pipe with 9 mm wall thickness was used as the base material for preparing samples. Test samples were cut along the pipe longitudinal axis. Features of phase transformation were revealed, using dylatometric studies [6], which are based on the phenomenon of change of material volume during polymorphous transformation. Determination of critical points A_{c_1} and A_{c_3} under the conditions of continuous cooling from 1300 °C was conducted in an argon-filled chamber. Rate of natural cooling was controlled by using samples with different cross-section. To determine temperatures, corresponding to points A_{c_1} and A_{c_3}, Shevenar dylatometer was used with simulation of furnace conditions in samples heating at the rate of 150 °C/h. Metallographic examination was conducted using light microscope «Neophot 32». Microstructure was revealed on polished sections by chemical etching in 2.5 % alcohol solution of nitric acid with addition of picric acid. Cold cracking susceptibility was evaluated by the implant method [7, 8] (called the method of inserts in local literature), using a special unit, developed at the PWI [9].

Testing by this method was conducted as follows. A cylindrical sample (insert) of steel 20KhN4FA with a spiral V-shaped thread was placed into a drilled hole in a plate, resting on supports and heated up to a certain temperature (Figure 1). Then, the sample-insert was welded to a plate by manual coated-electrode arc welding and was loaded up to specified magnitudes of inner stresses in the sample by applying a tensile force to its free end. The sample was fastened to a loading component through a threaded joint. In order to change the cooling conditions, preheating up to 150, 200, 250 and 300 °C was used. Loading of welded joints was performed 3–5 min after welding. Here the temperature in the welded joint area dropped approximately to the level of preheating temperature. Temperature was recorded with a welded to the sample chromel-alumel thermocouple, connected to KSP-4 potentiometer, calibrated for operation with this type of thermocouples. The supporting plate was of steel 20 of 20 mm thickness. The plate can be made of any steel. It is used for heat removal from the welding zone and sample heating in testing with preheating [7].

Loading stresses were established in a certain proportion to the yield point of the studied steel 20KhN4FA, for which purpose its strength properties were determined to GOST 6996–66: for smooth samples σ_t = 1018.7 MPa, $\sigma_{0.2}$ = 775 MPa; for samples with a circular notch σ_t = 1291.3 MPa (notch profile and dimensions are the same, as for testing by implant

method). Depending on the testing conditions, the sample either failed, or withstood the load without fracture. Proceeding from the authors' experimental data and experience of other researchers [8–10] it was established, that with the above method of testing the time to fracture may be from several minutes up to several hours (not more than 24 h). Therefore, unfailing samples were kept under the load for 24 h. This resulted in determination of maximal (critical) stresses, below which no fracture occurred within the above testing period. TMU-21U electrodes of 3 mm diameter were used for welding, which was performed in the following mode: welding current 120–130 A, arc voltage 24 V; welding speed 7.8–9.5 m/h. Diffusible hydrogen concentration in the deposited metal (alcohol test) was equal to 3.48 cm^3 per 100 g of metal.

Figure 2 shows a thermokinetic diagram of austenite decomposition, derived as a result of the conducted investigations. It does not have the section of equilibrium decomposition in the entire range of cooling rates, but has just the martensite or martensite-bainite regions. At cooling rate $w_{6/5} > 20$ °C/s in the temperature range of 600–500 °C 20KhN4FA steel forms martensite. At lower cooling rates, products of intermediate transformation appear in the steel structure in addition to martensite, the amount of these products growing with lowering of the cooling rate (Figure 3).

Results of dylatometric investigations demonstrate that under the conditions of delayed cooling ($w_{6/5} < 20$ °C/s) in welding of 20KhN4FA steel in the HAZ sections close to the fusion line, martensite formation will be accompanied by austenite transformations by the bainite mechanism with partial self-tempering of transformation products [11], characteristic of this process, and lowering of the level of metal strengthening, which should be favourable for the cold cracking resistance of welded joints.

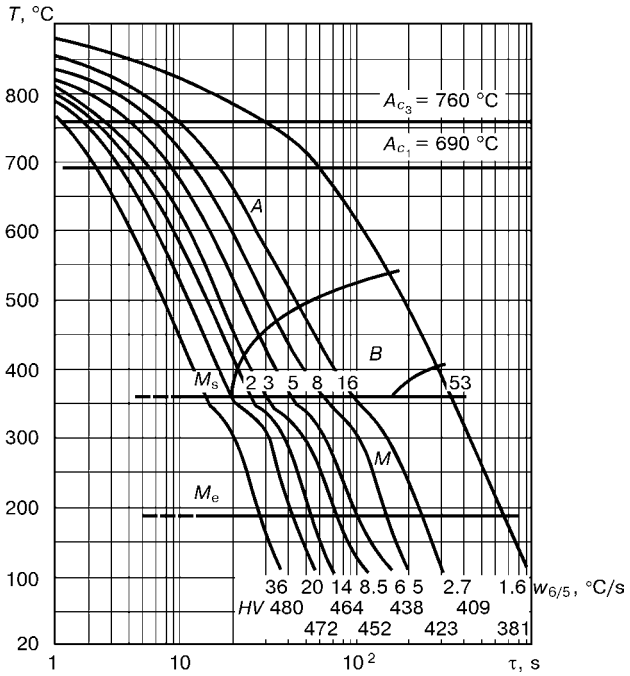

Figure 2. Thermokinetic diagram of austenite decomposition in 20KhN4FA steel: A — austenite; B — bainite; M — martensite; M_s and M_e — the start and end of martensite transformation, respectively

The data on the influence of preheating temperature T_p and level of tensile stresses on welded joint cracking resistance in testing by the implant method are given in Table 1. Obtained results showed that at $T_p > 200$ °C the level of tensile stresses, at which no fracture of welded joints occurs, is markedly increased. As was established during performance of experiments, during loading in the preheating temperature range of 250–300 °C the material being welded is capable of going through partial ductile deformation, whereas further on the susceptibility to crack initiation and delayed brittle fracture is not observed.

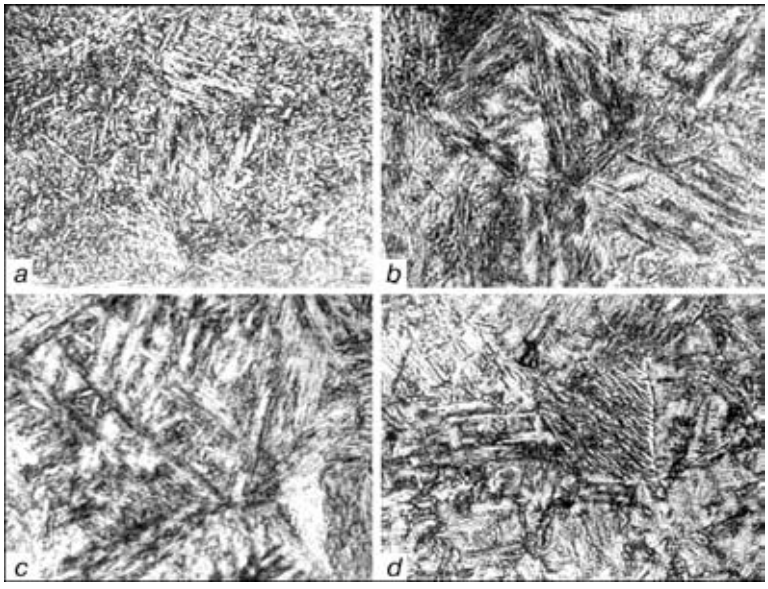

Figure 3. Macrostructure of 20KhN4FA steel in the initial condition (*a*) and after cooling in the dylatometer with different rates: *b* — $w_{6/5}$ = 20.0; *c* — 8.5; *d* — 1.6 °C/s (×200)

Table 1. Results of testing for crack resistance by the implant method

T_p, °C	Tensile stresses at loading							
	$0.47\sigma_{0.2}$	$0.65\sigma_{0.2}$	$0.79\sigma_{0.2}$	$0.94\sigma_{0.2}$	$1.023\sigma_{0.2}$	$1.1\sigma_{0.2}$	$1.19\sigma_{0.2}$	$1.26\sigma_{0.2}$
150	O	X	X		X			
200	O	O	X					
250			O	O		O	O	X
300								O

Note: X — sample fracture, O — no fracture.

For a quantitative estimate of preheating temperature influence on cold cracking susceptibility, it is convenient to use the calculation criterion I [8]:

$$I = \frac{NTS - LTS}{NTS}, \qquad (2)$$

where NTS is the strength of a notched sample; LTS is the critical stress, determined during testing.

Decrease of the values of I coefficient corresponds to an increase of cold cracking resistance. On the other hand, its values, close to a unity, characterize a high brittleness and low cracking resistance of the material. For critical conditions of testing with preheating up to 200, 250 and 300 °C, the values of embrittlement coefficient I = 0.61, 0.28 and 0.24, respectively.

As follows from calculation results, at transition from the temperature of 200 to 250 °C, I values markedly decrease, the cold cracking resistance rising almost 2.2 times. At preheating up to 300 °C, the cracking resistance rises more than 2.5 times, compared to welding with preheating to 200 °C. Nonetheless, it cannot be unambiguously stated, that preheating up to temperatures on the level of 200 °C will not be effective, as in the general case, the temperature mode of a welded joint, in addition to preheating temperature, is further affected by the amount of heat, applied in welding, which is determined by heat input q/v and conditions of heat removal. A conclusion on the dependence of cracking resistance just on preheating temperature will not be quite exact, and is, probably, valid only for the case of welding steel of one thickness

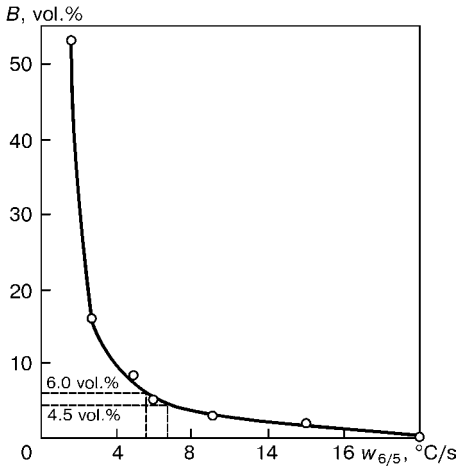

Figure 4. Influence of cooling rate $w_{6/5}$ of steel 20KhN4FA on the content of bainite B, formed at thermokinetic transformation of austenite

and by one specific method. For a more complete evaluation of the temperature mode in the HAZ the cooling rate of the metal being welded should be used, i.e. a generalized characteristic, allowing for the combined action of the above factors.

Table 2 gives the results of determination of the cooling rate of HAZ metal in bead deposition on 20 mm thick plate by manual arc welding with the heat input q/v = 10000 J/cm. Calculation was performed for average values of welding current I_w = = 125 A and welding speed v_w = 8.6 m/h by the known equation [12, 13] with the heat source efficiency η = 0.8. Thus, in preheating up to temperatures of 250 and 300 °C, providing the maximum cracking resistance, the metal cooling rate in the section of the most probable brittle fracture is 6.7 and 5.5 °C/s, respectively. Under such conditions bainite content depends on the cooling rate (Figure 4), and approximately from 4.5 up to 6.0 % of the bainite component forms in the metal structure.

Thus, the maximum admissible rate of HAZ metal cooling, equal to approximately 6.7 °C/s, may be regarded as a criterion of an optimal thermal mode in welding 20KhN4FA steel. Cooling at the rate below the above-mentioned one, provides a high resistance of welded joints to cold cracking. Such a rate may be achieved at different combinations of the temperatures of preheating (concurrent heating), welding heat input, metal thickness and item configuration. Therefore, selection of preheating temperature will depend on the specific case of welding.

As follows from published data, taken, for instance, from [13–18], in selection of preheating temperature the most preferable is low-temperature preheating (in some cases to 180 °C). This is substantiated by the possible occurrence of phenomena, causing metal embrittlement at temperature rise up to 350–400 °C. An opinion was also expressed [16], that increase of preheating temperature promotes development of higher residual stresses in the HAZ metal. In addition, as indicated by [15, 17], in welding of steels, having structural transformations in the intermediate area, preheating to lower temperatures promotes faster cooling of the metal and decomposition of austenite with formation of predominantly lower bainite, which is stronger and more ductile and tough than upper bainite.

In order to achieve high values of physico-mechanical properties of welded joints on hardening steels, it is recommended to maintain the level of the preheating temperature as close as possible to that of the

most complete decomposition of austenite [14]. In the case of steel 20KhN4FA the temperature of the end of martensite transformation is equal to $M_e \cong 190$ °C.

The above principle of low-temperature preheating was, probably, used as the basis of the calculation procedure to determine the preheating temperature T_p, developed by IIW [19], and improved by the authors of [20] for a wider range of values of P_ω parameter:

$$T_p = 350\{1 - \exp[-5(P_\omega - 0.27)]\}, \quad (3)$$

where P_ω is the generalized parameter of cracking susceptibility, determined from the ratio of $P_\omega = P_{cm} + [H]_{diff}/60 + S/600$. It is applicable for calculations by formula (3) in the range of values 0.27 up to 0.50 (here P_{cm} is carbon equivalent, equal to C + Si/30 + (Mn + Cu + Cr)/20 + Ni/60 + Mo/15 + V/10 + 5B; $[H]_{diff}$ is diffusible hydrogen concentration in the weld metal, $cm^3/100$ g; S is the steel thickness, mm).

In welding of 20KhN4FA steel 18 mm thick with scatter of chemical element composition from the lower level (see above) up to a level, corresponding to the value of P_ω index, equal to 0.50 (at composition, corresponding to the upper limit of concentrations, $P_\omega = 0.52$), we will use the above formula to determine the range of preheating temperatures. It is equal to approximately 165–240 °C.

Thus, preheating (concurrent heating) up to the temperature of 200–300 °C may be recommended, based on the results, obtained through experiments and calculations, as well as analysis of approaches to selection of preheating temperatures in development of the technology of welding 20KhN4FA steel. It is rational to perform final selection of the preheating temperature, based on welding of technological samples with monitoring of the rate of metal cooling in the HAZ area. It should be taken into account, that with adjustment of the thermal mode under the conditions of a delayed heat removal, the heat applied to the welded joint zone in multipass welding (self-heating) leads to reduction of the cooling rate (see Table 2, tests No.4 and 5) and to a gradual increase of the temperature of HAZ metal above that of initial preheating [14].

CONCLUSIONS

1. Based on analysis of the plotted thermokinetic diagram of austenite decomposition in 20KhN4FA steel it is found, that at cooling rates of $w_{6/5} < 20$ °C/s, structural transformation with bainite formation takes place, at $w_{6/5} > 20$ °C/s austenite undergoes hardening for martensite. In this case no area of transformation with formation of an equilibrium ferrite-pearlite mixture was found.

2. It is established that a high resistance of welded joints of 20KhN4FA steel to cold cracking is achieved at thermal modes of welding, providing not more than 6.7 °C/s rate of HAZ metal cooling near the weld, which is associated with establishment of more effective conditions for formation of the bainite component in the metal structure and partial self-tempering of hardening products.

Table 2. Influence of the thermal mode on cooling rate of HAZ metal in manual arc welding

Test No.	T_p, °C	*Conditions of performance of welding and deposition*	*Distance from fusion line to thermocouple, mm*	$w_{6/5}$, °C/s
1	100	Single-pass welding	1.5	12.3
2	150	Same	2.0	8.6
3	250	»	3.0	6.7
4	230	Welding with deposition of two parallel beads	2.0	6.7
5	250	Deposition of a section of about 20×60 mm in several passes	2.0	3.3
6	300	Single-pass welding	4.0	5.5

3. When developing the technology of welding 20KhN4FA steel, it is recommended to apply preheating in the temperature range of 200–300 °C. Selection of a concrete temperature of preheating (concurrent heating) should be performed on the basis of the results of studying the temperature modes, change of the rate of metal cooling in the HAZ and correction of the parameters of the modes of welding and heating for a concrete product.

1. (1989) *Handbook of steel and alloy grades*. Ed. by V.G. Sorokin. Moscow: Mashinostroenie.
2. Bejlinova, T.A., Yankovsky, V.M., Gordeeva, L.I. (1971) Structure and properties of 20KhN4FA steel after tempering. *Metallovedenie i Term. Obrab. Metallov*, **10**, 56–58.
3. Hrivnyak, I. (1984) *Weldability of steels*. Moscow: Mashinostroenie.
4. Yorioka, N. (1992) Welding of TMCP steels. *J. Jap. Weld. Soc.*, **4**, 50–66.
5. Zaks, A.I. (1996) *Electrodes for arc welding of steels and nickel alloys*. Refer. Book. St.-Petersburg: Welcome.
6. Geller, Yu.A., Rakhshtadt, A.G. (1989) *Science of materials*. Moscow: Metallurgiya.
7. Granjon, H. (1969) The «implant» method for studying the weldability of high strength steels. *Metal Constr. and British Weld. J.*, **11**, 509–515.
8. Sawhill, J.M., Dix, A.W., Savage, W.B. (1974) Modified implant test for studying delayed cracking. *Ibid.*, **12**, 554–560.
9. Kasatkin, B.S., Brednev, V.I., Volkov, V.V. (1981) Method of determination of deformations in delayed fracture. *Avtomatich. Svarka*, **11**, 1–3, 11.
10. Yoshinori, I., Masakiniko, I., Mutsuo, N. (1976) Study on estimation of lower critical stress for cold cracking at welds by implant test method. *J. Jap. Weld. Soc.*, **12**, 51–58.
11. Gulyaev, A.P. (1960) *Heat treatment of steel*. Moscow: Mashgiz.
12. Petrov, G.A., Tumarev, A.S. (1977) *Theory of welding processes*. Moscow: Vysshaya Shkola.
13. (1982) *Welder handbook*. Ed. by V.V. Stepanov. Moscow: Mashinostroenie.
14. Burashenko, I.A., Zvezdin, Yu.I., Tsukanov, V.V. (1981) Validation of preheating temperature in welding of chrome-nickel-molybdenum-vanadium steels of martensite class. *Avtomatich. Svarka*, **11**, 16–20.
15. Novikov, I.I. (1974) *Theory of heat treatment*. Moscow: Metallurgiya.
16. Lobanov, L.M., Mikhoduj, L.I., Pivtorak, V.A. et al. (1995) Influence of peculiarities of submerged-arc welding technology on the stressed state of high-strength steel welded joints. *Avtomatich. Svarka*, **9**, 21–23.
17. Novikova, D.P., Bogachek, Yu.L., Semenov, S.E. et al. (1976) Influence of cooling and deformation on impact toughness of weld metal in low-alloy steel welding. *Ibid.*, **10**, 21–23.
18. Kozlov, R.A. (1986) *Welding of heat-temperature steels*. Leningrad: Mashinostroenie.
19. Zemzin, V.N., Shron, R.Z. (1978) *Heat treatment and properties of welded joints*. Leningrad: Mashinostroenie.
20. Kasatkin, O.G., Musiyachenko, V.F. (1977) Calculation of welding conditions of high-strength low-alloy steel. *Avtomatich. Svarka*, **10**, 1–5.

INTERCRYSTALLINE CORROSION RESISTANCE OF AUSTENITIC DEPOSITED METAL MICROALLOYED WITH REM

N.G. EFIMENKO[1] and **S.V. NESTERENKO**[2]
[1]Ukrainian Engineering-Pedagogical Academy, Kharkiv, Ukraine
[2]Kkarkiv State Academy of Municipal Services, Kharkiv, Ukraine

Investigations were performed of the influence of microalloying chromium-nickel deposited metal of 18-10 type with yttrium and cerium oxide on its intercrystalline corrosion resistance. A positive role of modifying by cleaning the crystal boundaries and more favorable distribution of intermetallic inclusions is demonstrated.

Key words: *chromium-nickel-molybdenum austenitic deposited metal, rare-earth metals, microalloying, corrosion resistance, carbon diffusion, intercrystalline corrosion, non-metallic inclusions, grain boundaries, chemical microinhomogeneity, heat treatment, chromium carbides*

Carbon diffusion to the boundaries and boundary regions of grains and crystallites during heating in welding in the temperature range of its maximum mobility is the determinant factor of intercrystalline corrosion (ICC) resistance of Cr–Ni–Mo austenitic metal. In this case, the thermal cycling, related to the increase of the duration of metal staying at high temperatures, when making multipass welds, accelerates the process of carbide formation on the boundaries and depletion of boundary regions in chromium.

Works [1, 2] show that REM microalloying of austenitic Cr–Ni–Mo metal improves the corrosion resistance. However, the mechanism of this influence on ICC process is not considered. It is also established [3, 4] that yttrium delays carbon diffusion in the metal of welds on low-carbon and austenitic Cr–Ni steels. It may be assumed, that the cause for improved intercrystalline corrosion resistance of microalloyed Cr–Ni–Mo metals, is delaying carbon movement to grain and crystallite boundaries and depletion of near-boundary regions in chromium.

The purpose of this work was to study the influence of REM microalloying on ICC resistance of weld metal.

Metal was studied, which was deposited by the electric arc process with electrodes, containing 0.5 % Y + 0.8 % CeO_2, added though the coating [2]. Samples for investigations were produced by making multilayer deposits on the end face of a plate of 08Kh19N11M2 steel 20 mm thick and 150 mm long, in keeping with GOST 6996–78. Deposition was performed with electrodes of 4 mm diameter at currents of up to 130–140 A. Composition of the deposited metal, containing REM, is given in Table 1.

Deposited metal samples were heated in argon at the temperature of 660 °C with soaking for 0.2, 10 and 100 h.

Susceptibility of the deposited metal to ICC was evaluated electrochemically, using a cell with separate electrode spaces [5]. Samples polarization was performed with P5727-M potentiostate. Standard chlorine-silver electrode was used as reference electrode. Experimentally derived values of the potentials are given in hydrogen scale.

Investigations of chemical microinhomogeneity and distribution of elements on grain boundaries, as well as composition of non-metallic inclusions (NMI) were conducted, using electron microscopes Comebax and Comscan-4 with Link System 860 attachment for X-ray microanalysis. Samples for scanning electron microscopy were prepared by generally-accepted procedure, using known etchants.

Depth of ICC penetration was measured in keeping with GOST 6032–89 (AM method), using metallographic microscope.

Anode potentiometric curves of metals, studied in 1M $HClO_4$ + 0.1m NaCl solution, are given in Figure 1. The above electrolyte is characterized by high selective action on boundary regions of grains and crystallites, depleted in chromium. Straight-line shape of anodic potentiodynamic curves was obtained after taking the cathode curve from i_c = 10 mA/cm^2, starting with corrosion potential φ_c.

Table 1. Deposited metal composition, wt.%

Sample	*C*	*Cr*	*Ni*	*Mn*	*Si*	*Mo*	*S*	*Y*	*Ce*
Initial	0.060–0.075	18.2–19.0	10, 1, 10	0.80–0.95	0.45–0.60	2.0–2.3	0.016	–	–
Experimental	0.065–0.075	18.0–19.1	10, 15	0.80–0.90	0.40–0.60	2.1–2.3	0.015	0.019	0.021

Note. Composition of the deposited metal of both the variants includes 0.014 wt.% P.

Table 2. Corrosion resistance and depth of ICC penetration

Object of study	*Variant No.*	*Heat treatment duration, h*	*ICC depth, μm*	*Rate of corrosion in 1M H_2SO_4 at 60 °C, mm/year*
Metal without REM	1	0	45–57	0.18
	2	2	130–145	–
	3	10	215–226	–
	4	100	355–370	0.32
REM-containing metal	5	0	18–24	0.06
	6	2	38–56	–
	7	10	105–115	–
	8	100	145–155	0.12

Analysis of polarization measurements for samples of deposited metals shows that activation regions develop at heat treatment in the range of values of anode potentials of 0.15–0.4 V (Figure 1, curves *2′*, *2*, *3′*, *3*, *4′*, *4*). No such regions are found in the curves for samples without heat treatment (Figure 1, curves *1′*, *1*).

Degree of deposited metal susceptibility to ICC, according to [5], is determined by activation current i_a at φ_a = 0.3 V. It was experimentally established that i_a currents for microalloyed samples (Figure 1, curves *1′–4′*) are much smaller than those for the initial metal (Figure 1, curves *1–4*). In addition, i_a value increases with the increase of the duration of heat treatment, this growth being less pronounced for microalloyed metal than for the metal of the initial variant. ICC resistance was evaluated by the depth of its penetration. Gravimetric corrosion testing of samples in 1M H_2SO_4 solution at the temperature of 60 °C was conducted at the same time. Testing results are given in Table 2.

Data of Table 2, similar to electrochemical measurements, are indicative of a higher resistance to ICC and retardation of total corrosion of microalloyed metal in H_2SO_4 solutions.

It is found that in the metal without REM subjected to 100 h heat treatment, much more pronounced segregation of chromium on grain boundaries (0.8–2.0 wt.%) was registered, compared to its average content, as well as reduction of nickel content by 0.90–0.96 wt.% (Table 3, variant No.4).

Table 3. Chemical microinhomogeneity of deposited metal (heat treatment 100 h)

Variant No.	*Content, wt.%*					
	average		*on grain boundary*		*in the immediate vicinity of grain boundary (10 μm)*	
	Ni	*Cr*	*Ni*	*Cr*	*Ni*	*Cr*
4	9.228	19.209	8.562	21.756	9.246	19.246
8	9.872	19.810	10.250	20.201	10.382	20.208

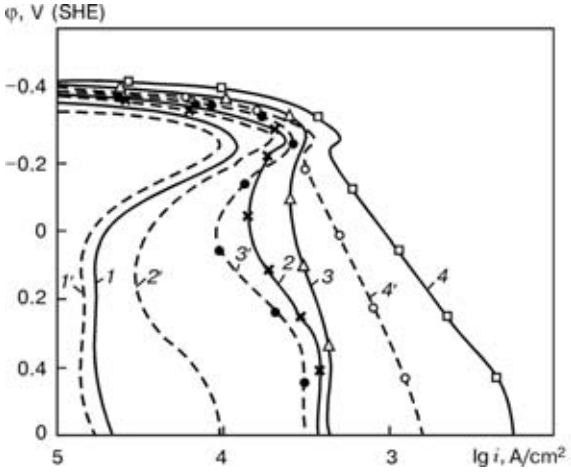

Figure 1. Anode potentiodynamic curves of deposited metal (*1–4* — without REM; *1′–4′* — with REM) in 1M $HClO_4$ + 0.1m NaCl solution at 650 °C temperature with different duration of heat treatments: *1* — 0; *2* — 2; *3* — 10; *4* — 100 h

No such change was observed in REM-containing metal, subjected to the same heat treatment (Table 3, variant No.8). No significant segregation of elements was found in samples, subjected to heat treatment for not less than 10 h.

Microstructure of REM-containing metal is refined, unlike the metal of the initial variant. It is further established that at heat treatment of the metal of the initial variant the grain boundaries become significantly thicker due to chromium carbide precipitation (Figure 2).

An intensive growth of the acicular phase is found (Figure 3, *a*; Table 3, variant No.4), which originates from the grain boundaries. The number of needles of the C-containing phase depends on heat treatment duration. Appearance of an observable amount of this phase was not noted for microalloyed samples even at heat treatment for 100 h (Figure 3, *b*; Table 3, variant No.8). In addition, no carbide precipitations or boundary thickening at grain boundaries was found

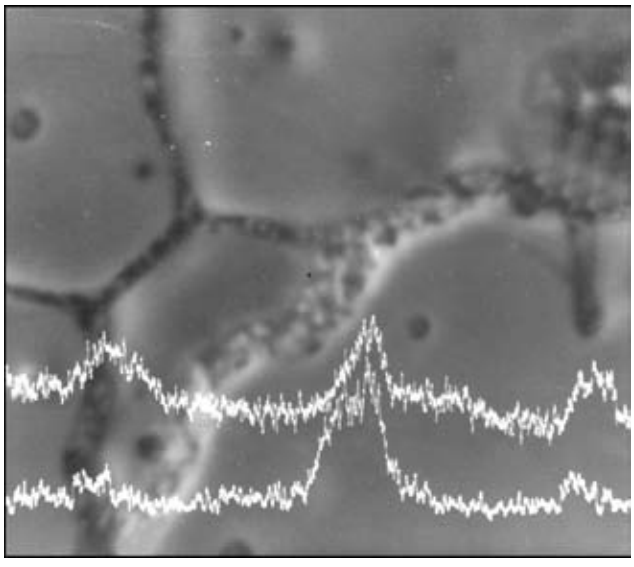

Figure 2. Chromium carbide precipitation on grain boundaries of initial deposited metal at heat treatment for 100 h (×4000)

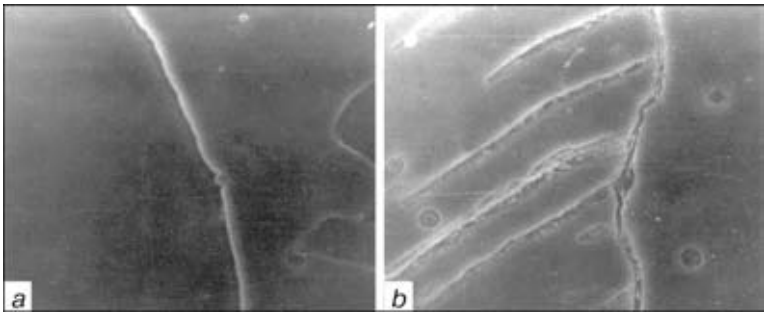

Figure 3. Grain boundaries of deposited metal (heat treatment 100 h) of initial variant (*a*) and with REM (*b*)

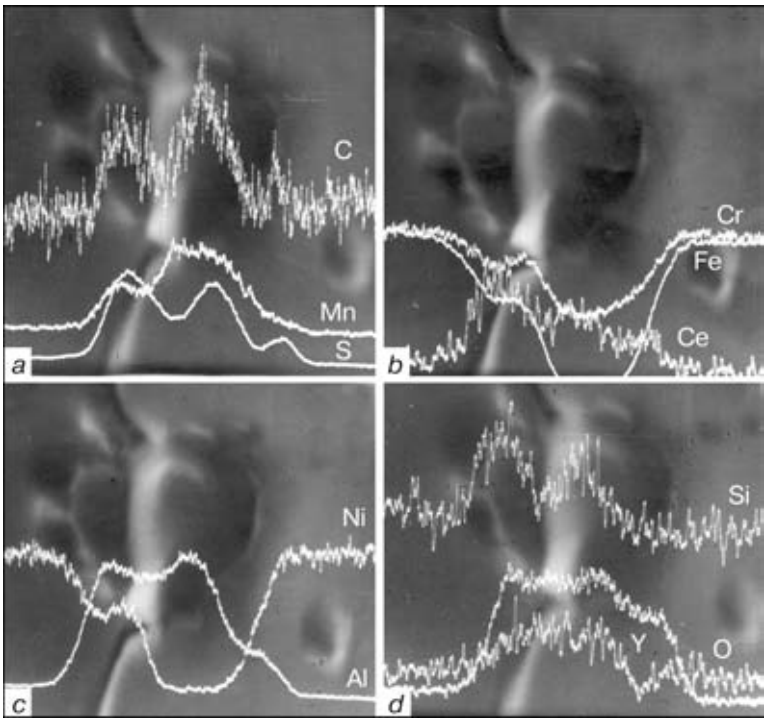

Figure 4. Distribution of chemical elements in NMI, located at the grain boundary (REM-containing metal, heat treatment 100 h)

Table 4. Typical composition of non-metallic inclusions

REM residual content in the metal, wt.%	*Brightness in reflected electrons*	*Weight fraction of elements, %*								
		Si	*Mn*	*Cr*	*Mo*	*Ti*	*S*	*Ca*	*Y*	*Ce*
No	Light	3.02	3.18	–	–	0.405	0.65	–	–	–
Same	Same	3.05	3.60	–	–	0.30	0.35	–	–	–
»	»	–	1.38	35.66	6.10	0.18	0.086	–	–	–
»	»	–	1.20	25.84	2.23	0.12	0.054	–	–	–
»	Dark	17.46	32.10	–	–	0.252	1.69	0.082	–	–
»	Same	13.78	16.01	–	–	0.458	0.082	0.011	–	–
»	»	7.30	14.07	–	–	0.66	1.016	0.05	–	–
»	»	6.82	10.83	–	–	0.802	1.14	0.071	–	–
»	»	6.256	13.849	–	–	1.45	0.711	0.07	–	–
0.0019Y + 0.0021Ce	»	20.54	34.60	–	–	15.19	0.67	0.77	0.87	4.16
Same	Light	1.50	2.80	26.059	–	0.128	1.80	0.258	–	0.60
»	Same	6.82	10.81	–	–	0.80	1.14	1.08	–	0.187
»	»	6.25	13.80	–	–	1.46	0.711	0.451	0.623	0.519
»	Dark	11.39	20.95	–	–	1.24	1.38	0.22	0.21	1.11
»	Same	24.76	26.76	–	–	3.55	1.33	6.69	–	1.01
»	»	19.046	25.38	–	–	2.30	1.80	1.98	0.469	0.924

for microalloyed samples under similar conditions (Figure 3, *b*; Table 3, variant No.8).

Investigation of NMI disclosed that in the initial metal they are located predominantly on grain boundaries. In REM-containing metal NMI are refined (0.8–1.0 μm) and uniformly distributed in the matrix, their shape being close to the spherical one. Sometimes, NMI of 3–8 μm size are found, part of them being located along grain boundaries.

In reflected electrons NMI have different colours — light, dark, sometimes light-grey. Their colour, as established by analysis, depends on the content of a particular chemical element. NMI composition is complex. Manganese, silicon and sulphur prevail in dark-coloured NMI in REM-containing metal. They also contain a significant amount of oxygen and carbon (Figure 4). Light-coloured inclusions are identified as REM oxysulphides and oxycarbosulphides. NMI in the initial metal are dark-coloured (silicates, silicon and manganese oxides, manganese sulphides) and light-coloured (mostly, manganese oxides and sulphureous compounds).

Composition of typical NMI is given in Table 4.

Positive influence of REM on ICC resistance of the metal can be presented, proceeding from the obtained experimental data and results of studies [3, 4, 6, 7]. High affinity of REM to oxygen and sulphur promotes formation of high-temperature NMI [4, 6] in the pre-solidification period. The mode of distribution of NMI in the solidified metal changes. They are found predominantly in the body of grains and crystallites [7]. Interdendritic and intergranualr boundaries become cleaner, and thinner. Structural constituents are modified [4]. The formed NMI, containing REM, have a complex composition; carbon is present in them in addition to oxygen and sulphur, i.e. carbides form [4]. Carbon diffusion is retarded in the temperature range of its maximum diffusion mobility [3, 4]. Chemical microinhomogeneity in the boundary regions becomes smaller [3, 6]. Retardation of carbon diffusion lowers the probability of formation of chromium carbides on the boundaries. Change of the nature of structure formation processes promotes decrease of the intensity of corrosion processes in the boundary regions.

CONCLUSIONS

1. High-temperature treatment of initial metal promotes the appearance of carbide phase on grain boundaries and of C-containing acicular phase. Number of these phases depends on the duration of metal soaking at the temperature of maximum mobility of carbon. No such phases are found in REM-containing metal, which is attributable to lowering of diffusion activity of carbon, i.e. stabilization of the structure.

2. REM addition to the deposited metal lowers the chemical microinhomogeneity, leads to modification of structural components, and cleaning of the boundaries of grains and crystallites.

3. In REM-containing metal the formed NMI have a complex composition, are distributed mainly in the body of grains and crystallites, contain a considerable amount of sulphur and oxygen, as well as carbon.

4. Electrochemical investigations and measurements of the depth of ICC penetration are indicative of a higher ICC resistance of REM-containing metal.

1. Lazebnov, P.P., Aleksandrov, A.G. (1988) Influence of modification on structure and properties of 12Kh18N10T steel welded joints metal. *Svarochn. Proizvodstvo*, **6**, 33–36.
2. Nesterenko, S.V., Efimenko, I.G. (1990) Increase of corrosion resistance in acid media of austenitic deposited metal by complex alloying with rare-earth metals. *Ibid.*, **10**, 19–21.
3. Efimenko, N.G., Balan, L.N. (1988) Effect of yttrium on hydrogen diffusion in welded joints. *Ibid.*, **7**, 32–36.
4. Efimenko, N.G. (1990) On the mechanism of effect of rare-earth metals on solidification process and formation of primary weld structure in welding of steel. *Ibid.*, **7**, 38–34.
5. Medvedeva, P.A., Knyazheva, V.M., Kolotyrkin, Ya.M. et al. (1975) Electrochemical method of quantitative evaluation of stainless steels susceptibility to intercrystalline corrosion. *Zashchita Metallov*, **6**, 699–705.
6. Nuji, Y., Ohashi, T., Hiromoto, T. et al. (1980) Solidification microstructure of ingots and continuously cast slabs treated with rare-earth metal. *Tetsu-to-Hagane*, **6**, 618–627.
7. Efimenko, N.G., Balan, L.N., Bakakin, G.N. (1985) Influence of yttrium on weld metal structure in fusion welding. *Svarochn. Proizvodstvo*, **4**, 19–21.

PHYSICAL-MECHANICAL NON-HOMOGENEITY OF WELDED JOINTS OF HIGH-NITROGEN Cr–Mn STEELS AND THEIR CORROSION RESISTANCE

A.I. BALITSKY, I.F. KOSTYUK and **O.A. KROKHMALNY**
G.V. Karpenko Physical-Mechanical Institute, NASU, Lviv, Ukraine

Formation of physical-mechanical heterogeneity in metal of welded joints depending on weld metal alloying is considered. The welds alloying with nitrogen provides the higher electrochemical homogeneity of the joints.

Key words: *welded joint, high-nitrogen Cr-Mn steels, non-homogeneity of properties, intercrystalline corrosion, hardness, mechanical tests*

The high-nitrogen Cr–Mn steels of 18-18 type find the more and more wide application in power engineering [1–3], including the electric power stations of Ukraine. At present, the austenitic Cr–Mn steel R900 (12Kh18AG18Sh) with a superequilibrium concentration of nitrogen is used for the manufacture of shrouds of rotors of the modern turbogenerators reaching 1000–1200 MW of unit power. The high content of nitrogen is attained by the electroslag remelting of casting in the medium of a high-nitrogen charge. A number of works was devoted to this technology both as regards to the new banding Cr–Mn steel of 18-18 type [4–13] and also traditional steels 60Kh3G8N8V and 40Kh4G18 [14,15]. The new steel possesses high values of strength and fracture toughness, resistance to a local corrosion and stress corrosion cracking [1]. Information about the stress corrosion resistance of Cr–Mn steels of the 18-18 type is rather limited [16–20]. The fracture of shrouds manufactured from steel R900 was not recorded until now, however, the cases of their corrosion-mechanical damages are known.

The technology of welding Cr–Mn steels of 18-18 type is similar to the technology of welding of other austenitic steels. However, the problems can occur with the formation of pores, reduction in strength, toughness and also corrosion resistance if not to follow a proper technology (low power of welding arc, small sizes of molten pool). The content of carbon, silicon and nickel in filler metal should be minimum, as these elements reduce the nitrogen solubility in the weld. In addition, high nickel concentrations predetermine the chemical and structural microheterogeneity and low corrosion resistance of welded joints (WJ), caused by it. Using wire with 0.4–0.8 % N and shielding gas, containing nitrogen up to 4 %, it is possible to produce the defect-free WJ. Therefore, the works are intensively carried out for the development of new, more effective fillers and technologies of welding of high-nitrogen austenitic steels [18, 19].

The physical-chemical and electrochemical heterogeneity of WJ from two high-nitrogen austenitic steels, close in composition, and their corrosion resistance in solutions of sodium chloride, hydrochloric acid and copper salts were examined. Properties of two-sided butt joints made of as-delivered steels 12Kh18AG18Sh and 08Kh19AG10Sh were studied. Table 1 gives chemical composition of parent and filler materials.

Welded joints No.1 of 12Kh18AG18Sh steel samples were made by the manual argon-arc tungsten electrode welding using a filler wire Sv-01Kh19N9. Welded joints No.2 of 08Kh19AG10Sh steel samples were made by the automatic arc welding in a special shielding atmosphere containing 4 % N_2. A special wire No.1 (Table 1), developed for welding high-nitrogen austenitic steels, was used as a filler material. Owing to a high content of chromium in it the pore-free welds are produced with a high level of mechanical characteristics.

Due to developing chemical and structural heterogeneity in different zones of high-alloy steel WJ, and,

Table 1. Chemical composition of parent metal of welded joints and filler wires

Material	*Elements, wt.%*							
	C	*Si*	*Mn*	*Cr*	*Ni*	*Mo*	*V*	*N*
Steel 12Kh18AG18Sh	0.12	0.36	18.70	19.19	0.16	0.01	0.05	0.64
Steel 08Kh19AG10Sh	< 0.08	< 0.50	10.00	19.00	< 1.00	< 0.50	–	0.50
Wire No.1	0.04	0.70	5.50	25.00	21.00	3.60	–	0.38
Wire Sv-01Kh19N9	0.08	1.00	2.00	19.00	9.00	–	–	–
Wire Sv-07Kh25N13	0.09	0.80	1.00–2.00	25.00	13.00	–	–	–

Table 2. Depth indices of corrosion (mm/year) of welded joints and parent metal in aggressive media

Medium	*WJ No.1*	*WJ No.2*	*PM No.1*	*PM No.2*
3 % NaCl	$1.6 \cdot 10^{-3}$	$1.0 \cdot 10^{-3}$	$6 \cdot 10^{-4}$	$9 \cdot 10^{-4}$
5 % HCl	3.51	2.63	1.56	1.70
22 % $CuSO_4$	0.09	0.07	0.10	0.06
22 % $CuCl_2$	3.11	3.03	2.78	2.99

Table 3. Corrosion potentials (E_c, mV) in different areas of welded joint

WJ No.	*WJ areas*	*3 % NaCl*	*5 % HCl*	*22 % $CuSO_4$*	*22 % $CuCl_2$*
No.1	PM	348	−272	416	−68
	HAZ	334	−254	407	−82
	Weld	415	−33	507	248
	WJ	360	−263	438	−71
No.2	PM	329	−283	358	−57
	HAZ	303	−285	361	−39
	Weld	368	−238	442	166
	WJ	343	−256	401	−36

first of all, in weld and HAZ metal, the WJ can be considered, as a whole, as a complex short-circuit multielectrode corrosion system. In the electrolyte solution the WJ surface can be considered equipotential, and each its region can be considered polarized with respect to a compromise potential of the corrosion system. The high-nitrogen steels have a narrow range of passivity in hot solutions of chlorides, therefore, it can be expected that the fillers with a higher potential will predetermine their contact corrosion. Samples were tested in solutions: 3 % NaCl, 5 % HCl, 22 % $CuSO_4$ and 22 % $CuCl_2$ during 720 h. The depth characteristics of corrosion of WJ parent metal (PM) were determined from mass losses reduced to the area of corrosion damage by weighing samples in scales VLR-20.

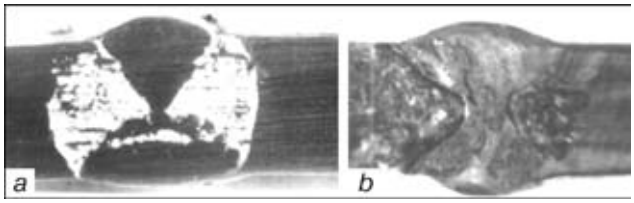

Figure 1. Samples of WJ No.1 after 240 h soaking in 5 % HCl (*a*) and 22 % $CuCl_2$ (*b*) solutions

During examination of mass losses of samples (Table 2) a high corrosion resistance of WJ of high-nitrogen austenitic steels in the following solutions was established: 3 % NaCl and 22 % $CuSO_4$ (2 and 5 marks, respectively, by GOST 13819–68). It can be noted that sample of WJ No.2, being more homogeneous in chemical composition, has a higher corrosion resistance in 3 % NaCl solution (almost 1.5 times). In 22 % $CuCl_2$ the rates of corrosion of both samples are almost similar and rather high. This proves, that WJ in the medium of chlorides have a low corrosion resistance (6 marks). Moreover, the more non-homogeneous metal of WJ No.1 has 1.5–2.4 times higher rates of corrosion than PM that is an indirect testimony of its high electrochemical heterogeneity.

The examination of macrostructure of a near-weld zone showed an absence of pores or other large defects. The visual inspection of the samples revealed their

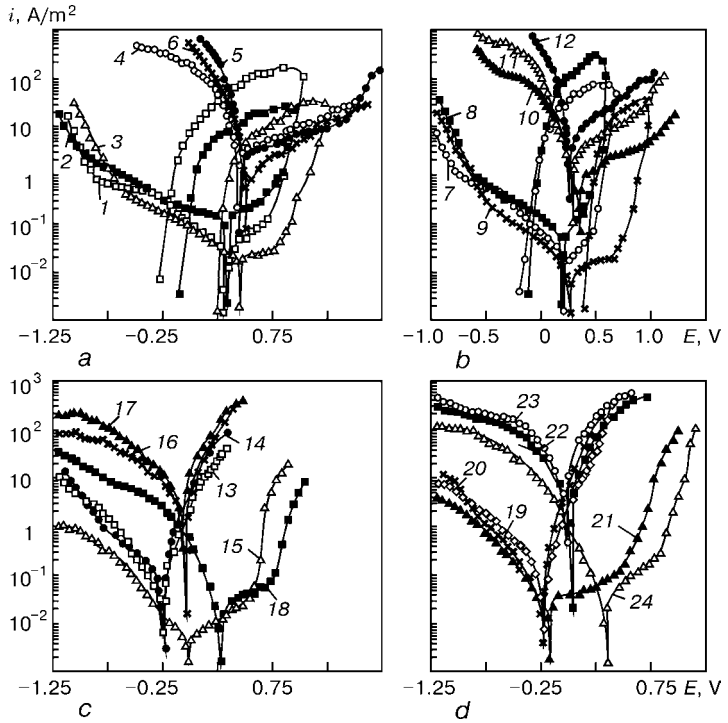

Figure 2. Polarization curves of regions of WJ No.1 (*a*, *c*) and No.2 (*b*, *d*) in 3 % NaCl (*1–3*, *7–9*), 22 % $CuSO_4$ (*4–6*, *10–12*), 5 % HCl (*13–15*, *19–21*) and 22 % $CuCl_2$ (*16–18*, *22–24*): *1*, *4*, *7*, *10*, *13*, *16*, *19*, *22* — PM; *2*, *5*, *8*, *11*, *14*, *17*, *20*, *23* — HAZ metal; *3*, *6*, *9*, *12*, *15*, *18*, *21*, *24* — weld

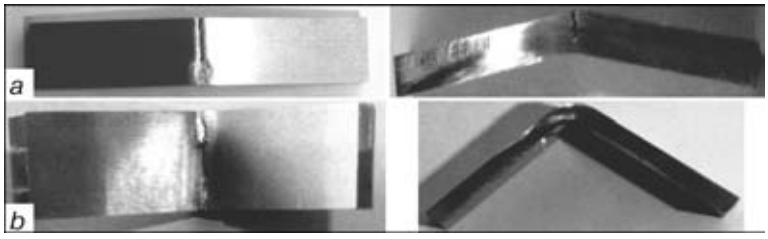

Figure 3. Appearance of samples after test for intercrystalline corrosion: *a* — bending angle 11°; *b* — 83°

non-uniform corrosion in PM–HAZ metal zone in solutions of 5% HCl and 22 % $CuCl_2$ (Figure 1). Weld corrosion was not observed in principle. Due to formation of a galvanopair on WJ No.1 in 22 % solution of $CuCl_2$ the intensive cathodic precipitation of copper with a simultaneous formation of shallow pittings in the fusion zone and HAZ metal was observed. In the fusion zone the tendency to a local corrosion damage in the form of an undercut (slot) is observed. The rate of corrosion of WJ No.2 is increased negligibly (1.01–1.34 times) as compared with PM.

The conclusion about the higher electrochemical homogeneity of WJ No.2 is confirmed by the results of measuring stationary potentials of corrosion of the WJ regions (Table 3). For both WJ the potentials of the weld zone are highest. For WJ No.1 in solutions of 3 % NaCl, 22 % $CuSO_4$ and 22 % $CuCl_2$ the corrosion dissolution of the material is concentrated on the HAZ metal, while in 5 % HCl solution it is concentrated on the PM, as these areas have the lowest potentials of corrosion.

For WJ No.2 in solutions of 3 % NaCl and 5 % HCl the potential of HAZ metal is lowest, while in solutions of copper salts the PM potential is lowest.

Difference between the potentials of the above-defined regions of WJ No.1 in 5 % HCl and 22 % $CuCl_2$ solutions is 239 and 330 mV, respectively, while in WJ No.2 it is 47 and 223 mV. In 3 % solution of NaCl the anodic polarization of PM and HAZ metal, stipulated by a contact with a more noble weld metal, accelerates negligibly the corrosion of WJ as a result of a low effectiveness of the cathodic process (Figure 2, *a*, curves *1–3* and 2, *b*, curves *7–9*). At a compromise potential of the given corrosion system, which is potential of WJ (see Table 3), these regions are located in a steady passive state, and the rate of their anodic dissolution is low (to 0.2 A/m^2). In 22 % solution of $CuSO_4$ the corrosion of WJ is accelerated by 1–2 orders due to a significant increase in effectiveness of the cathodic process (Figure 2, *a*, curves *4–6* and 2, *b*, curves *10–12*). However, due to absence of chloride-ions in the solution this does not cause depassivation of none of the WJ regions. The corrosion process is proceeding under the cathodic control.

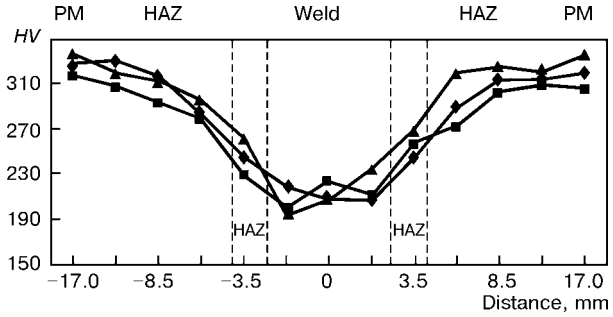

Figure 4. Values of hardness of three samples of WJ No.3

The presence of the chlorine-ions and low values of pH predetermine the activation of PM material and HAZ metal of WJ in 5 % solution of HCl, and material of weld remains passive (Figure 2, *c, d*). Corrosion process is proceeding under the mixed anodic-cathodic control at a high rate. Compromise potentials of the WJ corrosion systems, i.e. 22 % solution of $CuCl_2$, are shifted to the region of a pitting corrosion of regions of PM and HAZ metal, while the material of weld is located in a passive state. The high rate of corrosion of WJ in this medium is determined by the effectiveness of cathodic and low polarization of anodic electrode processes. The occurrence of an auxiliary electrode as a result of a cathodic precipitation of copper complicates the analysis of this multielectrode corrosion system. The polarization curves with a reverse trace could establish the potentials of pitting repassivation.

Welded joints No.2 were also investigated for their susceptibility to intercrystalline corrosion. Tests were performed in accordance with GOST 6032–89 using method AM. Samples were investigated in a water solution of copper of sulphuric acid, adding the copper chips. Before the tests the samples were degreased. After continuous boiling (24 h) they were rinsed with water and dried. Samples were bent for up to 90° in weld metal. Figure 3 shows samples after the tests. Cracks were observed at the surface of weld metal of the bent samples. It is typical that the bending angle was 83° for sample No.1 and 11° — for No.2. The experiments were interrupted after the appearance of cracks.

Samples of WJ No.3 from steel 12Kh18AG18Sh were welded with wire Sv-07Kh25N13 which does not contain nitrogen (see Tables 1 and 2). Hardness was measured normal to the weld. The hardness values were lower in weld and fusion zone. This is explained by the absence of nitrogen and different composition of weld and PM. It is typical that microhardness of weld metal is almost similar in all the samples.

CONCLUSIONS

1. In the weld zone a heterogeneity of main mechanical properties is observed due to decrease in nitrogen content in the weld material.

2. Investigation of susceptibility of Cr–Mn 18-18 type steel welded joints in saturated solution $CuCl_2$

to the corrosion-mechanical damage makes it possible to reveal the weakest zones of the weld.

3. Welded joints made by the arc welding using the N-containing fillers and shielding medium are characterized by the higher electrochemical homogeneity than those produced with electrode Sv-01Kh19N9. These welded joints are characterized by the high corrosion resistance in 3 % NaCl and 22 % $CuSO_4$ solutions. Test results give all grounds to recommend the N-containing fillers for welding high-nitrogen Cr–Mn steels.

1. Balitsky, A.I. (1999) *Current materials for power turbogenerators*. Lviv: FMI.
2. Speidel, M.O. (1981) Nichtmagnetisierbare Stähle für Generator-Kappenringe, ihr Widerstand gegen Spannungsreibkorrosion und Wasserstoffversprödung. *VGB Kraftwerktechnik*, **5**, 417–427.
3. Stein, G. (1980) Kappenringe — ein Krupp-Produkt mit Tradition und Zukunft. *Techn. Mitt. Krupp Werksbericht*, **2**, 69–72.
4. Kutkin, G.G., Vasiliev, L.M., Zuev, I.M. et al. (1990) ESR technology of high-nitrogen 12Kh18AG18 steel into ingots of 18 t mass. In: *Abstr. of pap. of 1st All-Union Conf. on High-Nitrogen Steels*, Kyiv, April 18–20, 1990. Kyiv.
5. Stein, G., Menzel, J., Kirshner, W. (1996) Manufacturing and operation of retaining rings made out of stress corrosion resistant steels. In: *Proc. of 1st MaTech'96 Int. Conf. on Development, Testing and Application of Materials*, Opatija, Oct. 2–5, 1996.
6. Stein, G., Menzel, J., Chondhury, A. (1989) Industrial manufacturing of massively nitrogen-alloyed steels in a pressure ESR furnace. *Steel Times*, **3**, 146.
7. Stein, G., Menzel, J., Dorr, H. (1987) *Möglichkeiten zur Herstellung von Smiedestücken mit hohen Stickstoffgehalten in der DESU-Anlage. Ergebnisse der Werkstoff-Forschung*. B. 1: Moderne Stähle. Thubal-Kain.
8. Medovar, B.I., Saenko, V.Ja., Grigorenko, G.M. et al. (1996) *Arc-slag remelting of steel and alloys*. Cambridge: Cambridge Int. Sci. Publ.
9. Medovar, B.I., Saenko, V.Ja., Medovar, L.B. et al. (1992) *New multilayer steel in welded structures*. Vol. 2. Part 2. New York: Harwood A.P.
10. Balitsky, A.I., Pokhmursky, V.I., Volkov, A.S. et al. (1998) Peculiarities of electroslag remelting and properties of high-strength tire steel. In: *Proc. of 4th Corrosion'98 Int. Conf.-Exhibition on Problems of Corrosion and Corrosion Protection of Materials*, Lviv, June 9–11, 1998. Lviv.
11. (1990) *Retaining rings: Product literature. Krupp Metallund Schmiedewerke*. Essen.
12. Medovar, B.I., Stupak, L.M., Bojko, G.A. et al. (1981) *Electroslag metal*. Ed. by B.E. Paton, B.I. Medovar. Kyiv: Naukova Dumka.
13. Medovar, B.I., Grigorenko, G.M., Pomarin, Yu.M. et al. (1995) Influence of flux composition and gas atmosphere on nitrogen absorption by steels and alloys during induction and arc melting. *Problemy Spets. Elektrometallurgii*, **3**, 6–14.
14. Pakhuridze, V.N., Chekotilo, L.V. (1974) Methods of manufacturing of rotor turbogenerator tire rings. In: *Special Electrometallurgy*. Issue 27.
15. Pakhuridze, V.N., Chekotilo, L.V. (1975) Nitrogen alloying of austenitic steels 60Kh3G8N8V and 40KhG18 during ESR. *Problemy Spets. Elektrometallurgii*, **1**, 40–45.
16. Balitsky, A.I. (1998) Estimation of susceptibility to corrosion cracking during welding and cutting of high-nitrogen chrome-manganese ESR steels. In: *Proc. of Int. Conf. on Welding and Related Technologies for the 21st Century*, Kyiv, Nov. 24–27, 1998. Kyiv: PWI.
17. Balitsky, A.I., Krokhmalny, O.A., Kostyuk, I.F. (2000) Corrosion mechanical strength of welded joints of high-nitrogen steels. In: *Abstr. of poster pap. of Int. Conf. on Welded Structures*, Kyiv, Oct. 2000. Kyiv: PWI.
18. Harzenmozer, M., Diener, M. (1997) Suitable filler material for welding of high nitrogen stainless steels. In: *Proc. of 18th Int. SAMPE Europe Conf. on the Society for the Advancement of Material and Process Engineering*, Paris, La Defense, April 23–25, 1997. Paris.
19. Coetzee, M., Pistorius, P.G.H. (1994) Elevated temperature phase transformations and weldability of experimental Cr–Mn–Ni stainless steels. Paper 48. In: *Proc. of Conf. on Duplex Stainless Steels*, Glasgow, Nov. 13–16, 1994.
20. Kostyuk, I.F. (2001) Heterogeneity of physicomechanical properties of welded joints from high-nitrogen chrome-manganese steels and their corrosion resistance. In: *Materials for power engineering.* Issue 1.

PILOT PLANT OF WELDING EQUIPMENT OF THE E.O. PATON ELECTRIC WELDING INSTITUTE OF THE NAS OF UKRAINE IN THE NEW CONDITIONS OF ECONOMY

V.A. TITOV, B.V. DANILCHENKO, A.N. VOLKOV, A.G. BRYZGALIN, S.M. POLISHCHUK, V.A. KORITSKY and **V.V. ANDREEV**
The E.O. Paton Electric Welding Institute, NASU, Kyiv, Ukraine

Peculiarities of the PWI Pilot Plant evolution in the conditions of transition to the market economy in Ukraine are considered. System and nomenclature ranges of the welding equipment manufactured currently are presented.

Key words: *pilot plant of welding equipment, power sources, serial welding equipment, transformers, rectifiers, semi-automatic machines, modification of equipment*

The planned economy has specialized manufacturers of welding equipment in very narrow ranges, classifying them by purpose, kinds, types, capacity, fields of application, mass and dimensions of the products. For examples, the manufacturers of power sources of welding arc were specialized by kinds of equipment (transformers or rectifiers), purpose (welding ferrous or non-ferrous and light metals), capacity (low, medium and high welding currents). This principle had certain advantages connected with a feasibility to manufacture a large quantity of single-type equipment of comparatively low prices and to deliver it for large distances to different consumers, not taking much into account the tariffs for transportation (which, certainly, were not too high).

The system was functioning successfully within one great state, never having practically the saturated market and, therefore, it was not intended and adapted originally to a flexible reaction to the continuously changing economic situation, demands of consumers and, finally, to the technical progress and different innovations. On the general background of thirty plants-manufacturers of welding equipment, low-sensitive to the innovations in manufacturing, the following plants were distinguished: Plant «Elektrik» (Leningrad), Kakhovka Plant of Electric Welding Equipment, Vilnius Plant of Electric Welding Equipment and Pilot Plant of Electric Welding Equipment (Kyiv), being in a continuous contact with own design bureaus or were supported by design bureau of research institutes. The products of these plants were superior, as a rule, to the products of other enterprises in quality and variety.

Restructuring, formation of CIS, transition to the new conditions of economy have led to the occurrence of custom barriers, barter and currency settlements, significant growth of tariffs for transportation, that caused the objective need in an abrupt increase in assortment of the products manufactured by each of the plants-manufacturers to saturate as much as possible the own market and its realization to partners from other CIS countries. The need in payments for cooperation deliveries of the materials and completing products, appearance of competition, exceeding of proposals over the demands, and, at last, the total situation in CIS countries characterized by a recession in economic activity, made the manufacturers of welding equipment not only to widen the nomenclature, but also to increase the technical level of products, coming to the new positions of reliability, quality and design.

The new conditions to run a business required appropriate organizing and finance reaction that was expressed at some plants by search and finding of investments of a finance, scientific and technical nature, and led in some cases to the change in organization forms, i.e. to the creation of joint stock societies and joint ventures (Plant «Fakel», Brovary, Ukraine; Vilnius Plant of Electric Welding Equipment; Power Machine-Building Plant, Simferopol, Ukraine, etc.). In these conditions the position of Pilot Plant of Welding Equipment (PPWE) of the PWI was ambiguous: from the one hand, the plant remained under methodological, scientific and organizational supervision by the PWI, used and realized the developments of its Experimental Design Technological Bureau, from the other hand, it became an ordinary entity of economic activity, obliged to function far beyond the sphere of scientific service. Under these conditions, no budget support in the form of fulfillment of orders within the scope of Government programs, orders of ministries and negotiated works on the research subjects of the PWI was given to the PPWE. The situation was worsened also by the fact that the government form of property of the enterprise was registered by the appropriate Statement of President of Ukraine, that could not but influence the inflow of private capital and investments from outside.

Figure 1. Equipment of the «Paton» series

New situation insisted on the development of a conception of adaptation to the changed conditions of an economical environment. The conception was based on an expediency of transition to the manufacture of serial welding equipment of a high demand with a large dominating of a volume of production of this equipment over the volumes of manufacture of pilot models of equipment and volumes of services of a scientific-technical nature. One of the key statements of the conception became the need in design and manufacture of equipment of the new generation within the whole spectra of needs of economy in kinds, types, purpose and capacity of welding units. Requirement for the design of equipment using single principles of development, designing and testing became the obligatory condition of a successful fulfillment of this work to provide high reliability and quality of all the nomenclature range.

The production of the PWI PPWE was distinguished from the equipment of other manufacturers by:

- reliability;
- assurance of optimum duty cycle depending on the purpose of the equipment;
- easy arc exciting;
- provision of units with instruments;
- refusal from use of extradevices (for example, from sensors and overheating relay);
- optimum relation between price and quality of production.

Conception was based on the necessity in assistance to preserve and develop the school of researchers-developers and designers, having single opinions as to the principles of design of unified units, furnishing and transition to computer designing of the equipment, close relation with industry, flexible links with production processes and requirements of market. Tendency to the creation of all the range of equipment in a single design was considered as obligatory, that had to lead finally to the formation of a certain image of enterprise and to contribute to consolidation of its positive reputation with the customer. The important decision was taken to name the equipment using the name of the founder of the Paton Institute, that put additional requirements to the quality, careful manufacture and reliability of products in parallel with an advertising attraction.

The realization of the conception made the parametric range of the equipment of the PWI development, designed for main types of arc fusion welding, more clear (Table 1). In addition, some models were not modified significantly (for example VMG-5000), a part of products was modified (STSh-250 and PS-250), some units were designed and manufactured for the first time.

Rectifier of the VD-309 type belongs to the most typical representatives of power sources of the new

Table 1. System range of welding equipment manufactured by the PWI PPWE

Type	*Range of welding current, A*									
	0–100	*100–140*	*70–250*	*200–250*	*250–315*	*315–400*	*400–500*	*500–630*	*630–1000*	*1000–2000*
MAW	TDS-125, TDS-140		STSh-250, STSh-251, STSh-252, PVS-250		VD-308, VD-309		STSh-500 SGD			
MAG	PS-100	BP-200		PS-250.1, PS-250.2, PS-250VPR6, PS-315			Not manufactured	BP-600		
MIG		STSh-252			Not manufactured		A-500UP	Not manufactured		
AW					Not manufactured					AD-381

Manual arc welding (MAW)

Welding purpose	*Household*	*Industrial*		
		Site	*Stationary stations*	*Stationary stations for welding with high-efficient electrodes and cutting with electrodes*
Current range, A	0–140	70–250	70–315	70–500
Description of equipment	TDS-125, TDS-140	STSh-250, STSh-251, STSh-252, PVS-250	VD-308, VD-309	STSh-500 SGD
Maximum thickness, welded per one pass without edge preparation, mm	3	5	8	12

Semi-automatic consumable electrode welding in active shielding gases (MAG)

Wire diameter, mm	0.6; 0.8	1.0; 1.2	1.4	1.6	1.8; 2.0	2.0
Maximum welding current, A	100	200	315	400	500	630
Description of equipment	PS-100	BP-200	PS-250.1, PS-250.2, PS-250VPR6, PS-315	Not manufactured		BP-600
Maximum thickness, welded per one pass without edge preparation, mm	4	6	8	10	12	14

Welding with non-consumable electrodes in inert gases (MIG)

Electrode diameter, mm	3–4	4–6	6–7	8	8
Maximum welding current, A	200	315	400	500	630
Description of equipment	STSh-252	Not manufactured		A-500UP	Not manufactured

Automatic welding (AW)

Welding purpose	*Welding of small and madium thicknesses, special-purpose equipment*	*Single-arc welding of medium and large thicknesses*	*Welding of large thicknesses, including multiarc welding*
Welding current, A	< 500	500–1000	1000–2000
Description of equipment	Not manufactured		AD-381

Table 2. Main characteristics of transformers for manual, semi-automatic and automatic arc welding of the «Paton» series

Parameters	*Type*							
	TDS-125	*TDS-140*	*STSh-250*	*STSh-251*	*STSh-252*	*STSh-500 SGD*	*TDFP-1250*	
Mains voltage, V	220	220	220/380	220/380	220/380	380	380	
Welding current, A	80, 125	90, 120, 140	70–250	7–250	70–250	25–125, 125–600	1250 Square	1600 Sinusoidal
Duty cycle, %	20	20	20	40	40	60	100	
Open-circuit voltage, V	63	64	65	65	65	63	112	
Consumed power, kW	7.8	8	16.3	16.3	16.3	32.5	125	
Cooling	Forced	Forced	Forced	Forced	Forced	Natural	Forced	
Mass, kg	19	25	49	58	65	200	1500	
Notes					Block of arc burning stabilizing	Block of arc burning stabilizing	Block of phase control	

generation, which, due to the combination of two steep-falling characteristics (Figure 2), provides a reliable arc exciting, stable process of welding and smooth filling of weld crater during the process completion. The VD-309 rectifier passed successfully all trials under the extreme conditions of the metallurgical production, in pipelines assembly in the field conditions, in critical repair jobs. Characteristics of the equipment, serial-produced by the PWI PPWE, are given in Tables 2–6.

Over the recent years the Plant has mastered the manufacture of lines for continuous production of spirally-welded polymeric pipes of 500–1100 mm diameter, 2–10 mm wall thickness, efficiency of line is up to 30 m/h. The manufacture of three types of equipment for welding polymeric pipes in field and shop conditions has been also mastered: units SAT-11OR (32–110 mm dia. pipes welded), SAT-180G (32–180 mm dia.) and SAT-315G (80–315 mm dia.). The detachable heating elements for welding thin-walled polyethylene shells and manual extrusion machines of different modifications used in manufacture of shaped elements of polymeric pipes and other products from polymeric materials are also manufactured. Table 7 represents comprehensively the work of the PWI PPWE on adaptation to new conditions of market economy.

At present the PPWE manufactures and realizes:

• transformers and rectifiers for manual and automatic arc welding (125–5000 A);

• semiautomatic welding machines (100–600 A) for welding with solid and flux-cored wires;

• machines for air-plasma cutting, strengthening, spraying, surfacing (45–350 A);

• installations for argon arc welding (250–600 A), units of autonomous cooling;

• complex electromechanical equipment, including equipment for multiarc welding of large-diameter pipes with transformers for 1250 A with a square shape of welding current (see in detail in Website www.paton-ozso.kiev.ua);

Table 3. Main characteristics of rectifiers for manual and semi-automatic arc welding of the «Paton» series

Parameters	*Type*							
	PS-100	*PVS-250*	*PS-250*	*PS-250VPR6*	*PS-315*	*VD-308*	*VD-309*	*BMG-5000*
Mains voltage, V	220	75	380	380	380	380	380	380
Welding current, A	40–100	70–210	50–320	50–320	50–100	45–125, 125–315	45–125, 125–315	50–5000
Duty cycly, %	60	50	60	60	60	60	60	100
Open-circuit voltage, V	40	100	40	40	40	70	96	60
Consumed power, kW	3.3	–	16.5	16–5	15	24	24	317
Cooling	Forced	Forced	Forced	Forced	Forced	Forced	Forced	Water
Mass, kg	35	12	110	115	180	170	185	1900
Kind of volt-ampere characteristic	Falling	Steep	Falling	Falling	Falling	Steep	Steep	Rigid
Notes		Attachment to transformer		Air-plasma cutting up to 6 mm				Provides operation of up to 30 stations of MAW

Table 4. Main characteristics of semi-automatic machines (SAM) and feeding units (FU) for arc welding of the «Paton» series

Parameters	*Type*					
	PS-100	*BP-200*	*PS-250*	*PS-250.1*	*PS-315*	*BP-600*
Maximum welding current, A	100	200	320	320	400	600
Number of rollers, pcs	2	4	4	4	4	4
Wire feed speed, m/min	0.8–5.0	2–12	1–16	1–16	2–20	2–25
Diameter of welding wire, mm	0.8	0.8–1.2	0.8–1.4	0.8–1.4	0.8–1.6	1.0–2.5
Mass of wire on reel, kg	5	5	15	15	15	15
Feasibility of welding with flux-cored wire	–	–	+	+	+	+
Mass, kg	8	12	22.6	125	200	21.6
Notes	FU	FU	FU	SAM	SAM	FU

Table 5. Main characteristics of installation for argon-arc non-consumable electrode welding

Parameters	*Type*	
	STSh-252	*A-500 UP*
Mains voltage, V	220 and 380	380
Welding current, A	70–260	50–500
Duty cycle, %	40	60
Open-circuit voltage, V	65	80
Consumed power, kW	16.3	40
Mass, kg	65	50 (without power source)
Welding of aluminium and its alloy	+	+
Notes	Block of arc burning stabilizing	Quality welding of aluminium without etching

Table 6. Main characteristics of machines for air-plasma cutting

Parameters	*Type*			
	«Kiev-1»	*«Paton PPR-200»*	*«Kiev-3»*	*«Kiev-4»*
Mains voltage, V	380	380	380	380
Operating current, A	45	200	300	315
Duty cycle, %	25	60	100	100
Open-circuit voltage, V	140	280	300	320
Consumed power, kW	10	60	75	77
Plasmatron cooling	Air	Water	Water	Water
Mass, kg	45	300	800	900
Thickness of metal being cut, mm:				
steel	6	60	80	90
copper	2	25	45	50
aluminium	5	50	60	70

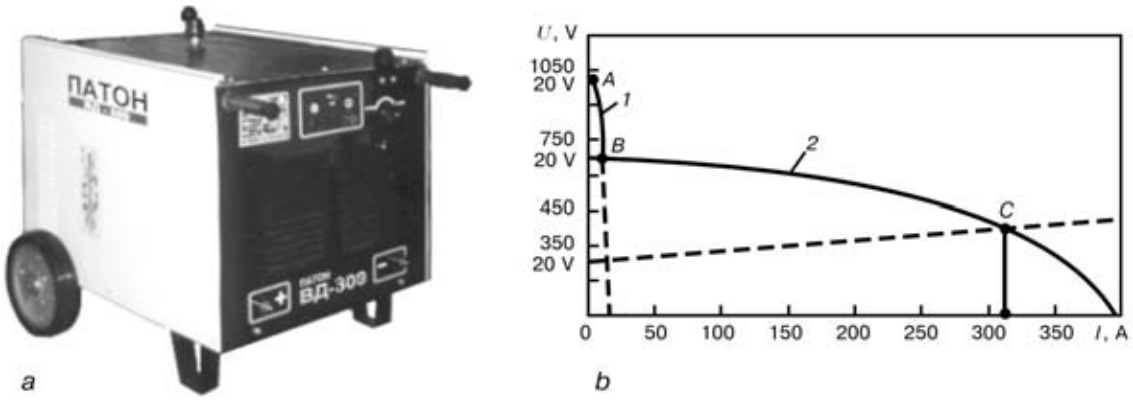

Figure 2. Appearance of rectifier VD-309 (*a*), volt-ampere characteristic of auxiliary (*1*) and operating (*2*) rectifier (*b*)

Table 7. Manufacture of new equipment

Description of product	*Quantity of models*				
	Before 1998	*1998–2000*		*2001*	
		in total	*including new models as compared with 1998*	*in total*	*including new models as compared with 2000*
Transformers	2	4	2	7	3
Rectifiers	6	7	3	8	2
Semi-automatic machines	4	5	3	6	1
Machines for air-plasma cutting	3	4	1	4	–
Installations for argon-arc welding	–	1	1	2	1
Plasma cutters	3	4	1	4	–
Gas torches	2	2	–	4	4
Units of autonomous cooling	–	1	1	2	1
Models in total	20	28	12	37	12
including those of main welding equipment	15	21	10	27	7

• welding units (250–500 A), including those for automobiles, tractors, etc.;

• full sets of lines for manufacture of welding electrodes (1–5 t per shift);

• complex works on mechanical treatment of massive components (see in detail in Website);

• welding electrodes, wires, consumables for surfacing (wires, strips, tungsten carbide, etc.);

• equipment for welding polymers; extruders (up to 2.5 kg/h, mass of unit — 4.8 kg), installations for butt and fillet welding of pipes (630 mm dia.), installations for manufacture of polymeric large-diameter shells (up to 1200 mm), butt welding of sheets, heating elements (detachable) and others;

• welding accessories: TIG, MIG/MAG welding torches, terminals, electrode holders, special cloth, etc.;

• welding tractors (500–2000 A) with power sources;

• manufacture of welded metal structures of any category of complexity and dimensions;

• equipment for electroslag technologies (including power sources up to 10000 A);

• invertor welding engineering (including sinergetics and pulsating systems).

In the near future the PWI PPWE will start manufacture of chopper attachments and invertor power sources.

Nomenclature of the products, volume of their production and realization in 2000 and 2001 allow us to make the conclusion about overcoming of the crisis situation by the plant.

DETONATION SYSTEM «PERUN-S» FOR DEPOSITION OF PROTECTIVE COATINGS

E.A. ASTAKHOV
The E.O. Paton Electric Welding Institute, NASU, Kyiv, Ukraine

Basic units were developed and a prototype of the automatic detonation system was made for deposition of coatings with widened operational capabilities, allowing it to be successfully applied for handling both research and production problems.

Key words: *detonation equipment, deposition technology, channels, feeders, control systems, powdered material, energy parameters, pulsed flows, coating properties*

The general trend now is to recover industry of Ukraine and other CIS countries and to gradual increase in their productive capacities. This undoubtedly will involve practical application of various coating methods to protect surfaces of parts operating under severe conditions of intensive wear and corrosion.

In this regard, detonation deposition of coatings is still one of the most efficient methods of thermal spraying [1–5]. Ensuring high quality of resulting coatings requires the appropriate high-productivity equipment.

This article considers designs of basic units of detonation equipment «Perun-S» and the system as a whole in terms of providing not only improved properties of sprayed coatings, but also widening of technological capabilities of the process.

Figure 1. General view of the ADS «Perun-S»

Automatic detonation system «Perun-S» is a joint development of the E.O. Paton Electric Welding Institute and Institute for Superhard Materials of the National Academy of Sciences of Ukraine. It is based on the scientific and practical experience accumulated from building and application of detonation systems «ADK-1» and «Prometej». Also, it incorporates new scientific and technical solutions. Design documents were developed, on the basis of which the pilot-commercial manufacture of the above system was arranged at Research and Production Company «Orgtekhavtomatizatsiya» (Simferopol, Ukraine)*.

Specifications of ADS «Perun-S»

Shooting rate (frequency of work cycles), Hz	3.3; 6.6
Length of the basic channel, mm	590
Length of an additional section, mm	500
Coating area deposited per cycle, mm^2	320
Coating thickness provided per cycle, μm	3–12
Powder utilisation factor, %	40–60
Flow rate of working gases, m^3/h:	
acetylene	1.0–1.2
propane-butane	0.9–1.1
hydrogen	3.2–3.6
oxygen	2.0–2.4
nitrogen	4.6–5.2
compressed air	4.6–5.2
Limits of displacement of coating device, m:	
right-left	1.50
forward-backward	0.85
up-down	0.20
Power consumption, kW	2
Supply voltage, V	220; 380
Frequency, Hz	50

The general view of the system «Perun-S» is shown in Figure 1.

The system comprises a device for abrasive treatment and deposition of coatings (gun), gas distribution panel, gun displacement device (manipulator), gun and manipulator control units, and device for monitoring of the coating deposition process. To be commercially applied, the system needs a noise-proof box (with an area of not less than 15 m^2) equipped with forced ventilation means, and an operator's room (8 m^2) connected to the box and having a viewport looking to the box. The process is controlled remotely from the operator's room.

Functioning of the coating deposition device is based on a method differing from that used before in that the working gases, e.g. oxygen and acetylene are continuously fed to the combustion chamber in the

* The author expresses gratitude to his colleagues who participated in building the ADS «Perun-S»: V.S. Klimenko, V.S. Skadin, A.I. Kildy, A.A. Polonsky, V.N. Kolesnichenko, Yu.N. Ilchenko, A.A. Mozzhukhin, as well as to managers of the E.O. Paton Electric Welding Institute, Institute for Superhard Materials and Company «Orgtekhavtomatizatsiya» for their assistance in arrangement of the work for production of pilot-commercial equipment and industrial implementation of the process.

form of a mixture in the stationary flow mode, while periodicity of the process in the absence of contact of the fuel gas mixture with the detonation products is achieved through a periodic feed of a neutral gas (nitrogen, air) in intervals between feeding of a powdered material and ignition of the gas mixture. Here, exceeding of 2.5–3 times in the purging pressure of nitrogen, compared with pressure of working gases, provides cut-off of the latter.

Although the cyclic character of the process does persist in this case, a finished portion of the fuel mixture with a preset concentration of components is fed per cycle, thus allowing quality of the coatings to be improved owing to a volume homogeneity of the gas mixture [5].

Channel. One of the main and most important components of detonation systems is a channel (explosion chamber) [3, 4], where the fuel mixture is mixed with a spray material powder and where a high-velocity flow of the detonation products with the suspended spray material particles is formed.

The channel should provide the required level of energy parameters of a pulsed flow of the combustion products, sufficient for heating and acceleration of the optimal portion of powder with the most efficient utilisation of energy released in combustion of the fuel mixture.

Channels of the prior art had length of 1300–2500 mm [3, 6, 7]. Our case presents a pioneering use of a channel with length reduced to 590 mm in practice of detonation spraying. This allowed consumption of working components to be decreased, and shooting rate to be increased with an unchanged initial pressure of feeding them to the channel, thus raising productivity of the spraying process.

The channel is of a sectional type. This makes it possible to control the degree of heating of particles. Elongation of the main channel to 1100 mm is done through adding an extra section.

Feeder. The system uses a feeder with a pulsed axial feed of a spray material. Feeders of this type have as a rule a limited volume of the hopper, as the powder portion injected into the channel is in direct dependence upon the level of powder in the hopper. Decreasing it is accompanied by decrease in the powder portion being injected [8]. This requires a constant filling up of the feeder with powder. The developed extra blowing system (increase in the pressure of nitrogen for transportation of powder as it leaves the hopper) made it possible to stabilise to some extent the portions and increase the time of operation of the equipment to refilling the feeder, but involved some increase in a nitrogen flow rate and, hence, deterioration in properties of coatings.

This drawback was eliminated in the design of the feeder used in ADS «Perun-S» (Figure 2).

The feeder developed consists of a cylindrical cup *1* with cover *2* connected to the internal cup *7*. Two fastened rubber gaskets *8* and *9* form a movable bottom of the casing. On the bottom the feeder is pressed by

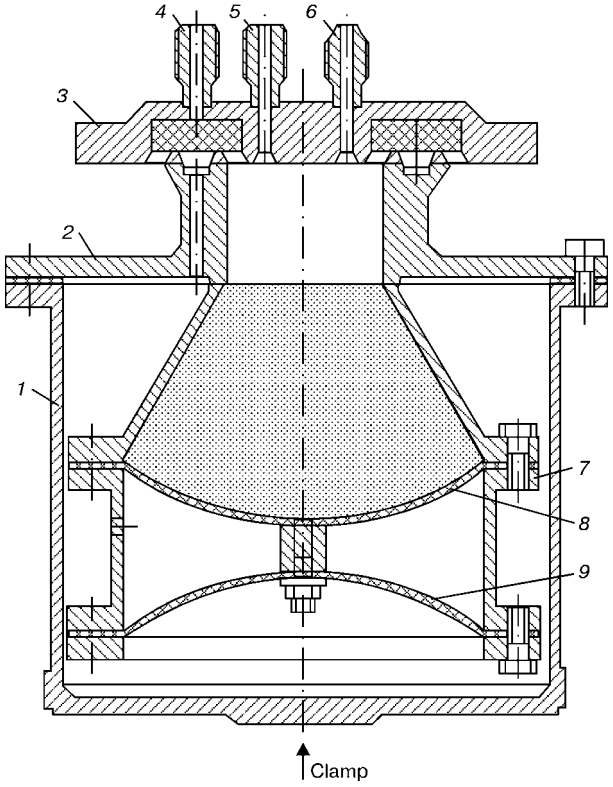

Figure 2. Design of the feeder with casing having a movable bottom (see designations in the text)

a pneumatic cylinder to cover *3* of the feeder installation unit. The cover has three unions *4–6*. Transporting gas which carries the powder is fed through union *6*. The gas-powder mixture is fed through union *5* to the channel. The bottom of the casing is raised with utilisation of powder during the spraying process. This provides maintaining of a constant level of powder in the feeder to ensure a stable density of the gas-powder mixture during the spraying process. The bottom is raised by means of compressed air fed through union *4* to the space between the external cup and the bottom. Air pressure is regulated using distributors of the pneumatic unit controlled by the system for monitoring the presence of powder in the detonation products.

Capacity of one feeder provides a consistent feed of powder, e.g. for 2 h of continuous operation of the equipment at a shooting rate of 3.3 Hz.

Systems for on-line diagnostics of the process. The current procedure for assessment of quality of thermal spray coatings is through testing witness specimens made from similar coatings. Reliable means for non-destructive testing of coatings applied to actual parts are unavailable so far. Therefore, increased requirements are imposed on detonation units for stability of their operation to guarantee consistent properties of coatings on parts. Stability of operation of a unit implies consistency of energy characteristics of the spray material particles in formation of coating layers.

Experience of operation of detonation equipment evidences that there are cases where readings of the registration instruments installed in gas lines vary within permissible limits, while the process techno-

logy and coating formation conditions suffer sever violations. Most often the cause of such violations is a change in a powder portion fed to the channel prior to detonation of the gas mixture. This occurs either because of a decrease in section of the gas line channel connecting the feeder to the channel (because of sticking of baked powder particles to the channel walls), because of violation of air tightness in this line, or because of decrease in the amount of powder in the feeder hopper.

The special device for monitoring parameters of the pulsed metallising powder was made to quickly and timely reveal violations in the spraying technology [9].

The monitoring device is intended to visually detect (on the basis of readings of a measuring instrument) the presence or absence of the spray material powder in the detonation products flowing out from the system channel after initiation of the detonation. Also, it enables (after preliminary calibration) determination of the amount of powder contained in the detonation products. For this, the measuring device is calibrated either for the powder content in weight percent or for thickness of a coating formed per cycle.

The principle of operation of the device is based on increase in the intensity of light emitted from the high-temperature flow of the detonation products in the case when it contains heated particles of the spray material powder. The intensity of light was found to increase with increase in the amount of powder contained in the detonation products.

The device for monitoring the presence of powder in the combustion products can affect operation of the actuators of the detonation equipment through its control system.

In the case of absence of powder particles in the detonation products, as well as in the case of misfire, i.e. miss of a shot because of non-ignition of the fuel mixture in the chamber, the sensor in the feedback circuit will send a signal to the control unit, and the equipment will be switched off.

With just one misfire the equipment may not be switched off. In this case the next shot directly following the missing one, containing an increased powder portion, will get to the safety gate which closes at this moment the surface of a workpiece, thus ensuring the consistent quality of a spray coating.

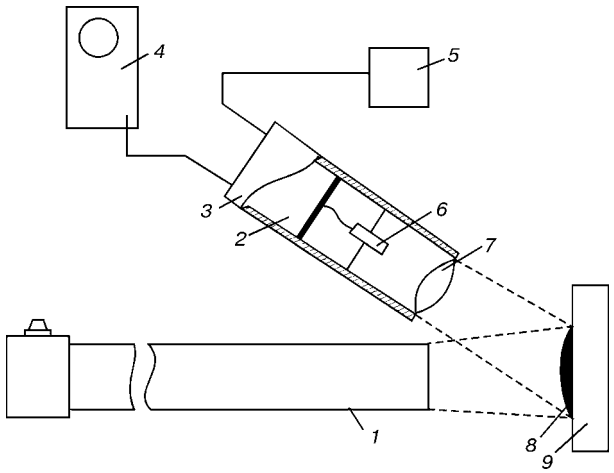

Figure 3. Schematic of the device used to reveal latent defects in a coating layer during spraying (see designations in the text)

However, the possibility of monitoring the intensity of light emitted from the metallising flow does not always guarantee formation of a quality coating. For example, the sprayed coating may separate from the substrate because of poor cleaning or insufficient abrasive treatment of the substrate surface. This defect can be detected immediately after deposition of a coating by visual examination using a magnifying glass or by grinding.

The method was suggested and device was made during the development of the «Perun-S» system for detection of latent defects with an area of more than 0.2 cm^2 directly during spraying of the detonation coatings.

When the spray material powder particles heated to a melting point hit the substrate, their rapid deformation (for 0.1–0.3 μs) and cooling occur [6, 7]. This is accompanied by simultaneous physical-chemical processes which promote adhesion of individual particles to each other and to the substrate. Latent macrodefects (of the separation type) are formed immediately after formation of a coating and its cooling. Changes in conditions of heat transfer to the substrate within the defect zone, caused by high-temperature gas or metallising flows affecting the coating, can reveal effects the registration of which allows separations and coarse pores to be detected in it. Theoretical description of these effects is based on results of calculations of surface temperature T_s of deformed particles fixed to the substrate during spraying.

Analysis of the results of calculation of T_s in spraying nickel and aluminium oxide allowed the following conclusions [10]:

- in the presence of a macrodefect between the upper layer of a coating and a workpiece (with or without a coating) the surface temperature of a new sprayed layer immediately after its formation is much higher than that of a defect-free region of the coating;
- with growth of thickness of the coating over the macrodefect its surface temperature after spraying of new layers will decrease.

Functioning of the device providing such monitoring is schematically shown in Figure 3. Workpiece *9* on the surface of which coating *8* is to be deposited is placed in front of the exit section of channel *1*. Photosensor *3* consisting of optical system *7*, photoelement *6* and preamplifier *2* electrically connected to it is mounted on channel *1*. Photosensor *3* is placed so that its optical axis is directed to the centre of coating spot *8*. Preamplifier *2* is connected to the constant voltage source *5*, while the output of preamplifier *2* is connected to the input of oscillograph *4*.

The high-temperature flow of the detonation products is periodically ejected from the channel *1* during operation of the detonation equipment. The flow contains heated (up to a pre-melting point in the optimal

case) particles of the spray material powder. Light emission or brightness of the spot of coating *8* being formed is first very high at the moment of formation of the detonation coating layer due to impact on the surface of workpiece *9* by the heated powder particles. This is evidenced by peaks (Figure 4) of signals from photosensor *3*, which are used to estimate the surface temperature of coating spot *8* on the oscillograph screen.

During a time between two regular shots made by the detonation equipment (300–600 ms) the surface temperature of coating *8* decreases almost to a temperature of workpiece *9*, which is also fixed on the screen of oscillograph *4* owing to the signals sent by photosensor *3*, the amplitudes of which reduce during this time actually to zero. Rapid decrease in temperature of the surface is caused by an intensive heat transfer into the bulk of workpiece *9* due to a good contact with it over the entire plane of the sprayed layer of coating *8*.

In the case of formation of a microdefect (e.g. crack) under the sprayed layer the cooling rate at the surface of coating *8* dramatically decreases, i.e. the coating over the defect remains heated much longer due to a poor heat transfer through the crack. The fact of formation of a microdefect is fixed by oscillograph *4* from a relative increase in the amplitude of a signal received from photosensor *3* 20–40 ms after the shot with which a defective coating was deposited. The level of this signal will no longer decrease to zero, like in the case of formation of defect-free layers deposited with previous shots. In this case it will decrease much more slowly. This is caused by the fact that coating with a crack located under it emits light for a much longer time.

Spraying process control and regulation system. The control panel of ADS «Perun-S» consists of three independent units located in one casing:

- positioner which includes all the elements for control and monitoring of displacements made by the manipulator, as well as setting of the displacement mode and speed;
- control unit housing all elements for control of operation of the equipment, setting of operation cycles for actuators and operation modes for feeders, maintaining the level of powder in them during spraying, and fixing the number of working cycles in feeding the powder from the first and second feeders;
- unit for monitoring the quality and composition of the metallising flow, its weight and component distribution, as well as channel temperature.

The moment of locking the corresponding sealed-contact reed relay by a rotating magnet is used to send signals to make the actuators operate. This design allowed drawbacks of an electromechanical command apparatus [6] to be avoided and a flexible system for variation of time ranges for their operation relative to each other to be provided.

Gas distribution panel for feeding working media. A distinctive feature of a multichannel panel is that each of the working medium lines has high-frequency pressure-gradient regulators, which stabilise output parameters of gas flows independently of their variations at the input and pressure drop in gas bottles.

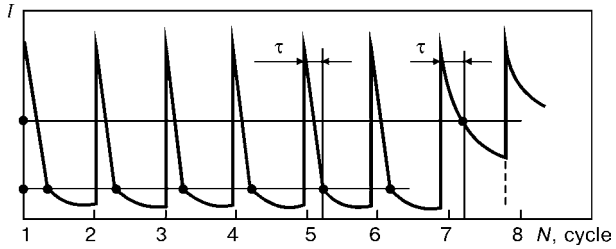

Figure 4. Plot of variations in the intensity of light I from the coating surface layer in the case of presence or absence of defects in it (N — number of cycles)

The use of a fluorine-plastic float in a rotameter to feed gas to the feeder and direct throttling of its flow provide a high-accuracy feed of the spray material powder (even that of a low looseness). This provides an increase in reliability of operation of the entire system.

Equipment displacement manipulator. The three-axis manipulator for displacement of the equipment allows spraying on flat surfaces of any size. To spray parts of the type of bodies of revolution, it is necessary to additionally equip the manipulator with a rotator. The versatile welding rotator of model 1111020 [11], featuring smooth step-free regulation of the rotation frequency within a range of 0.1–5.0 rpm, was proved good for practical application. Its maximum load-carrying capacity is 100 kg.

Basic technological capabilities of ADS «Perun-S». The equipment developed can operate with different working gases (propane-butane or hydrogen can be used as a fuel gas in addition to acetylene; nitrogen or compressed air can be used for transportation of powder, purging of the coil and channel and dilution of the fuel mixture).

Classical version of operation of the detonation systems is based on the use of acetylene as a fuel gas, as its mixtures with oxygen are characterised by a high detonation velocity, high dynamic head and temperature of the gas flow behind the detonation wave front. In addition, they have almost no pre-detonation mode.

The use of acetylene-oxygen mixtures requires careful adhering to safety regulations imposing severe requirements both on operation of the equipment and on a spraying production shop as a whole. All this makes designs much more sophisticated, as it is necessary to additionally fit the equipment with blow-back safety systems and units.

Analysis of literature data [12] and calculations are indicative of the fact that dynamic characteristics of the gas flow behind the detonation front in stoichiometric acetylene-oxygen, propane-butane and methane-oxygen mixtures are almost identical, and those of propane-butane and oxygen even higher by 5–10 %. Achievement of practical results and building of the corresponding equipment by the I.N. Frantsevich Institute for Materials Science Problems, E.O.

Designation of parts	*Spraying location*
Magnetic recording devices	Company «Mayak», Kyiv, Ukraine
Hydraulic cylinder rods, bearing components, piston pins, supporting necks of shafts, crankshafts of ship engines	Company «Yugrybsudoremont», Sevastopol, Ukraine
Commercial sewing machine knives, high-voltage terminals of power supplies, edge seals of electric valves	Company «Orgtekhavtomatizatsiya», Simferopol, Ukraine
Mating surfaces of parts and assemblies for aircraft engineering (shrouds of compressor impellers, segments of gas turbine engine fans, fuel-injection nozzles)	Kazan Branch of R&D Institute for GTE, Kazan, Russia
Saw disks for cutting hot rolled products, hydraulic rods, die casting moulds	Vitkovice Metal Works, Ostrava, Slovakia
Units of oil pumps (impeller sleeves, plain bearings, labyrinth packs)	«Druzhba» Oil Pipeline Agency, Rovno, Ukraine
Agricultural machinery parts	Agricultural Academy, Kaunas, Lithuania
Casings and rotors of hydrogen pumps, screening machine plates, pump shafts	«Scancoating» Company, Tammisaari, Finland

Paton Electric Welding Institute, Institute for Superhard Materials of the NAS of Ukraine, and Polytechnic Institute (Kalinin, Russian Federation) became a reality owing to theoretical calculations made by associates of the M.A. Lavrentiev Institute of Hydrodynamics of the Siberian Division of the Russian Academy of Sciences (Novosibirsk) under the leadership of T.P. Gavrilenko [13].

While solving the problem of using hydrogen as a fuel gas, the focus of the developers was on replacement of gas bottles by electrolytic cells for gas supply. The small-size machine «Perun-M» characterised by an increased independence is based on this principle. Its casing houses a device for abrasive treatment and deposition of coatings, noise-proof chamber, workpiece manipulator, gas generator (electrolytic cell) and control and monitoring unit. The floor area it needs is about 5 m^2, and it needs just electric power to function. Arrangement of commercial manufacture of increased-productivity electrolytic cells combined with the use of a compressor, will make it possible to solve the problem of gas supply using hydrogen and oxygen for the «Perun-S» system, and its normal functioning under industrial conditions where the gas supply from bottles is difficult to apply.

The control unit for operation of the equipment allows spraying at a shooting rate of 6.6 and 3.3 Hz, as well as variations of location of the spray material particles in the channel relative to the moment of initiation of a working mixture. This makes it possible to vary within wide ranges their velocity and degree of heating at the moment of formation of a coating layer, affect the extent of their oxidation and vary chemical and phase composition.

Fitting the equipment with two independently controlled powder feeders makes it possible to change from the mode of detonation-abrasive treatment to the coating mode without switching off of the machine, perform abrasive treatment and coating in one working cycle, spray two-component coatings without the need to preliminarily prepare the mixtures and regulate their chemistry, vary composition of the working mixture along the length of the channel (one feeder supplies gas without a powder), spray uniform coatings or coatings with a minimum allowance for machining on large surfaces, owing to a stable operation of the feeder (variations in portion of an injected powder during operation are not more than 8 %).

Design of the sectional channel allows the use of special nozzles to change profile of the spraying spot, redistribute concentration of spray particles in a flow across the section of the channel and deposit coatings on inside surfaces of pipes.

The Table gives a list of main ranges of parts treated by detonation spraying, as well as companies that arranged special shops for these purposes using ADS «Perun-S».

The equipment developed is used for research purposes at the PWI (Kyiv), Institute for Superhard Materials (Kyiv), Institute of Thermoelectricity (Chernovtsy, Ukraine) of the NAS of Ukraine, Technical University (Tallinn, Estonia) and University of Technology (Tampere, Finland).

Specialists of the PWI and Institute for Superhard Materials rendered technical assistance in arrangement of spraying production shops, assembly and setting up of equipment, training of personnel in operation of the equipment, development and mastering of the spraying technology.

Service of this equipment for 10 years proved the efficiency of the implemented design and technology solutions (this applies particularly to control systems and feeders).

Owing to deposition of wear- and corrosion-resistant coatings the service life of parts treated is extended by a factor of 1.5–10.

The list of basic materials used for detonation spraying and properties of the resulting coatings are described in detail in studies [1, 5, 6, 14].

CONCLUSIONS

1. The possibility of using propane-butane as a fuel gas for detonation spraying was proved, which allowed design of the equipment involved to be simpli-

fied and requirements to production shops imposed by safety regulations to be decreased.

2. The use of the process monitoring device allowed stability of operation of the powder feeder to be objectively estimated through registration of the amount of powder in a high-temperature pulsed flow, thickness or weight of the deposited coating to be predicted, and quality of the formed layers to be controlled by revealing latent macrodefects.

3. The pioneering method was suggested and device was developed for combining abrasive treatment of the substrate and deposition of coating on it in one cycle, which allowed the productivity of the process to be raised and its cost to be reduced.

4. The use of the equipment displacement manipulator combined with a rotator enabled spraying of parts of any sizes with simple or complex profile.

5. Long-time operation of the automatic detonation system «Perun-S» under various production conditions proved that it is a high-productivity stationary equipment. Its commercial application is especially efficient for mass or large-scale production of a wide range of coated parts. Technological capabilities of the system opened up wide prospects for conducting research in order to further improve the detonation equipment and technology, deposit various compositions, investigate methods for their preparation and the effect of a character of distribution of components in them on properties of composite coatings.

1. Tyurin, Yu.N. (1999) Improvement of detonation coating equipment and technologies. *Avtomatich. Svarka*, **5**, 13–18.
2. Astakhov, E.A., Borisov, Yu.S., Kildy, A.I. (1998) Commercial detonation coating technology and equipment. In: *Proc. of Int. Conf. on Welding and Related Technologies for the XXI Century*. Kyiv: PWI.
3. Kharlamov, Yu.A. (2001) Barrels of units for detonation spraying of coatings. *The Paton Welding J.*, **10**, 12–16.
4. Gavrilenko, T.P., Nikolaev, Yu.A., Ulianitsky, V.Yu. (1992) New materials and technologies. In: *Theory and practice of material strengthening under extreme conditions*. Novosibirsk: Nauka.
5. Yushchenko, K.A., Astakhov, E.A., Klimenko, V.S. et al. (1990) Detonation spraying of strengthening coatings and ways of its development. In: *New processes and equipment for thermal spraying and vacuum deposition*. Kyiv: PWI.
6. Zverev, A.I., Sharivker, S.Yu., Astakhov, E.A. (1979) *Detonation coating*. Leningrad: Sudostroenie.
7. Shorshorov, M.Kh., Kharlamov, Yu.A. (1978) *Physico-chemical principles of detonation coating*. Moscow: Nauka.
8. Astakhov, E.A., Zverev, A.I., Sharivker, S.Yu. et al. (1979) Detonation coating feeders. *Poroshk. Metallurgiya*, **3**, 75–78.
9. Klimenko, V.S., Skadin, V.G., Astakhov, E.A. et al. (1980) Reflex detonation units. In: *Detonation coatings*. Kalinin.
10. Klimenko, V.S., Borisova, A.L., Skadin, V.G. (1983) *Detonation coating technology*. Kyiv: IPM.
11. (1986) *Catalogue of mechanical welding equipment*. Moscow: VNIITEMP.
12. Dvukraev, B.N. (1976) Gas-thermodynamic parameters of detonation coating. *Poroshk. Metallurgiya*, **2**, 62–65.
13. (1986) Problems of application of detonation in technological processes. In: *Transact. of Institute of Hydrodynamics of USSR AS SD*. Novosibirsk.
14. Astakhov, E.A., Filippov, D.T. (1988) *Detonation spraying for repair and strengthening of shipyard items*. Kyiv: Znanie.

STATE-OF-THE-ART OF UNDERWATER WELDING AND CUTTING IN UKRAINE

V.Ya. KONONENKO

Enterprise «Ekotekhnologiya», Kyiv, Ukraine

The paper analyzes the state-of-the-art of underwater welding and cutting in Ukraine. It is established that coated-electrode wet welding now is the main process of underwater welding. In Ukraine practically all the metal structures are cut underwater by applying tubular-electrode oxy-electric cutting. Other underwater cutting processes have not been used lately.

Key words: *wet underwater welding, flux-cored wire cutting, oxy-electric cutting, coated electrodes, flux-cored wire, exothermal electrodes*

Underwater welding and cutting in the former USSR began to be applied from the middle of 1930s [1] in repair of underwater pipelines, as well as in salvaging and reconditioning of ships with combat and navigation damage. The main customer for development of these technologies and equipment was the Ministry of Defense of the Soviet Union. Several organizations conducted work in this area. In 1967 a team was set up at the PWI, which was later re-organized into a specialized laboratory on investigation and development of electrode materials, technologies and equipment for different processes of welding and cutting under the water.

Coated-electrode underwater welding. In Ukraine underwater welding has been performed for a long time with coated electrodes of grades LPS-4, LPS-5, EPS-5, EPS-35, EPO-55, EPS-52, EPS-A, etc. [2–4], developed in 1940–1950. The main manufacturer was «28th Military Plant» in the city of Lomonosov, Russia. Several electrodes were manufactured directly by the performers of underwater technical works. Underwater welding with the above electrodes was characterized by unstable arcing. High beads with coarse-rippled surface formed, and slag crust detachment was difficult. In welding of a multipass welded joint deterioration of the second and subsequent welds was found.

Electrodes of EPS-52 grade had the most satisfactory welding-technological properties. Mechanical properties of joints, produced in underwater welding with these electrodes, corresponded to those, made in air with electrodes of E34 type. Production of EPS-52 electrodes has now been resumed in Enterprise «28th Military Plant». Electrodes of EPS-A grade are designed for welding under the water the higher strength hull steels of AK type. Satisfactory welding-technological properties of the welds were provided only in performance of downhand and vertical welding. The metal, deposited with these electrodes, had a deeply-austenitic structure. However, EPS-A electrodes have not been produced for more than 10 years now.

Wet underwater welding with coated-electrodes has its positive and negative features. The following may be stated as the positive features:

- high flexibility of the process;
- ability to use widely accepted mobile welding units with a self-sufficient drive;
- small weight and dimensions of equipment for underwater application;
- higher degree of protection of the molten metal drop due to a lip, formed at the electrode tip, than in welding with self-shielded flux-cored wires;
- ability to produce root weld with back bead formation.

The following features are negative:

- low efficiency of the process;
- large amount of gas phase and mechanical suspension in the reaction zone, hindering visual inspection of arcing and weld formation;
- considerable scatter of strength and ductile properties of the metal of welded joints, depending on the depth of work performance and qualification of diver-welder.

Ukrainian market of welding consumables is currently offering the possibility of supplying electrodes of E38-LKI-1P type for underwater welding of carbon and some low-alloyed steels, developed at St.-Petersburg Marine Technical University together with Company «Electrodny Zavod» [5]. They are manufactured to order by «Elektrodny Zavod». These electrodes have not yet been used for conducting welding operations in Ukraine.

Based on numerous systematic studies the PWI has produced a gas-slag composition, which allowed development of a new coated electrode for wet welding under the water in all positions [6, 7]. Electrodes of EPS-AN1 type feature good welding-technological characteristics and are designed for underwater welding of a number of carbon and low-alloyed steels at down to 20 m depth. They provide mechanical properties of weld metal on the level of those of electrode metal E-42. By their welding-technological and mechanical properties they are superior to electrodes of E38-LKI-1P type.

Electrodes of EPS-AN1 grade were used to perform underwater repair of a pulp-feed line in Kyiv. They were also applied in mounting of metal structures of underground facilities, having a water layer on the surface. These electrodes were used in 2001 for welding galvanic-action protectors to a berthing foundation for oil unloading in the region of the city of Odessa. They are currently produced in small batches to order under laboratory conditions.

It should be noted that a number of companies, selling diving gear in Ukraine, offer electrodes for underwater welding, manufactured by various companies. These electrodes are certified to international standards. Their cost is 3–5 times higher than that of similar local electrodes.

Wet mechanized underwater welding. A unique technology of wet mechanized welding with self-shielded flux-cored wires was developed as part of the work with Navy [8–11]. The main element of the technology was self-shielded flux-cored wire of PPS-AN1 type. Its design and technological features of its manufacturing allowed placing the wire into the water-filled cavity of feed mechanism of a semi-automatic machine. In this case there was no need to feed shielding gas into the arcing zone or inner cavity of the semi-automatic machine. Reduction of the volume of gas phase and suspensions in the reaction zone enhanced the ability to visually control the arcing process and formation of weld metal. Such technological features enabled the PWI Design Bureau developing a successful design of a specialized semi-automatic machine for operation at considerable depth. Two of its modifications A1450 and PSh141 have passed government trials and were accepted for fitting Navy rescue units. Their batch production was organized in the PWI Pilot Plant of Welding Equipment. In addition to semi-automatic machines, accepted for supplying the Navy, semi-automatic machines of grades A1660 and PSh146 were produced for the needs of national economy.

Flux-cored wires of grades PPS-AN1 and PPS-AN5 (wire for welding in sea water) for underwater welding were batch-produced by the PWI Pilot Production and Pilot Plant of Welding Consumables. When welding with flux-cored wire the structures of steels VSt.3sp, 09G2, 09G2S and 19G in fresh and sea water at down to 20 m depth, mechanical properties of welded joints were equivalent to those of joints, made in air with E-42 electrodes. In welding at greater depths the welding-technological characteristics and mechanical properties of the metal deteriorated. Batch-production of these wires in the PWI Pilot Plant of Welding Consumables and Pilot Production was interrupted in 1994.

Since 1991 the PWI has been producing PPS-AN2 flux-cored wire (modification of PPS-AN1 wire) to a specification in the laboratory conditions. This wire provides good welding-technological properties in welding at down to 20 m depth. Testing of PPS-AN2 wire, conducted in 1992 in the USA, demonstrated that the water, in which welding is performed, impairs

Electrode material grade	σ_t, *MPa*	σ_y, *MPa*	δ_5, %	KCV_{-20}, J/cm^2	*Bend angle, deg, class B AWS AWS D3.6M:1999*
EPS-52	340–400	Not specified	≤ 6	N/D	N/D
EPS-AN1	420–460	320–350	≥ 10	≥ 25	180
E38-LKI-1P	400	Not specified	≤ 8	N/D	N/D
PPS-AN1	400–430	300–320	14–18	≥ 10	180
PPS-AN2	400–440	300–340	13–18	≥ 25	180
PPS-AN5	420–460	320–360	13–17	≥ 25	180
PPS-EK1	400–460	300–360	14–18	≥ 25	180

the ductile properties of the welded joint metal. Mechanical properties of welded joints, produced, when using this wire in fresh water, are given in the Table.

In 1997 Enterprise «Ekotekhnologiya» developed a self-shielded flux-cored wire of PPS-EK1 grade for mechanized underwater welding of structures of carbon and low-alloyed steels of VSt.3sp, 09G2 type etc. at the depth of down to 20 m. The wire is batch-produced to TUU 14288312.000–97 specification, has the certificate of Ukrainian Certification Center UkrSEPRO and is supplied for performance of underwater operations in repair of port facilities and ships afloat in the Baltic Sea and oil-producing offshore platforms in the Caspian Sea. Mechanical properties of welded joints are given in the Table. PPS-EK1 wire can be used instead of PPS-AN1, PPS-AN5 and PPS-AN2 wires with semi-automatic machines of type A1660, A1450, PSh141 or PSh146 for underwater welding.

Since 1981 the PWI has developed a number of demonstration samples of flux-cored wires for wet underwater welding of HSLA steels. Strips of stainless steel with different content of nickel and nickel strips were used as the sheath. Demonstration samples of wires ensured wet welding of steels with more than 0.4 carbon equivalent in all positions. Flux-cored wires of austenitic class were developed for automatic welding in deep waters. Experiments, performed in the simulation test chamber, demonstrated the ability to weld carbon and low-alloyed steels, as well as hull steels of AK type at down to 1000 m depth.

In 1985 to fulfill a Navy order a demonstration sample of a unique unit A1802 was developed for automatic welding of ship-lifting lugs to deep-water objects, and its full-scale testing was conducted. The unit allowed performance of two-sided multipass welds by two arcs in the downhand position. Slag crust was removed after each pass with a multi-pin gauging tool of an ingenious design. A mock-up of a deep-water immersible power source USIP was developed to ensure the unit operation. Its full-scale testing was conducted using A1802 unit. The source had a flat and falling external volt-ampere characteristics, which allowed performance of automatic welding with flux-cored wires and coated electrodes. Equipment and electrode materials (flux-cored wires of austenite class) were accepted by a government commission and approved for subsequent introduction. However, lack of funding did not permit continuing work in this area.

Technology of wet mechanized welding is an extremely successful technological solution in terms of restoration of practically all the kinds of metal structures under water. Low weight of the equipment, its compactness and reliability and fast mastering allowed performing a large amount of work both in the territory of Ukraine, and outside it [12–14]. In Ukraine underwater welding was used to repair underwater passages across the Dnieper and Seversky Donets rivers, Donuzlav lake, water ducts and pulp-feed lines, water works at upgrading low-level water intake facilities in Krivoj Rog (SevGOK) and to lift sunk ships. Unique repair of an underwater passage of a gas pipeline across the Dnieper river was performed. The pipeline was made of steel of X60 type with 22 mm wall thickness, its working pressure was 7 MPa. Welding was conducted with flux-cored wire, which provided a deep austenitic structure of weld metal. A lot of underwater welding was used in 1974, when salvaging «Mozdok» motorship sunk in the area of Odessa city.

The market of services, related to application of mechanized underwater welding, has shrunk right now. Funding of the work by Russian Navy was cut in 1992. Number of divers, who were trained in the PWI facilities, became smaller. Batch production of semi-automatic machines for underwater welding was stopped in 1993. No components are manufactured for them, either. A new modification of a semi-automatic machine for underwater welding with mechanical switching of feed rate is being tested now. Wide introduction of this semi-automatic machine is improbable, because of its limited technological capabilities.

Mechanized underwater welding with local drying of the working zone. In Ukraine work is being conducted by one businessman on improvement of the technology and equipment of mechanized underwater welding with local drying of the working zone. The main element of the equipment system is a closed gas-filled feed mechanism with a stock of wire for welding and a mini-chamber, where the welding process is run and the weld forms. Mini-chamber is pressed to the structure being welded by the welder-diver. He also switches the wire feed on and off. The other process parameters are controlled by an opera-

tor, who is on the surface. Water driving away from the reaction zone is achieved with CO_2 gas or argon in a mixture with oxygen. Welding is performed with Sv-08G2S wire. Based on the author's information, testing, conducted in Chernomorskoe township, demonstrated rather high performance of this equipment system. Further testing was conducted in the USA. In underwater welding at down to 20 m depth of a number of samples of low-alloyed steels, high mechanical properties of the joints were produced, corresponding to class A AWS D3.6M:1999.

Mechanized underwater cutting. During development of flux-cored wires for underwater welding, it was found that a number of components, added to the wire composition, provide a deeper penetration of the base metal. Obtained investigation results were the basis to develop specialized flux-cored wires for underwater severing [13–16]. These wires provide effective melting and oxidation of the metal being cut. Cut cavity blowing after removal of the molten metal was performed by adding gas-forming components to the core charge composition. In flux-cored wire severing semi-automatic machines for underwater welding of A1660 or A1450 type («Neptun») and arc power sources, applicable in this case, can be used. Cutting of up to 20 mm thick metal was performed at currents of 300–600 A. If the cut metal thickness is greater, larger diameter wire should be used, and power source, providing working current of 900–1000 A, should be applied. Experiments on cutting, made in the simulation chamber, showed that the process can be conducted even at more than 600 m depth. Cutting process efficiency becomes somewhat higher with the increase of depth.

In 1979 a specialized semi-automatic machine and deck power source were developed for cutting up to 50 mm thick metal under the water to fulfill a Navy order. During its testing, however, it was found that the diver is tired quickly, as the holder designed for 1000 A current, has a considerable weight, flux-cored wire of 3 mm diameter is rigid, and the weight of the immersible mechanism with the wire is more than 50 kg. This equipment system did not become widely applied, but it was used to perform unique work on cutting out a hole in the casing of a submarine reactor compartment [17].

Equipment upgrading was carried on, in view of the high effectiveness of the process of underwater severing and elimination of oxygen from the processing sequence. A specialized smaller-weight semi-automatic machine PSh131 was developed, which was put into production at the PWI Pilot Plant of Welding Equipment. Flux-cored wires for cutting are batch-produced by the PWI Pilot Plant of Welding Consumables and Pilot Production. Manufacturing of wires for underwater cutting is now interrupted because of a lack of orders. This technology was used to perform a number of operations of underwater severing of ships and other metal structures [15, 17–19]. Flux-cored wires for cutting were used in preparation of underwater metal structures for welding.

Underwater cutting with coated electrodes. A number of operations of electric-arc cutting (EAC) under water were performed, using coated welding electrodes of EPS-52 type. This method allows cutting metals 5–10 mm thick [2, 3]. However, despite the low efficiency, this process is often used due to its simplicity, inexpensiveness, and no need to apply oxygen in the technological process. In order to improve the efficiency of cutting, the PWI developed specialized coated electrodes of grade ANR-5P for underwater cutting [20]. A layer of polyethylene was applied onto the coating surface to provide hydraulic insulation. One electrode of 4 mm diameter allows making a cut 120 mm long on 10 mm thick steel. These characteristics are significantly higher than when EPS-52 electrodes are used. Electrodes are manufactured to order at the PWI in small batches under laboratory conditions.

Oxy-electric cutting under the water. Alongside with coated-electrode EAC, oxy-electric cutting (OEC) under the water with electrodes of grade EPR-1, developed in 1950s, became widely accepted [2, 3]. Batch production of electrodes has been mastered at Enterprise «28th Military Plant». The electrodes were in constant demand, however, comparative testing of EPR-1 electrodes and of their foreign analogs, conducted at the end of 1980s, showed that the speed of cutting with the former is lower. The PWI developed a new electrode of ANR-T8 grade and holder for OEC. Hydraulic sealing of the coating is performed with a thermosetting tube. Length of a cut, made with one electrode on 20 mm thick steel, is up to 400 mm. Electrodes are currently produced at the PWI under the laboratory conditions.

Underwater cutting with exothermal electrodes. The PWI developed samples of electrodes for underwater exothermal cutting, ordered by Navy. In 1991 full-scale testing of the electrodes was conducted under the conditions of the Baltic Fleet. Batch-production of these electrodes was not organized, as work by the orders of FSU Navy was stopped in 1992. These electrodes are not produced in Ukraine now.

Based on the results, obtained during performance of R&D together with FSU Navy, specialized equipment was developed and a shop section was set up to manufacture exothermic electrodes in St.-Petersburg. These electrodes are currently produced to order. Manufacturing of specialized holders for these electrodes was simultaneously set up at Enterprise «28th Military Plant». Electrodes and holders are finding limited application. They have not been used in Ukraine so far.

In conclusion it should be noted that underwater welding with coated electrodes currently prevails in Ukraine, because of stopping production of semi-automatic machines for mechanized underwater welding and components for them. In view of the absence of investments into development and production of a

new semi-automatic machine, designed using modern components, the technology of wet mechanized underwater welding may be completely lost for the user in the near future.

OEC is again becoming the major process of underwater severing in Ukraine. This process is fully provided with electrode materials and equipment, made locally. EAC process is little in demand because of its low efficiency. The process of underwater flux-core wire arc cutting is not applied, in view of the absence of specialized equipment.

1. Khrenov, K.K. (1946) Underwater electric welding and cutting. In: *Coll. of pap., dedicated to 70th anniversary and 50 years of scientific activity of Evgeny Paton*. Kyiv.
2. Madatov, N.M. (1965) *Underwater repair of ships and vessels*. Moscow: MO SSSR.
3. Madatov, N.M. (1967) *Underwater welding and cutting of metals*. Leningrad: Sudostroenie.
4. Avilov, T.I. (1957) *Some problems of metallurgy in underwater welding with high-grade electrodes*. Syn. of Thesis for Cand. of Sci. Degree. Moscow.
5. (1997) Company «Elektrodny Zavod». In: *Welding electrodes*. Catalogue. St.-Petersburg.
6. Gretsky, Yu.Ya., Maksimov, S.Yu. (1994) Influence of electrode coating components on weld metal formation in manual underwater welding. *Avtomatich. Svarka*, **7/8**, 15–17.
7. Gretsky, Yu.Ya., Maksimov, S.Yu. (1995) Structure and properties of low-alloy steel joints in underwater wet welding with coated electrodes. *Ibid*., **5**, 7–11.
8. Savich, I.M. (1969) Underwater flux-cored wire welding. *Ibid*., **9**, 70.
9. Savich, I.M., Smolyarko, V.B., Kamyshev, M.A. (1976) Technology and equipment for semi-automatic underwater welding of metal structures. *Neft. Stroitelstvo*, **1**, 10–11.
10. Asnis, A.E., Savich, I.M., Grishanov, A.A. et al. (1978) Physical-mechanical properties of welded joints produced by underwater flux-cored wire welding. *Avtomatich. Svarka*, **5**, 48–51.
11. Paton, B.E., Savich, I.M. (1987) 100 years of underwater welding. *Ibid*., **12**, 1–2.
12. Kononenko, V.Ya., Gritsaj, P.M. (1994) Wet mechanized welding in repair of ship hulls. *Morskoj Flot*, **11/12**, 21–22.
13. Kononenko, V.Ya., Rybchenkov, A.G. (1994) Experience of wet mechanized welding with self-shielded flux-cored wires in underwater repair of gas- and oil pipelines. *Avtomatich. Svarka*, **9/10**, 29–32.
14. Kononenko, V.Ya., Gritsaj, P.M., Semenkin, V.I. (1994) Application of wet mechanized welding in repair of ship hulls. *Ibid*., **12**, 35–38.
15. Danchenko, M.E., Savich, I.M., Nefedov, Yu.N. (1988) Underwater arc cutting with flux-cored wire. *Ibid*., **4**, 59–61.
16. Danchenko, M.E., Savich, I.M., Nefedov, Yu.N. (1989) Influence of hydrostatic pressure on technological parameters of underwater arc cutting with flux-cored wire. *Ibid*., **1**, 48–49.
17. Savich, I.M., Maksimov, S.Yu. (2001) Application of mechanized cutting in salvaging of a submarine. *Ibid*., **2**, 59–60.
18. Danchenko, M.E., Nefedov, Yu.N. (1991) Selection of optimum parameters of underwater cutting with flux-cored wire. *Ibid*., **11**, 61–65.
19. Danchenko, M.E., Nefedov, Yu.N. (1990) Flux-cored wire underwater cutting using a semi-automatic welding machine. *Ibid*., **1**, 70–71.
20. Danchenko, M.E., Lappa, A.V. (1993) Underwater cutting with stick electrodes (Review). *Ibid*., **8**, 35–37.

RESTORATION BY EXPLOSION WELDING OF CONNECTING SURFACES OF COUPLER LOCKS

A.N. KRIVENTSOV, V.I. LYSAK, V.I. KUZMIN and **M.Ya. YAKOVLEV**
Volgograd State Technical University, Volgograd, Russia

Technology for repair of worn out connecting surfaces of coupler locks by explosion welding is described. Parameters of the process of explosion welding of cladding plates to the locks and results of mechanical and full-scale tests of repaired locks are given.

Key words: *connecting surface of the lock, cladding plate, explosion welding, soft interlayer, contact strengthening, edge lacks-of-penetration*

Connecting surfaces of locks, which are responsible for the reliability of automatic coupler closing, wear in the most rapid manner. At the depth of wear, reaching the limit admissible value, the locks are repaired or taken out of service. The Instructions, approved by the Head Administration of Carriage Fleet of the Ministry of the Railways and Head Administration on Repair of Rolling Stock and Fabrication of Spare Parts [1] permit only one process to be used for restoration of such surfaces, namely electric arc surfacing. Unfortunately, this cannot always be fulfilled, as it requires special equipment, appropriate surfacing materials and precisely following the technology, developed by All-Union R&D Institute of Railway Transportation. On the other hand, it is known that explosion welding can successfully compete with surfacing in restoration (strengthening) of parts of mechanisms and machines (cylinder bushings, pistons, shares, various guides and other parts), designed for operation not only under the conditions of high pressures and temperatures, but also in the abrasive media. It has been proved that restoration by explosion welding of working surfaces of steel cylindrical and flat parts for different purposes shortens the restoration cycle, reduces material consumption and scope of machining and improves the wear- and corrosion resistance [2]. In this connection, investigations on development of the technology of restoration (cladding) of worn connecting surfaces of locks by applying wear-resistant steels by explosion welding were conducted at the Chair of Welding of Volgograd State Technical University by the order of carriage depot of Volgograd Branch of Nizhne-Volzhskaya Railways. The developed technology was to meet the following requirements:

1) guarantee preservation of the shape and restoration of geometrical dimensions of the repaired locks of automatic couplers to those, specified by documentation, approved by Head Administration of Carriage Fleet of the Ministry of the Railways and Head Administration on Repair of Rolling Stock and Fabrication of Spare Parts;

2) enable application of the traditional and composite wear-resistant materials in repair of locks, capable of extending the term of the lock safe operation 2 to 3 times, compared to similar locks, restored by electric arc surfacing;

3) guarantee producing a reliable welded joint of the cladding layer with the lock being repaired over the entire surface being restored;

4) completely eliminate the possibility of lock failure or appearance of any hazardous defects (hidden microcracks, cracks, coming to the surface, spallation, etc.) in them during their restoration by explosion welding.

Strips of 65GS steel (with initial Brinell hardness *HB* 180) of 70 × 350 mm size and 2–4 mm thickness (depending on the degree of wear) were used to restore the worn connecting surfaces of locks. It is known that the range of explosion welding parameters, guaranteeing production of a strong joint of 65GS steel with other steels, including those which are used to make the locks (20FL, 20GL, 20FGL, GOST 977–75), is quite wide. Therefore, third requirement seemed to be easy to fulfill. The lock proper was mounted on a base of metal shot, which is known [3] to be capable of easily absorbing the energy, accumulated in the system being welded, and, thus, minimizing the distortion of the lock shape and probability of formation of cracks and spallations in it, i.e. ensuring fulfillment of first and fourth requirements. The cladding (flyer) plate was mounted above the connecting surface of the lock with a certain gap so, that one of its side edges were located above the inner boundary of the contour of the lock connecting surface, and the other, similar to its two end faces, were outside the external boundary of the contour of this surface of the lock.

This should promote a considerable reduction (if not complete elimination) of the so-called edge lacks-of-penetration, i.e. one of the characteristic defects of explosion welding [3]. Such defects were not observed on the external boundary of the contour of the connecting surface of the lock in the first experiments, which, actually, was something to be expected. However, shallow edge lacks-of-penetration were found every time on the inner boundary of the contour of the lock connecting surface from test to test, which is exactly what required making some changes in the preparation of the cladding plates for welding and

the sequence of welding proper, which consisted in the following.

First of all, one of the side edges of the cladding plate, which during the system assembly for welding should be above the inner boundary of the contour of the lock connecting surface, was chamfered, i.e. the thickness of the cladding plate was smoothly reduced. This should compensate the inevitable lowering of the pressure pulse on its edge, due to penetration of the unloading wave into the zone of the formed detonation products from the side boundary of the reacting explosive charge, leading to a drop of the acceleration velocity.

Secondly, during the system assembly for welding a thin interlayer of a third metal, namely copper, was placed into the gap between the lock and the cladding plate, which allowed welding to be performed in the so-called soft mode, as the range of explosion welding parameters, guaranteeing production of a strong joint of copper with any of the steels, is wider than that for «steel + steel» pair, and, more over, it is shifted towards lower v_c and v_{cont} values, where v_c is the velocity of collision and v_{cont} is the velocity of the point of contact. Thus, this change in the welding sequence should also have contributed to elimination of the edge lack-of-penetration.

It is further important to note that addition of the copper insert, in which $R_{Cu} \cong R_{st}$ (here $R_{Cu} = \rho_{Cu}c_{Cu}$, $R_{st} = \rho_{st}c_{st}$ is the acoustic stiffness of copper and steel, respectively; ρ_{Cu}, ρ_{st} is the density of copper and steel; c_{Cu}, c_{st} is the velocity of sound in copper and steel) did not bring about a qualitative change of the pattern of shock-wave interaction, always favourable (in terms of preservation of the forming joint) in welding of materials with similar or close acoustic stiffnesses, and did not lower the zonal strength of the mechanically inhomogeneous welded joint (see below), as the accepted thickness (≈ 1 μm) of the «soft» interlayer falls in the range of thicknesses, where the factor of contact strengthening becomes active [4]. Welding by this sequence was performed, using a blasting explosive of lower strength with detonation rate $\Delta = 2500$ m/s and bulk density $\rho_0 \approx 0.9$ g/cm^3.

All the repaired locks were subjected to ultrasonic and parametric control. None of these revealed any discontinuities in the clad zone, or shape distortion or any noticeable deviations of their geometrical dimensions from those specified by the above documentation.

In addition, one lock was selected from each repaired batch to conduct mechanical tests to evaluate

Repaired lock and samples for mechanical tests, made of cut out parts of its clad zone

the zonal strength of the cladding layer (65GS steel) and welded joint [3], which was performed by determination of the indentation resistance. It is established that the hardness of this layer, i.e. of the connecting surface, increased from 180 up to *HB* 250–260. Welded joint resistance to layer pulling out was assessed by the results of mechanical tests of special samples, which were made of elements, cut out of the clad zone of the repaired lock (Figure). It is established that the welded joint strength exceeds the initial strength properties of the materials of the lock and the cladding layer and is equal to not less than 400 MPa.

Positive results of laboratory tests were the basis to conduct full-scale testing of restored locks under the actual conditions of their service in Volgograd–Moscow railway section. Analysis of the results of these tests and their comparison to basic data suggest that the developed technology of restoration of the connecting surfaces of locks in automatic couplers of railway rolling stock will allow extending the periods of safe service of these components at least 2 to 3 times, as well as reducing the labour and power cost of their restoration-repair. In addition, the developed technology of restoration of quickly wearing surfaces allows using not only the traditional, but also new composite wear-resistant materials, susceptible to strengthening, which will, probably, yield even higher results.

1. (1989) *RTM 32 TsV 201–88.* Manual on welding and surfacing in repair of cars and containers. Moscow: Transport.
2. Ivanyutenko, A. (1979) *Efficiency of explosion surfacing and welding*. Novosibirsk.
3. Konon, Yu.A., Pervukhin, L.B., Chudnovsky, A.D. (1987) *Explosion welding*. Moscow: Mashinostroenie.
4. Bakshi, O.A., Shakhmatov, M.V., Erofeev, V.V. (1984) Influence of internal defects on static strength of mechanically inhomogeneous welded joints. *Avtomatich. Svarka*, **11**, 7–11.

OPTICAL SENSOR FOR BUTT FOLLOWING AT GAP SIZES CLOSE TO ZERO

F.N. KISELEVSKY, G.A. BUTAKOV, V.V. DOLINENKO and **E.V. SHAPOVALOV**
The E.O. Paton Electric Welding Institute, NASU, Kyiv, Ukraine

Approach is suggested to the construction of optical sensor system for determination of the trajectory of a butt made without edge grooving with a gap close to zero. The sensor allows eliminating several disadvantages of the luminous section method and can serve as a beneficial addition to it.

Key words: *optical sensor, digital filtering, signal/noise ratio, surface roughness, luminous section, infrared illuminator*

To solve the problems of butt following in automatic welding a system of sensors (electric arc, inductive, tactile, optical, etc.) has been developed, whose principle of operation is based on using phenomena of a different physical nature.

Requirements, specified to the sensors in the systems of arc welding control, are very strict as regards to resistance against mechanical, thermal and electromagnetic actions, however, the price for these sensors should be acceptable [1].

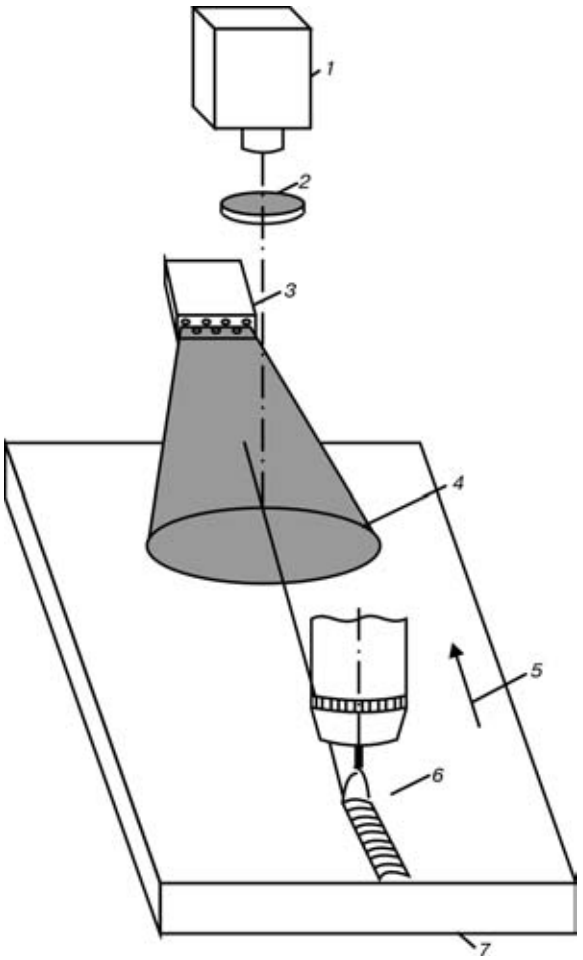

Figure 1. Principle of operation of system of following the butt with the gap close to zero: *1* — CCD-camera; *2* — interference filter; *3* — illuminator; *4* — scattered light; *5* — welding direction; *6* — welding zone; *7* — workpiece

The general tendency in the development of works in the field of creation of sensor systems for welding industry is connected with a design of optical sensors that is stipulated by their advantages as compared with other systems from the point of view of information completeness [2, 3]. Optical sensors provide, except data about the butt position, the information about its geometric sizes (gap, change in groove shape, etc.), and can measure in a number of cases the sizes of the weld being formed and/or the weld pool.

Among the optical systems used in automatic arc welding, the sensors operating on the basis of a luminous section method found the wide spreading.

Unfortunately, the use of the method of a luminous section in welding well-fitted parts without edge preparation is very difficult or even impossible, as the probability of an erroneous determination of butt is greatly increased, in particular if the surfaces being welded are prepared unproperly or have defects. When following the butt with V-shaped grooving in the process of welding parts made from the material with high coefficient of reflection (stainless steels, aluminium alloys), the parasitic re-reflections at the groove facets may occur that influences the correct finding of its position.

At the E.O. Paton Electric Welding Institute an optical scheme of butt following in a transverse direction has been developed for the case when the gap size is close to zero. The principle of operation of the system is shown in Figure 1.

The main system element is a digital video camera, containing a device with a charge coupling (CCD-camera), whose data are processed using a personal computer.

To increase the signal/noise ratio under the conditions of intensive light radiation of the arc an interference infrared filter is used, which working length of wave is selected from the following conditions:

- CCD-camera should be characterized by a sufficient sensitivity in the range of wave lengths passing through the infrared interference filter;

• light radiation of the arc in welding should be as minimum as possible in the working range of the interference infrared filter.

To provide stable conditions for CCD-camera operation an illuminator, assembled of several infrared light diodes (5–6 pcs) is sufficient. Casing of the illuminator serves simultaneously as a radiator for cooling. The illumination scattering is attained as a result of mutual intersection of directivity diagrams of radiation of light diodes, when the distance from illuminator to the surfaces being welded much exceeds the sizes of light diodes. The information input is realized in a real time. The rate of image processing is 5 frames per second.

The initial image, presented by an array of numbers, is processed using a linear or non-linear filtering to intensify the luminosity differences. Abrupt changes (breaks) in luminosity are the simplest symptoms in defining the configurations of objects. Optical properties of the parts surface, i.e. roughness, presence of surface defects (oxides, scratches), coefficient of reflectivity and others, influence the selection of filtering algorithm.

One of the simplest method of linear filtering consists in calculation of discrete differences that is similar to a continuous space differentiation. Underlining of vertical differences is realized by a horizontal (line-by-line) discrete differentiation. As a result an array of elements is formed:

$$G(j, k) = F(j, k) - F(j, k + 1),$$

where j, k are the coordinates of point on image; $F(j, k)$ is the luminosity of this point. Similarly, the underlying of horizontal differences is performed. As a result, an array of elements is obtained:

$$G(j, k) = F(j, k) - F(j + 1, k).$$

Diagonal underlying can be obtained by calculation of differences of levels of diagonal pairs of image elements.

In non-linear systems of detection of differences to contrast the pre-threshold limitation the non-linear combinations of luminosity values of image elements are used. In most methods the processing of windows of 2×2 or 3×3 pixels is only used.

To contrast and distinguish the differences the following non-linear operation of two-dimensional discrete differentiation, suggested in [4] is used:

$$G_R(j, k) = ([F(j, k) - F(j + 1, k + 1)]^2 + [F(j, k + 1) - F(j + 1, k)]^2)^{1/2}.$$

The non-linear method of detection of differences based on homomorphous processing of images is also often used [5]. According to this method, the point is located on a difference if the logarithm from luminosity of this point exceeds the mean value of logarithms of luminosity of four near-adjacent elements for some fixed value. Element of contrast image is determined as

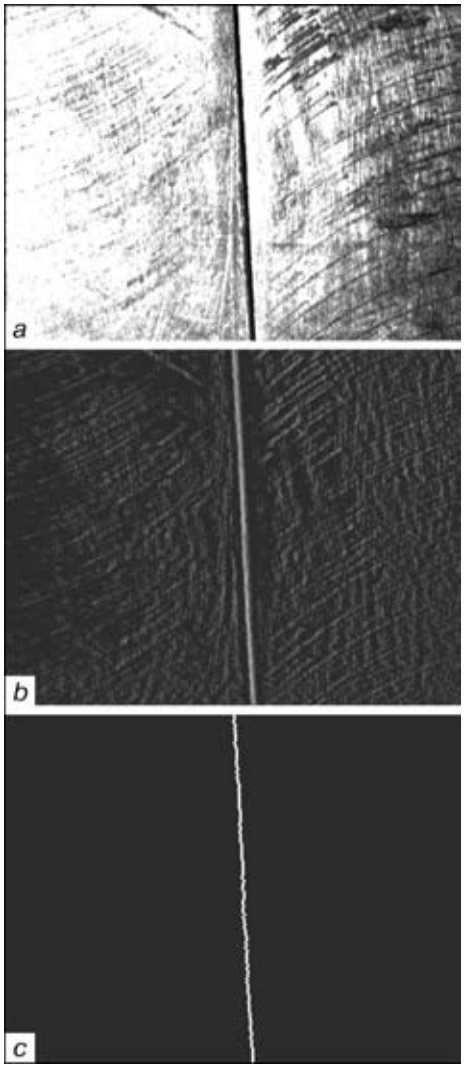

Figure 2. Images obtained using programs of processing: *a* — initial; *b* — after filtering; *c* — search and distinguish of butt

$$G(j, k) = \log | F(j, k) | - \frac{1}{4} \log (A_1) - \frac{1}{4} \log (A_3) - \frac{1}{4} \log (A_5) - \frac{1}{4} \log (A_7),$$

where A_1, A_3, A_5, A_7 are the luminosities of four adjacent points with respect to point with coordinates (j, k) or

$$G(j, k) = \frac{1}{4} \log \left\{ \frac{[F(j, k)]^4}{A_1 A_3 A_5 A_7} \right\}.$$

Comparison of $G(j, k)$ with upper and lower threshold values is equivalent to the comparison of fraction in brackets of expression with a modified threshold. Therefore, it is not necessary to make precise calculation of values of logarithms. The main advantage of a logarithmic detector of differences, consists in the fact that, except simplicity of calculations, it is not sensitive to multiple changes in luminosity level [6].

The logarithmic method of contrasting can be considered as a linear contrasting using Laplas's operator, whose element levels are equal to logarithms of lu-

minosity. Other methods of contrasting can be also easily presented in the form of sequence of non-linear element-by-element operations with a next linear contrasting of differences and threshold limitation.

The initial imaging of surfaces welded in a scattered light obtained using CCD-camera in the process of a sensor operation is given in Figure 2, *a*. Imaging after preliminary filtering is shown in Figure 2, *b*. The next step in algorithm of processing consists in search and distinguish of the butt. Figure 2, *c* shows the result of operation of subprogram of search and finding of the butt trajectory.

The optical sensor described does not allow us, unfortunately, to obtain information about the displacement of edges or change in groove depth and to define exactly the distance from torch to the butt. In this connection it is rational to use this method as an addition to the sensor of a luminous section.

The described method of butt following in the scattered light seems very promising. In addition to other optical methods it gives the best results, in particular in following the butt with the gap close to zero.

1. Koelbl, V. (1989) *Optical system of weld following and different cases of its application*. Vortrag DER.
2. Ushio, M., Oshima, K., Asai, S. et al. (1999) The-state-of-the-art of arc welding in vessel and pipe. IIW Doc. XII-1585–99.
3. Lee, C.W., Na, S.J. (1996) A study on the influence of reflected ARC light on vision sensors for welding automation. *Welding J.*, **11**, 379–387.
4. Diakonov, V., Abramenkova, I. (2002) *Signal and image processing*. Special Refer. Book. St.-Petersburg: Piter.
5. Prett, U. (1982) *Digital image processing*. Vol. 2. Moscow: Mir.
6. Kiselevsky, F.N., Butakov, G.A., Dolinenko, V.V. et al. (2001) Increase in weld following quality on the base of technical vision. In: *Proc. of Int. Sci.-Pract. Conf.-Exhibition on Problems of Quality Assurance in Welding Production*, Kyiv, April 3–6, 2001. Kyiv.

DEVICE PKR-3 FOR CONTROL OF VARIATIONS IN THICKNESS OF WELDING ELECTRODE COVERINGS

M.F. GNATENKO

Company «Velma», Kyiv, Ukraine

Methods for evaluation of variations in thickness of electrode coverings are considered. Specifications of a new device of the PKR-3 model are given.

Key words: *arc welding, covered electrodes, variations in thickness, evaluation methods, electromagnetic devices*

Analysis of the economic development of the CIS countries shows that manual arc welding using covered electrodes will still be dominant in the welding industry for some more decades. Therefore, production of electrodes should be further developed and improved. Quality of electrodes is an indispensable part of successful production and application of welded joints with required service properties. Basic quality indicators are regulated by GOST 9466–75 «Metal Electrodes for Manual Arc Welding and Surfacing». One of the most important quality indicators is variation in thickness of an electrode covering. This indicator determines eccentricity of location of the electrode axis relative to the rod axis. Uniformity of melting of the electrode covering (lip), arc stability, welding-technological properties of electrodes and, as a result, quality of welded joints and their performance depend to a considerable degree upon the variations in thickness of the electrode coverings.

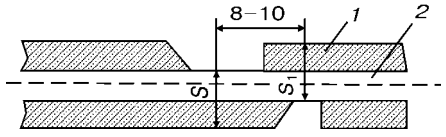

Figure 1. Schematic of measurement of electrode covering thickness variations: *1* — covering; *2* — rod

Requirements to permissible thickness variations are very stringent: not more than 5 % of the electrode diameter. In practice the trend is to make this tolerance as low as 2 times, i.e. not more than 2.5 %. The best electrode manufacturers make electrodes with thickness variations of about 1 % of the electrode diameter or not more than 0.05 mm. The method used to measure the electrode covering thickness variations is specified in GOST 9466–67. However, it is labour- and time-consuming, and features an insufficient accuracy.

According to this method «variations in thickness of the electrode covering, e, should be determined at three points located at a distance of 50–100 mm from each other along the length and at a distance of 120 ± ± 15° on the circumference. Measurements at each point are performed by using a micrometer in accordance with a diagram shown in Figure 1 at an accuracy of up to 0.01 mm.

Value e in millimetres is calculated using the following formula:

$$e = S - S_1.$$

There are also other methods and special devices (magnetic, capacitance etc.) permitted to check the

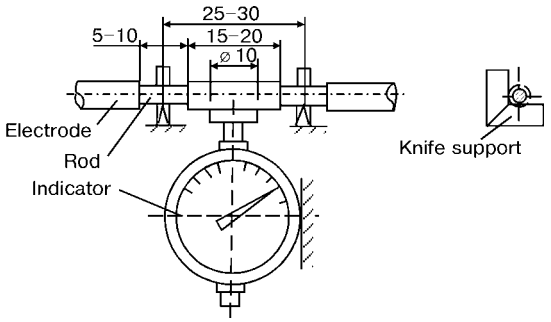

Figure 2. Schematic of measurement of electrode covering thickness variations (new GOST edition)

covering thickness variations, providing the required measurement accuracy».

It is suggested that the new edition of the GOST, which is to be approved during this year, should read: «The primary method to evaluate electrode covering thickness variations *e* is the method based on rotation of an electrode on two angular knife-shaped supports (for bare portions of the rod) with a measuring head located between the knives (under the electrode covering) (Figure 2). Prior to measurements, the electrode should be cleaned from the covering in locations where the knife supports are to be installed, the rod should be thoroughly cleaned with no damage to its surface, placed on the supports of the device and rotated to not less than one revolution by pressing the knife supports to angles and recording the extreme readings of the indicator with an accuracy of 0.01 mm The difference between these indications will correspond to a value of the electrode covering thickness variation. Measurements at one electrode should be made at three points: at the beginning, in the middle and at the end, to find the maximum value. Testing the covering thickness variation *e* can also be done using special devices to ensure a high response of control with no damage to the covering (magnetic, capacitance, X-ray etc.)».

Electromagnetic devices have gained the widest acceptance. Company «Velma» has developed, manufactures and supplies such a device of the PKR-3 model (Figure 3). It is intended for non-destructive testing of all grades of welding electrodes with ferrous and non-ferrous rods to variations in thickness of their coverings according to GOST 9466–75.

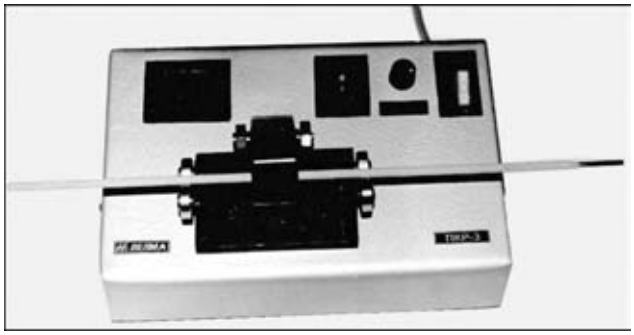

Figure 3. Device PKR-3 to control electrode covering thickness variations

Specifications of PKR-3 device

Sizes of electrodes tested, mm:	
rod diameter	2–5
covering thickness	0.35–2.00
Range of measurement of covering thickness variations, mm	0.01–0.25
Indication discreteness, mm	0.01
Measurement time, s	≤ 3
Mains voltage, V	220
Power consumption, V·A	5
Overall dimensions, mm	250×170×80
Weight, kg	2.7

Characteristic features of the device are as follows:

• control of variations in thickness of electrode coverings can be done in two modes with digital indication:

✧ current value,

✧ fixation of a maximum value;

• possibility exists of determining the plane in which difference in thickness of an electrode covering is maximum, and of establishing the direction of regulation of the forming sleeve;

• presence of only one measuring sensor located either on the top or on the bottom of an electrode placed on roller supports;

• simplicity of calibration of the device to different standard sizes of electrodes using a reference film;

• rapid response and high accuracy of control of thickness variations;

• operational reliability.

The use of the PKR-3 device provides the highest possible response in piece-by-piece control of variations in thickness of electrode coverings and prevents reject of electrodes on the basis of this indicator. Considering simplicity, operational reliability and low cost of the device, its efficiency is very high.

Developed at the PWI

METHOD AND EQUIPMENT FOR PULSED-ARC MIG WELDING WITH AUTOMATIC STABILISATION OF THE PROCESS

The method for pulsed-arc MIG welding with automatic regulation and stabilisation of energy parameters of the process, as well as equipment for realisation of this method have been developed. Advantages of the method and equipment are as follows:

- efficient control of metal transfer, allowing welding to be performed in any spatial position;
- decrease in critical value of the welding current, providing a wider range of working currents and reduced metal spattering;
- possibility of welding various steels (from low-alloy to stainless ones) and many non-ferrous metals, such as aluminium, copper and titanium alloys.

Compared with TIG welding, the new method allows the level of welding stresses and strains in workpieces to be substantially decreased, accuracy of geometric sizes of welded structures to be increased, welding speed and productivity of the process to be raised 2–3 times, and consumption of shielding gases to be reduced 3–4 times.

In addition, the use of the systems for automatic stabilisation and regulation of mean values of welding current and arc voltage makes it possible to decrease the effect of disturbing factors which usually accompany the welding process (variations in gaps, edge displacements, deviations in electrode extension, wire feed speed, torch travel speed, mains voltage and arc length according to deviations in geometric sizes of the welds from the set values), reduce the probability of defects of the type of oxide films, lack of fusion and pores, avoid subjective factors affecting the work of a welding operator, decrease requirements to his skill and training time, make labour conditions of welders much better, and program operating parameters in orbital welding.

Developers: P.P. Shejko, A.M. Zhernosekov, Yu.O. Shimanovsky

For additional information please contact:
Tel. (38 044) 227-44-78, 261-52-31

INTERNATIONAL SEMINAR «MODERN TECHNOLOGIES AND NEW STRUCTURAL MATERIALS IN CHEMICAL ENGINEERING AND INDUSTRY»

The International Seminar «Modern Technologies and New Structural Materials in Chemical Engineering and Industry» was held in Kyiv at the E.O. Paton Electric Welding Institute from 25 till 27 November, 2002. The Seminar was organised by the National Academy of Sciences of Ukraine, Ministry for the Industrial Policy of Ukraine, E.O. Paton Electric Welding Institute, Open Joint Stock Company «UkrNIIkhimmash» and International Association «INTERM» of the PWI. Chairman of the Seminar Organising Committee was Prof. K.A. Yushchenko, Deputy Director of the PWI and Corresponding Member of the NAS of Ukraine, and Deputy Chairman was Dr. Yu.B. Danilov, Deputy Director of the Company «UkrNIIkhimmash».

The Seminar was attended by more than 100 scientists and engineers from research and development institutes and higher education establishments, representatives of chemical engineering and oil-and-gas industry, chemical and oil-and-gas factories, specialists in production and realisation of steels, alloys and parts for chemical and petrochemical engineering and oil-and-gas industry from Ukraine, Germany, Austria and Portugal.

Prof. B.E. Paton, President of the NAS of Ukraine, noted in his welcome address and opening remarks to the Seminar participants that a prolonged depression in economics of Ukraine had a negative effect on the state of chemical, petrochemical and oil-and-gas industries. The major part of basic equipment of chemical engineering facilities exhausted their designed life long ago and need replacement and repair.

The sustained growth of economics of Ukraine observed since 2001 allows the problems associated with renovation and further development of these industries to be solved at a qualitatively new level.

The most important tasks for the immediate future are as follows:

- building of advanced apparatuses and equipment for chemical, petrochemical and oil-and-gas enterprises, making of new materials (steels, alloys etc.), and development of corrosion protection methods;
- development of reliable methods and instruments for evaluation of state of active equipment without interruption of its operation and estimation of residual life of the equipment, as well as new approaches to its repair;
- catching up with the backlog in application of new certified technologies, materials and equipment for preparation and welding production;

Prof. K.A. Yushchenko is making presentation at the Seminar

- development and realisation of new quality assurance systems for manufacture and repair of equipment at a level of international standards;
- increase in number of different levels of welding specialists certified in compliance with international standards;
- reduction of manual labour in manufacture of equipment.

It was gratifying that the Seminar was attended by specialists from all regions of Ukraine, as well as from such known companies as «ThyssenKrupp VDM Austria GmbH» and «Voest Alpine», which are the major manufacturers of high-quality structural materials.

Prof. B.E. Paton thanked all the attendees on behalf of the Organising Committee and wished the Seminar to be a success.

Mr. I.D. Ruchko, Head of Department for Chemical Engineering and Accessories at the Ministry of Industrial Policy of Ukraine, Prof. K.A. Yushchenko and Dr. Yu.B. Danilov in their presentations emphasised an importance of chemical and oil-and-gas industries for further development of industrial potential of Ukraine, its agriculture, social policy of the country to handle the needs of the population and export of products. Basic equipment of the majority of chemical, petrochemical and oil-and-gas enterprises of Ukraine is worn out to a considerable degree. Therefore, the scientific substantiation for application of new materials, building of new advanced equipment, upgrading and repair of existing equipment is an important and pressing problem.

Given below is the list of presentations with their short summaries.

During the Seminar

Dr. Yu.B. Danilov *(Open Joint Stock Company «UkrNIIkhimmash», Kharkiv) «Main trends in development of new structures for chemical and oil-and-gas industry enterprises».* Chemical engineering is the industry characterised by a rapid change of ranges of products and processes. Therefore, its most important task is to make a fundamentally new equipment, upgrade and repair existing facilities, automate processes and equipment, and develop methods to increase corrosion resistance. Ukraine has a sufficient scientific and industrial potential to cope with the above tasks.

Eng. Yu.Ya. Nekhaenko *(Severodonetsk State R&D Institute for Chemical Engineering) «Research and development activities of the Severodonetsk NIIkhimmash in manufacture of apparatuses for chemical enterprises».* The Institute is involved in research and development aimed at elaboration of integrated methods for diagnostics and repair of equipment in operation at chemical and petrochemical enterprises, design and manufacture of vessels and apparatuses with a working pressure of up to 16 MPa.

Dr. G.D. Samojlenko *(Limited-Liability Company «Topol», subsidiary of the Nikopol Yuzhnotrubny Works) «Ranges of the «Topol» Company Products».* The Company produces high-quality seamless welded and centrifugally cast pipes, as well as wire and branch pipes from carbon and low-alloy steels, medium- and high-alloy steels and alloys for chemical and petrochemical industries. The Company has a research base and specialists for development of technologies for manufacture of the above products.

Dr. H. Portisch *(ThyssenKrupp VDM Austria GmbH) «Nickel in a nutshell — the role of nickel in engineering, its production, supply and typical applications».* The Nickel Development Institute, where Dr. Portisch is a staff member, is active in promotion of nickel and nickel-base alloys to industry, publishes «Nickel Magazine», collects and disseminates information on the world production of nickel and nickel-containing alloys, as well as products of these materials. The Institute can provide free publications on this subject matter.

Mr. I. Sajer, G.D. Surguchev *(ThyssenKrupp VDM Austria GmbH) «ThyssenKrupp VDM Austria GmbH — Organisation and Products».* The Company incorporates 300 enterprises and makes about 1 million tons of steel. The Company has melting furnaces of differing capacities, including a 30 ton furnace with $Ar–O_2$ purging and continuously operating ESR furnace. The Company produces carbon steels, stainless steels with a nickel content of more than 25 %, nickel-base alloys, titanium and various parts of the above materials for chemical engineering etc.

Dr. H. Alves *(ThyssenKrupp VDM, Portugal) «High-quality materials of ThyssenKrupp VDM Austria GmbH for chemical engineering».* This division of the Company produces stainless steels of the 304L and 316L grades, alloys 926, 31, 32, C278, C4, C22, C50, B2 and B4 resistant to wet corrosion in chemical production environments. Alloy 31 is resistant to corrosion in sulphuric acid at concentrations of 98–99 and 78–80 % and at different temperatures.

Mr. B. de Bör *(ThyssenKrupp VDM, Germany) «High-temperature materials of Thyssen Krupp VDM Austria GmbH for gas-and-oil, aircraft and power engineering».* Melting, pouring and casting of alloys for application at temperatures of up to 1200 °C are performed in open arc furnaces by the VAR and ESR methods using 20 ton furnace. Alloy 602CA has been recognised the best one for operation in carburisation environments at 800–1200 °C.

Dr. J. Lettner *(Voest Alpine and ThyssenKrupp VDM Austria GmbH) «Hot-rolled bimetal plates for chemical, gas-and-oil and aircraft engineering».* Bimetal billets are produced by the Company using a traditional stack method. The billets are rolled to plates of different thickness at a customer's request. Bimetal is tested to bending and shear. The degree of diffusion of elements in the zone of adhesion of the layers is also checked.

Prof. I.K. Pokhodnya *(E.O. Paton Electric Welding Institute) «Welding consumables. State-of-the-art and development trends».* Arc welding will be dominant among numerous welding processes during the next decades. This area will require development of methods to control structure and properties of welds and joints in order to provide their high strength, ductility and operational reliability. These properties will be achieved through optimisation of systems of alloying of the welds and thermal welding cycles, through finding new methods to control melting and electrode metal transfer processes, as well as processes of penetration of the base metal, solidification of the weld pool and cooling of the welds. New types of efficient equipment will be made, reliable technologies for production of welding consumables will be developed, systems for computer-aided analytical control of production of welding consumables will be built on the basis of the latest physical and chemical analysis methods and instruments. The advanced standards, meeting the European requirements, should be worked out to establish quality assurance systems for production of parts, materials and consumables, as well as for certification of products.

Prof. K.A. Yushchenko *(E.O. Paton Electric Welding Institute) «Current trends in application of new technologies for welding of different grades of steels and bimetals».* In addition to traditional welding processes, there are also new technologies and equipment for arc welding of high-alloy steels

and alloys that found wide application. They include arc welding methods using microplasma, hybrid plasma + laser methods, welding using activators (PA-TIG) and self-shielding flux-cored wires, solid-state joining (friction stir welding, manufacture of structural members by explosion welding). Repair technologies using welding, cladding and spraying show high promise for maintaining performance of chemical and oil-and-gas industry equipment. The PWI is prepared to assist enterprises in mastering both new and traditional technologies.

Prof. K.A. Yushchenko, Dr. Yu.N. Kakhovsky, G.V. Fadeeva, V.I. Samojlenko, *and* ***Dr. A.V. Bulat*** *(E.O. Paton Electric Welding Institute) «New electrodes of the ANB series for welding high-alloy steels and alloys»*. The E.O. Paton Electric Welding Institute developed covered electrodes of the ANB-29, ANB-35, ANB-17 and ANB-17U, and ANB-42 (E-07Kh20N9, E-08Kh20N9G2B, E-02Kh19N18G5AM3 and E-04Kh23N24G4M3D3, respectively) grades for welding metal structures for chemical engineering. These electrodes are superior in a combination of their welding-operational properties, technological strength of weld metal and corrosion resistance to the known electrodes — analogues of the OZL-8 (E-07Kh20N9), TsL-11 (E-08Kh20N9G2B), EA-400/10U (E-07Kh19N11M3G2F) and OZL-17U (E-03Kh23N27M3D3G2B) grades.

Dr. V.F. Topolsky *(E.O. Paton Electric Welding Institute) «New processes for welding titanium and its alloys»*. The alloy on the base of titanium of the T-110 grade, having strength of 1100 MPa in the annealed state, as well as technology for welding this alloy and a number of other alloys were developed. Proposals for the manufacture of drill pipes from titanium-base alloys for drilling of wells to a depth of 5000 m were substantiated. The PWI offers cooperation in mastering these advanced developments.

Dr. V.A. Anoshin *and* ***Dr. V.M. Ilyushenko*** *(E.O. Paton Electric Welding Institute) «Advanced technologies for welding copper and steel + monel bimetal»*. The PWI developed and is applying advanced technologies for welding of copper using paste-like fluxes, in a nitrogen atmosphere, by plasma and ESW methods. Available are the technology and filler metals (wire, electrodes of the ANTs-3M grade) for welding of copper and steel + monel bimetal. Specialists of the PWI are prepared to assist industry in mastering these technologies.

Dr. I.V. Dovbishchenko *(E.O. Paton Electric Welding Institute) «Improvement of corrosion resistance of welded joints on aluminium equipment used to produce concentrated nitric acid»*. The PWI developed technologies for improvement of corrosion resistance of welded joints on reaction vessels (autoclaves, bleaching columns, refrigerators, pipelines etc.) and parts made from commercial aluminium AD00 and AD000 of an increased purity by heat treatment. The technology recommended will allow service life of the equipment to be extended.

Dr. E.F. Pereplyotchikov *(E.O. Paton Electric Welding Institute) «Modern technologies and equipment for surfacing and hardening of pipeline valves»*. the PWI developed technologies and substantiated the efficiency of using plasma-powder cladding for pipeline valve components. Provided was the information on new powders and equipment for plasma-powder cladding of valves. Examples of their efficient application for production and repair of valves were given.

Prof. A.Ya. Nedoseka, Dr. S.A. Nedoseka, M.A. Yaremenko *(E.O. Paton Electric Welding Institute),* ***A.A. Yolkin, Yu.F. Kurbatov, A.S. Vasiliev*** *(Odessa Port Factory) «Monitoring of technical state of equipment in operation»*. Available are the advanced technologies for monitoring of quality of welded joints and estimation of specified service life of equipment. The technologies are based on analysis of the material condition vector (MCV technology). The system for technical diagnostics of equipment of the EMA-3 family was made and introduced into industry.

Prof. S.G. Polyakov *(E.O. Paton Electric Welding Institute) «Scientific principles and hardware for utilisation of electrochemical methods for corrosion monitoring at petrochemical enterprises»*. Theory and practice of measurement of corrosion rate by the kinetic and polarisation resistance methods, as well as estimation of the effect of distribution of local corrosion centres on corrosion fracture susceptibility of a workpiece were worked out. Elements of the corrosion-measurement hardware (electrochemical cells, sensors etc.) were made and introduced into production. The developments are recommended for wide application at industrial enterprises.

Dr. V.A. Kachanov *(Open Joint Stock Company «UkrNIIkhimmash») «Investigation of corrosion behaviour of welded joints in new structural materials in aggressive environments»*. Investigations were conducted to study corrosion resistance of the ThyssenKrupp VDM alloys 31, 33, 59 and B4, Russian alloys 06KhN28MDT and KhN65MBU and zirconium E-110 in environments containing sulphuric acid, alloys 33 and 06KhN28MDT in titania production processes, as well as alloys 201, 33 and 06KhN28DDT in concentrated caustic environments. Recommendations for their applications were given.

Dr. V.A. Kachanov *(Open Joint Stock Company «UkrNIIkhimmash») «Increase in corrosion cracking resistance of metals in a structure»*. Recommendations for heat and hydraulic treatment of welded joints and equipment of steels 09G2S and St.3sp5 were developed and introduced into production in order to increase resistance to corrosion cracking.

Eng. S.V. Nesterenko *and* ***N.G. Yefimenko*** *(Kharkiv State Municipal Academy),* ***Dr. V.A. Kachanov*** *(Open Joint Stock Company «UkrNIIkhimmash») «Effect of REM and their master alloys on corrosion resistance of welds in austenitic steels»*. Microalloying of weld metal of the 12Kh18N10T, 07Kh19N11M3, 04Kh18N9, 10Kh20N9G6T types with of 0.0019 and 1.0035 % of yttrium and cerium, respectively, leads to inhibition of corrosion in aggressive environments containing H_2SO_4, HNO_3 and NaOH.

Eng. G.E. Shepil *(Open Joint Stock Company «UkrNIIkhimmash») «Metallography of corrosion*

fractures of high alloys». Metallography of the ThyssenKrupp VDM alloys 31, 33, 59, B4 and 201 and welded joints in environments characteristic of titania and caustic soda production revealed both advantages and disadvantages of each of the above alloys. Certain heat treatment conditions were recommended to improve corrosion properties of welded joints of alloys 31 and 59.

Dr. B.A. Gru *(State R&D Institute «Khimtekhnologiya», Severodonetsk) «Corrosion of steels and alloys in some chemical engineering environments»*. The Institute is active in research on corrosion resistance of steels, alloys and metals in specific aggressive environments characteristic of chemical engineering. It was established, in particular, that in production of potassium saltpetre steel 06KhN28MDT exhibited an acceptable corrosion resistance in an intermediate product of NOCl at a temperature of 20 °C, alloys KhN78T and KhN65MV exhibited an absolute resistance in a mixture of $NOCl + Cl_2 + N_2O_4$ at 20 °C, and the ThyssenKrupp VDM alloy 59 (03Kh22N60M15) was the best in organic chlorine at 600 °C.

Eng. A.I. Kabashny *(Open Joint Stock Company «UkrNIIkhimmash») «Peculiarities of the technology for manufacture of heat exchangers from plates»*. The Company «UkrNIIkhimmash» developed designs and technologies for manufacture of heat exchanging elements of the plate and panel types from plates. Thermal efficiency of such elements is 1.5 times as high as that of tubular elements.

Eng. V.M. Dolinsky, D.G. Ryauzov, V.I. Cheremskaya *(Open Joint Stock Company «UkrNIIkhimmash») «Operation and monitoring of technical equipment with defects in welded joints»*. The Company «UkrNIIkhimmash» developed and successfully verified under industrial conditions the model test method allowing estimation of the residual safe life of chemical engineering structures. To apply this method in industry, it is necessary to revise standards on admissibility and inadmissibility of operation of equipment.

Eng. I.I. Kovalev *(Rubezhansk State Chemical Factory) «Experience in operation, manufacture and repair of ferrosilicide equipment»*.

Eng. A.S. Gerashchenko *(Joint Stock Company «UkrTATnafta», Kremenchug) «Problems of repair, operation, assurance of quality and reliability of petrochemical equipment supplied to Joint Stock Company «UkrTATnafta»*. The Kremenchug Oil Refinery, which is capable of refining 18 million tons of oil per year, has in operation 2977 vessels and apparatuses, 1750 pumps, 124 compressors, 492 tanks, 6600 pipings and 1700 pieces of other service equipment. A wish was expressed that a centralised production of special electrodes with a guaranteed quality for chemical and oil-and-gas enterprises be arranged in Ukraine.

Dr. L.I. Aslamova, Dr. I.M. Kadenko *(T. Shevchenko Kyiv National University) «Training of personnel working with the equipment comprising ionisation radiation sources»*. In Ukraine for the first time the «State Sanitary-Hygienic Rules and Regulations for Radiation Safety while Working with Metal Scrap» were developed. They have been introduced into effect since March 15, 2002. The Kyiv National University arranged courses on the above subject matter for legal and natural entities.

Dr. P.P. Protsenko, Prof. K.A. Yushchenko *(E.O. Paton Electric Welding Institute) «International system for training and certification of specialists involved in welding and related processes»*. The International Training and Certification Centre for training of international-qualification specialists, such as welding engineers, welding technologists, welding specialists, welding practitioners and welding inspectors is functioning on a regular basis at the E.O. Paton Electric Welding Institute.

Eng. V.V. Progolaev *(Open Joint Stock Company «UkrNIIkhimmash»),* ***Dr. G.G. Monko*** *and* ***Dr. L.V. Chekotilo*** *(E.O. Paton Electric Welding Institute) «Development of new standards and specifications for chemical and oil engineering»*. The Company «UkrNIIkhimmash» developed and introduced into effect basic branch standards for chemical, petrochemical and oil-and-gas engineering: GSTU 3-17-191–2000 and GSTU 3-020–2001 (developed with participation of PWI), national standards: DSTU 4003–2000 and DSTU 4026–2001, as well as standards harmonised with EN: DSTU EN 286.1–2002 and DSTU EN 286.2–2002. The standards are available at the Company «UkrNIIkhimmash».

Participating in the round-table discussion were representatives of industrial enterprises, R&D institutes and other organisations: P.P. Elagin, B.P. Kisly, B.Yu. Zhukovsky, L.E. Marchenko, A. Salnikov, A.P. Korop, S.V. Firsov, A.E. Noravsky, I.D. Groisman, I.V. Yavorsky, V.A. Bas, V.A. Barilyuk, T.V. Suprun, V.G. Fartushny and others. The participants expressed an interest in having such seminars held on a regular basis.

In the closing speech K.A. Yushchenko and Yu.D. Danilov thanked representatives of Ukrainian organisations, research and industrial enterprises, as well as specialists and scientists from Austria, Germany and Portugal, the «ThyssenKrupp VDM Austria GmbH», «Voest Alpine» companies and the Nickel Development Institute for participation in the Seminar and support rendered to its holding.

The Seminar demonstrated a high potential of science and industry for further improvement of chemical and oil-and-gas industries of Ukraine.

Dr. L.V. Chekotilo